On agricultural eddy covariance atmospheric storage term: Developing a system to measure carbon dioxide concentrations and energy exchange inside a maize canopy

A Dissertation Presented for the

Doctor of Philosophy

Degree

The University of Tennessee, Knoxville

Taqi Raza

August 2025

ACKNOWLEDGEMENTS

This endeavor would not have been possible without the inspiration, dedication to science, and the opportunity from my mentor, Neal S Eash. Each of my committee members has been instrumental in getting me here by being generous with their knowledge, expertise, and recommendations: Bruce B Hicks, Nebila Lichiheb, Thomas J Sauer, James Zahn, John J Goddard, and Dayton Lambert. I could not have undertaken this journey without this study being made possible by the funding support of DuPont company, University of Tennessee Knoxville and Chateaubriand fellowship (France). Specifically, I would like to thank David Smith (technical specialist), Scot K Tucker (technical specialist), Wesley C Wright (Research associate) for their technical support throughout the study. I would also like to thank Jash Watson (farmer) for his support along with the use of his property for a multi-year field study. In addition, I want to thank the knowledgeable staff at UT Knoxville including Julie Carrier, Sandra A Marin, Lesia Rucker, and Ruth Watt-Yats, for their help and support with many logistical details.

A special thank you to Joel Nathaniel Oetting (postdoc) for his help with field and lab work, dedication to the field, and moral support.

Thank you to my family and friends, your support, encouragement, and faith has kept me motivated and thankful during this entire process.

To my beloved parents, whose love, sacrifices, and values continue to guide me every day. Though you are no longer with me, this achievement is as much yours as it is mine.

ABSTRACT

This dissertation examines CO_2 and H_2O fluxes, and energy storage terms over a maize field. An experimented program conducted in 2023 at a site in eastern Tennessee utilized a new multiport profile system to assist in the interpretation of eddy fluxes and to determine atmospheric storage rates of heat and CO_2. Flux measurements were made within and above the canopy. Energy balance closure was calculated with and without considering energy storage terms. CO_2 fluxes were partitioned to gross primary production (GPP) and ecosystem respiration (Reco) to estimate net ecosystem exchange (NEE). Additionally, the pooling effect of carbon dioxide was explored. The results demonstrate the need to assess storage rates in field studies of the surface energy budget and to account for the heat used to support photosynthesis. Both depend on the time of day and the prevailing meteorology, as well as subsurface properties like the soil water content. Depending on the time of day and prevailing meteorological conditions, photosynthesis can contribute 7 to 18 W m^{-2} to the surface heat energy imbalance reported elsewhere.

TABLE OF CONTENTS

LIST OF TABLES

LIST OF FIGURES

LIST OF ACRONYMS

Acronyms	**Definition**	**Unit**
Fc	CO_2 flux	$\mu mol\ m^{-2}s^{-1}$
Rn	Net radiation	W m^{-2}
LE	Latent heat flux	W m^{-2}
EC	Eddy Covariance	—
PAR	Photosynthetically Active Radiation	µmol m^{-2} s^{-1}
CHS	Canopy Heat Storage	W m^{-2}
SHS	Soil Heat Storage	W m^{-2}
T	Transpiration	mg H_2O m^{-2} s^{-1}
H	Sensible heat flux	W m^{-2}
IBL	Internal Boundary Layer	
IRGA	Infrared Gas Analyzer	
IRs	Infrared Radiometers	
BREB	Bowen Ratio Energy Balance	
Atm	Atmospharic	
GHGs	Greenhouse Gasses	
ppm	part per million	
β	Bowen Ratio	
ABRA	Augmented Bowen Ratio Analysis	

Carbon dioxide concentration	[CO_2]	$\mu mol\ m^{-2}s^{-1}$
Water vapor concentration	[H_2O]	$mmol\ m^{-2}s^{-1}$
SEB	Surface Energy Balance	
SBL	Stable Boundary Layer	
L, λ	Latent heat of vaporization	J kg^{-1}
E	Evapotranspiration	mm $hour^{-1}$
G0	Ground heat flux at top 0-meter soil	W m^{-2}
LAI	Leaf Area Index	
IRs	Infrared sensors	
IRGASON	Integrated CO_2 and H_2O Open-Path Gas Analyzer and 3-D Sonic Anemometer	
NEE	Net Ecosystem Exchange	$\mu mol\ m^{-2}s^{-1}$
GPP	Gross Primary Production	$\mu mol\ m^{-2}s^{-1}$
Re, Reco	Ecosystem respiration	$\mu mol\ m^{-2}s^{-1}$
ICOS	Integrated Caron Observation System	
LT	Local Time	
UTC	Universal Time Coordinated	
V5-V7	Vegetative stage	
VT	Tasseling stage	
R1-R5	Reproductive stage	

R6	Dent stage	
PE_storage	Photosynthesis heat storage	W m^{-2}
H_storage	Sensible heat storage	W m^{-2}
LE_storage	Latent heat storage	W m^{-2}
total_storage	Total heat storage	W m^{-2}
ET	Evapotranspiration	mm $hour^{-1}$
SURFATM	Surface and Atmosphere	
Lem	Measured latent heat flux	W m^{-2}
LEs	Simulated latent heat flux	W m^{-2}
Hm	Measured sensible heat flux	W m^{-2}
Hs	Simulated sensible heat flux	W m^{-2}
Nem	Measured Net Ecosystem Exchange	$\mu mol\ m^{-2} s^{-1}$
NEEs	Simulated Net Ecosystem Exchange	$\mu mol\ m^{-2} s^{-1}$
Recom	Measured Ecosystem Respiration	$\mu mol\ m^{-2} s^{-1}$
Recos	Simulated Ecosystem Respiration	$\mu mol\ m^{-2} s^{-1}$
ρ_m	Air molar density	Kg m^{-3}
$\overline{w'c'}$	covariance between wind speed (w) and CO_2 concentration	
$F co_2$	Carbon dioxide (CO_2) flux	$\mu mol\ m^{-2} s^{-1}$
$F h_2 o$	Water vapor (H_2O) flux	$mmol\ m^{-2} s^{-1}$
ρa	Air density	kg m^{-3}
c_p	Air heat capacity	J K^{-1} kg^{-1}

$\overline{w'T'}$	covariance between wind speed (*w*) and air temperature (*T*).	K m s^{-1}
J_c	CO_2 storage term	*μmol mol*$^{-1}$ *m*$^{-2}$$s^{-1}$
Δz_i	Thickness of layer	m
ΔT	Change in soil temperature above of heat flux plate	K
Δt	Time period	s
φ_f	Soil porosity	g/cm^2
P_b	Soil bulk density	Mg m^{-3}
P_s	Particle density	Mg m^{-3}
C_m	Soil volumetric heat capacity	MJ m^{-3} K^{-1}
C_w	Water volumetric heat capacity	MJ m^{-3} K^{-1}
θ	Soil volumetric water contents	m^3 m^{-3}

INTRODUCTION

Climate change is impacting food-water security throughout the world resulting in changes to cropping patterns (O'Dell et al. 2020; Syed et al. 2022). In the USA, significant areas of land have been converted into a maize (*Zea mays)*-soybean (*Glycine max*) production system where grass were once the native vegetation. Under such agricultural practices, greenhouse gas emissions and temperature become fundamental problems for environmental sustainability. Globally, continuous shifts in temperature and CO_2 are alarming. In nature, positive feedback for CO_2, water vapor, and temperature exists among soil, plant, and the environment (Held and Soden, 2000; Law et al. 2002; Luo, 2007). Any imbalance in these can create a situation of negative feedback and influence plant activities.

Studies have shown that gases (especially CO_2), water vapor and energy, behave differently inside the plant canopy than above the canopy (Grace, 2006; Baldocchi, 2014). Inside canopy received less light, limited air movement, lower wind speed and variation, higher CO_2 and H_2O concentration, while the above canopy has a reverse phenomenon. A central issue relates to the role of vegetation, with stomatal activity affecting water vapor and CO_2 exchange whereas sensible heat transfer entails the thermal characteristics of the foliage and the air within and above the canopy. All such influences vary with time and generalization is difficult. However, accurate modeling and understanding of source-sink relationships requires better understanding of how the plant environment changes as the climate changes, and how plant productivity is affected. Obtaining the observations necessary to examine the many physical, biological and perhaps chemical processes of relevance is demanding, most often requiring extensive measurement over areas that satisfy the basic constraints of the observing protocols that are used — primarily micrometeorological.

In agriculture or forestry, water use efficiency, plant growth and climate adaptation strategies are directly influenced by the surface energy balance (SEB). SEB represents the balance of energy (net-radiation) between in- and out-going energy at the land surface over a specific time. Achieving balance remains a significant challenge. Errors in SEB calculations can arise from neglecting to account for the fluxes not measured by eddy covariance (EC) techniques.

Our aim is to explore these matters in a growing maize crop. Maize canopies hold particular interest because understanding their dynamics is crucial to developing improved methods to manage irrigation and optimize crop yield. This research is an opportunity to explore SEB research issues in agricultural systems.

Justification of the Study

In the last few decades, significant work has been conducted to enhance the understanding of gas exchanges between soils, plants, and the atmosphere. These improvements have been incorporated into land-surface models and numerically based weather prediction as well as into assessment of atmospheric fluxes of carbon dioxide (Lamas Galdo et al., 2021), water vapor (Wang et al., 2023), and heat over vegetated landscapes. Eddy covariance is a common and widely accepted method to quantify the atmospheric flux of CO_2, H_2O, and heat in the ecosystem (Nicolini et al., 2018). Globally, almost 1000 EC locations are monitored (c.v. Flux net; Pastorello et al., 2020). However, at most sites the energy budget is not balanced ($R_n - G = H + LE$). Reasons include the loss of low/high frequency components of eddy fluxes, inappropriate coordinate-rotation, mismatched averaging periods, errors in measurement and data processing, spatial and temporal variations, advection and convection, and using the wrong fetch footprint (Massman and Lee, 2002; Meyers and Hollinger, 2004; Oetting et al. 2024).

Forest ecosystem studies increasingly highlight the importance of considering soil and canopy heat storage in SEB calculations. Neglecting these

factors can lead to significant discrepancies in SEB estimates (McGaughy and Saxton, 1988; Haegeum and Nelson, 2023). Accurate estimation and incorporation of heat storage terms are crucial for precise calculation of energy fluxes, directly influencing climate-smart modeling and strategies. Understanding and quantifying these energy balance components including heat storage terms are essential to study crop growth, water use efficiency, and the overall microclimate of agricultural fields.

During photosynthesis, plants store biochemical energy that can vary from 1-2% of available energy (Okae, 1987). The plant utilizes energy during photosynthesis for the formation of glucose and oxygen as end products from the *Rn*. Similarly, heat stored in plant biomass is also a considerable portion of *Rn* (Michiles and Gielow, 2008; Lindroth et al., 2010). Soil as a natural body can store heat energy that can be determined from any point of interest or depth above the reference point of a soil heat flux plate. This stored heat (energy) could be either a significant or minor component of the SEB, depending upon location. Heat stored in soil is emitted back to the surrounding atmosphere via different processes, affecting surface energy balance and the surrounding atmospheric conditions. A measurable portion of energy (*Rn*) is dissipated as latent (*LE*) and sensible heat (*H*). However, a measurable portion of *LE* and *H* is also stored within the canopy and potentially impacting the overall energy balance (Imukova et al. 2016). A study by Foken (2008) reported that the extent of energy balance error associated with different vegetation surfaces can reach as high as 20-50% for storage terms, 20-50% for soil heat flux (*G0)*, 5-20% for *H*, 5-20% for *LE* and 5-20% for *Rn.*

Accurate quantification of each energy balance component and heat storage term is essential for researchers to resolve problems of energy balance closure in agricultural ecosystems. Measuring heat storage terms accurately requires innovative methods and analysis techniques. Appropriate methods or new method development will help to develop a better understanding of CO_2, H_2O and heat variations, and their vertical profiles, thereby facilitating precise assessments of their exchanges, storage, and overall balance in the growing agricultural ecosystems.

Overview of the Study

To conduct this study, a multiport system was developed to examine the exchange of [CO_2], temperature (heat), and [H_2O] from maize fields and the overlying atmosphere by partitioning into below and above canopy profiles. The recommended FLUXNET (Wilson et al., 2002) and ICOS (Montagnani et al., 2018) methods were followed to measure CO_2, H_2O, and heat fluxes and their storage terms. Details of the following methods are explained in the later sections. The system is designed to maintain continuous airflow through all intake tubes, to cycle through all four measurement heights in less than one minute (7.5 seconds for each height), and to minimize the switching time between samplings.

The performance of the system for measurement of [CO_2] and [H_2O] profiles was examined in the lab before its field deployment. The system was deployed in the field during the first week of May 2023, and measurements were conducted until crop harvesting in the middle of October 2023. The 5 Hz raw data was averaged into 15-minute runs to calculate the CO_2, H_2O, *H*, and *LE* fluxes. Additionally, *Rn* and *G0* fluxes were measured to calculate surface energy balance. Furthermore, the data was used to calculate CO_2 and H_2O storage fluxes, and heat storage terms (canopy, latent/sensible and photosynthesis storages). A summary of the research parameters recorded during the study are given in **Table 1**.

Objective of the Study

The objective of study was to measure the [CO_2], [H_2O], and temperature from both within and above of a maize canopy to elucidate how the inside canopy airspace communicates with the outside airspace. Canopy profile data have been used with CO_2, *LE* and *H* flux to calculate NEE and heat storage terms over a maize canopy. The storage terms have been used as an additional parameter in energy balance equations to calculate the energy balance closure of maize. The maize surface energy balance is evaluated to determine whether including heat storage term improves the energy balance closure calculation.

Why Profile System for Flux Measurement

Accurate measurements of surface energy balance remain a major challenge through traditional EC systems (Wilson et al., 2002; Foken, 2008). Energy balance closure errors refer to fluxes measured by EC that fail to account for full surface energy balance (SEB). For example, at most agricultural and forest sites, recorded latent and sensible heat fluxes (*H* + *LE*) were found to be relatively lower than the available energy (*Rn*-*G0*), resulting in energy balance closure errors. Additionally, a good portion of energy (*Rn*) is also used during photosynthesis, stored in the canopy, in plant biomass as well as in soil. This is called the heat storage term. During

Table.1. Research parameters considered during the study.

Variable	Derivation	Measurement
Crop height	Directly	1-2 times a week
Plant population	Directly	1-2 times
Plant biomass	Directly	1-2 times
CO_2 concentration	Gas Analyzer	Continuous
Temperature variation	Partitioned	Continuous
Moisture contents	Partitioned	Continuous
Evapotranspiration	Eddy Covariance	Continuous
Wind speed within the canopy	2D sonic anemometer	Continuous
Wind speed above the canopy	3D sonic anemometer	Continuous
Within and above canopy temperature	Infrared temperature sensor And thermocouples	Continuous
Heat flux	Soil heat flux plate	Continuous
Spatial average of PAR	Quantum sensors	Continuous
Energy capture by plant	Line quantum sensor	Continuous

traditional flux measurements, these storage terms are often overlooked and underestimated, thereby impacting the accurate energy balance calculation (Wilson et al., 2002; Leuning et al., 2012). Errors in SEB closure calculations can be the consequence of differences in the measurement methods. Therefore, careful consideration of storage terms in addition to SEB components is a particularly important area of focus to address these challenges.

Other SEB errors are caused by the underlying assumptions endemic to EC. EC requires a horizontally homogeneous surface that is flat and uniform to permit reliance on the common algorithms describing the turbulent exchange. However, the scenario in the real world is different and the situation is different at most field research sites, e.g., site complexity, non-homogeneous landscape (e.g. advection and convection), edge effect, and measurement uncertainties especially by sonic anemometers. In agriculture, understanding flux-gradient relationships is important because these relationships are needed to calculate water loss, and to study flux-gradient exchanges between the crop and the air. With the EC method, the closure problem or energy imbalance remains an unsolved issue (Wilson et al., 2002; Foken 2008; Franssen et al., 2010; Foken et al., 2011; Leuning et al. 2012; Masseroni et al., 2014; Anderson and Wang 2014; Russell et al., 2015; Liu et al., 2017; Gao et al., 2017).

Fixing SEB errors presents a significant challenge due to difficulties in SEB measurement (Foken 2008; Foken et al. 2011; Anderson and Wang 2014), and other sources of discrepancies including ignoring storage terms (Zuo et al., 2011; Leuning et al., 2012; Russell et al., 2015; Liu et al., 2017). Aubinet et al. (2012) and Stoy et al. (2013) emphasized that including storage terms in SEB calculations improves SEB calculation estimates, increases flux measurement accuracy, and improves ecosystem-atmosphere models. Measuring storage terms is required to capture temporal and spatial variation of temperature, CO_2, and H_2O within and above the plant canopy. To account for this complexity, a multi-profile system is essential that considers two heights within the canopy and two above the canopy to calculate these storage terms.

CHAPTER 1: LITERATURE REVIEW OF THE STUDY

Abstract

Understanding soil-plant-atmosphere exchange of mass and energy is crucial for a better understanding of the terrestrial environment. To validate land-surface models using fluxes requires surface energy balance closure; however, these requirements are not fully satisfied when available energy is greater than the total vertical fluxes. Heat storage (whether within the canopy or in the soil) receives less attention from micrometeorologists for several reasons including that a fraction of the water vapor, gases, and heat are stored in the plant canopy (called canopy storage), and the amount stored is dependent upon the environmental conditions. Many studies reported that storage terms are consistently smaller in crops (which may be the reason it is often neglected) than forest ecosystems. Studies also reported that underestimation of storage terms in the energy balance closure can be a major reason for imbalances. Storage terms are significant contributors that have not been fully explored in agricultural crops although attempts have been made in forest studies. Including these storage terms will improve SEB closure.

Literature Review

Over the last few decades, several studies have been conducted to evaluate energy and mass exchanges between plant surfaces and the atmosphere to study ecosystem services, water resources management, and climate change impacts (Zalewski, et al. 2021). These studies improved the prediction of evapotranspiration and eco-hydrological response of agricultural ecosystems to extreme events (e.g., drought, floods). Naturally, water and temperature are tightly interconnected because a large portion of solar radiation (*Rn*) is converted into latent (*LE*) and sensible heat (*H*). In *LE*, *L* represents latent heat of vaporization, and *E* represents evapotranspiration which also determines the H_2O flux and energy exchanges in relation to near surface atmosphere conditions. *Rn*, *LE* and *H* are the major components of the SEB. *LE* and *H* fluxes also determine properties (e.g., physical) of planetary boundary layers and several climatological processes. *LE* flux influences the biogeochemical and hydraulic cycles by changing the SEB and *ET*. It indirectly controls the runoff and soil moisture regimes of the ecosystem (Wilson and Baldocchi 2000). As *LE* flux is the major component of the SEB, it provides a detailed understanding of water balance and climate change impact. Other SEB components such as ground heat flux (*G0*) and evapotranspiration (*ET*) play a key role in agricultural water management, irrigation scheduling, and hydrological water balance. Further, soil-plant-atmospheric interactions and agricultural productivity are influenced by the SEB and its components (Irmak et al., 2014). The land surface energy balance equation determines the amount of available net energy and its partitioning into numerous components. The SEB equation is described using the equation number 1 shown in **Figure** 1.

$$Rn = G0 + H + LE \qquad (1)$$

Here, the SEB is represented by *Rn* (net-radiation), *G0* (soil heat flux), *H* (sensible heat flux) and *LE* (latent heat flux/evapotranspiration).

This equation does not include the amount of heat stored in the soil and canopy (latent and sensible heat storage). It also does not include the amount of energy plants use during the process of photosynthesis (photosynthesis storage term).

Several studies have evaluated the role of energy storage terms. According to Meyers and Hollinger (2004), storage terms individually represent less than 5% of Rn.

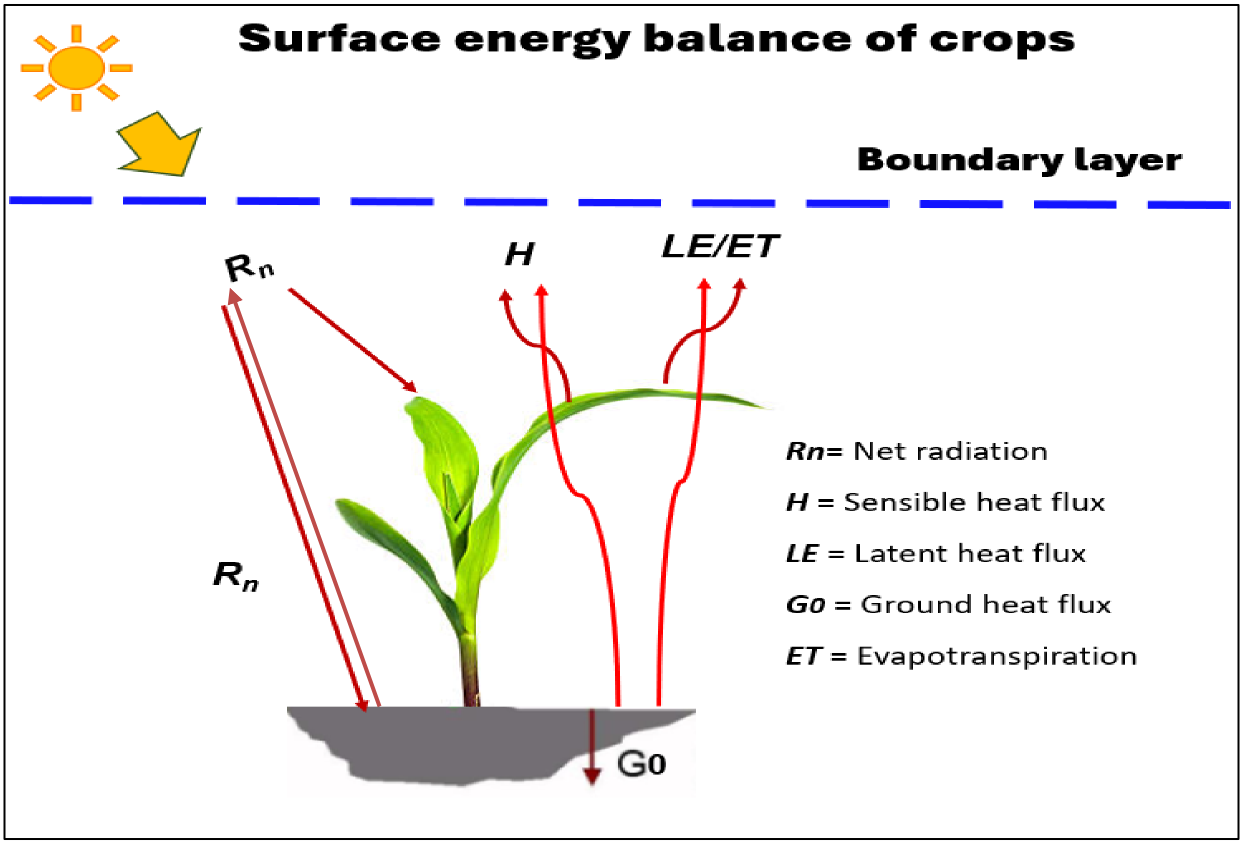

Figure 1. Scheme of the surface energy balance of crops

They also reported that during the early morning (0600-1200 hours) when the canopy is fully developed, the sum of canopy heat storage, soil heat storage and photosynthesis storage terms (energy in the carbohydrate bonds during the photosynthesis) account for approximately 15% and 7% of total Rn for maize and soybeans respectively. Jarvis et al. (1997) stated that in a mature forest, the canopy and soil heat storage fluxes are less than 5% of Rn collectively. Atmospheric CO_2, H_2O, and temperature are directly involved in photosynthesis, plant growth and crop yield. Any imbalance in them can create a situation of negative feedback and affect the plant growth and yield (Lal 2007; Duell et al., 2019). In forest ecosystems, Jarvis et al. (1976) reported that only 1% of net-radiation is utilized during photosynthesis while almost 93% of the radiation is converted into sensible/latent heat flux. Therefore, adding these heat storage term in the SEB equation is important (Foken, 2008; Twine et al. 2000).

There are several methods available to determine the energy balance components, but eddy covariance (EC) is considered the most accepted and widely used direct method to measure *LE* and *H* (Burba 2013). However, EC often underestimates surface energy by 10-30% of the surface energy flux (*Le* + *E*) (Wilson et al., 2002; Twine et al.,2000). Interestingly, in a recent study by Mauder et al. (2024), it was reported that at most FLUXNET sites, EC measurements had an average energy balance closure of 0.85 per site.

Accurately measuring surface energy balance closure remains a major challenge (Wilson et al., 2002; Foken, 2008). Energy balance closure error refers to fluxes measured by EC that fail to account for full surface energy balance. For example, at several agricultural and forest sites, recorded SEB is not closed ($Rn\text{-}G \neq H + LE$) because latent and sensible energy fluxes ($H + LE$) are lower than the available energy ($Rn\text{-}G$) resulting in energy balance closure errors.

Errors in SEB closure calculations can be the consequence of differences in the measurement methods, their interpretation, and comparison with varying model simulations. Therefore, careful consideration of storage terms in SEB components is a very important area of focus to address challenges of SEB and NEE (Leuning et al., 2012).

The energy imbalance (also referred to as residual energy or energy balance closure error) problem from the EC system has been studied extensively by researchers for a variety of vegetation surfaces (Franssen et al. 2010; Barr et al. 2012; Cava et al. 2008; Foken 2008; Wilson et al. 2002). With the EC method, the closure problem or energy imbalance remains an unsolved issue (Wilson et al. 2002; Foken 2008; Franssen et al. 2010; Foken et al. 2011; Leuning et al. 2012; Anderson and Wang 2014; Masseroni et al. 2014; Russell et al. 2015; Gao et al. 2017).

Fixing SEB errors is challenging due to difficulties in the SEB measurement (Foken 2008; Foken et al. 2011; Anderson and Wang 2014), and other sources of discrepancies including ignoring energy storage (Zuo et al. 2011; Leuning et al. 2012; Russell et al. 2015). Other differences are due to the generation of mesoscale eddies (> 2km) caused by energy advection under non-homogeneous landscapes (Mauder et al. 2010; Foken et al. 2011; Stoy et al. 2013; Eder et al. 2015; Gao et al. 2017; Xu et al. 2017) and uncertainties in the measurements by sonic anemometers (Kochendorfer et al. 2012; Frank et al. 2013; Horst et al. 2015). In the case of small canopy vegetation (e.g., wheat), the scale of energy differences varies site to site, vegetation to vegetation, and the fraction of the vegetation cover fraction (Leuning et al. 2012). Furthermore, greater exposure to soil and heat stored in the upper soil layer is also a source of energy closure discrepancies (Foken 1998; Foken 2008). A study on semi-arid land by Yue et al. (2011) found that accounting for heat stored above the soil heat flux plate substantially improved the energy balance closure of grass. Contrastingly, Franssen et al (2010) reported that based on analyses from a station of European FLUXNET sites the storage term has no significant role in the overall energy balance closure.

Aubinet et al. (2012) and Stoy et al. (2013) emphasized that including these storage terms in SEB calculations improves SEB calculation estimates, increases flux measurement accuracy, and improves ecosystem-atmospheric models.

This review evaluates previous studies on storage terms and their role in SEB closure to identify knowledge gaps so that surface-atmosphere exchange can be better quantified and modeled. Our review aims to collect the literature on the storage terms, shed light on their role in attaining energy balance closure, highlight their underestimation, and identify knowledge gaps to enhance our understanding of processes involved in surface-atmosphere exchange e.g. mass energy exchanges. Considering storage terms increases the SEB closure see in **Table 2**.

Conclusion

The literature study reported here highlights the importance of storage terms on the energy balance equation for the agricultural ecosystem to achieve close surface energy balance. Energy fluxes of land surface and atmosphere significantly influenced by the heat storage of canopy and soil. Discrepancies during the calculation of energy balance can be due to overlooking these terms. It also influences our understanding of the responses of crops to climate conditions. Research to estimate accurate heat storage terms and their incorporation are critically important to calculate energy flux precisely which consequently influences modeling and other climate smart strategies. By identifying and quantifying the contribution of storage terms, researchers can upscale the accuracy of the model's work based on surface energy balance.

Table 2. Impact of storage terms on SEB values.

Vegetation type	**Storage term effect on SEB (%)**	**References**
Deciduous forest	+20-50	(Foken, 1998)
Maize and soybean	+6-10	(Meyers, 2004)
Rapeseed	+6	(Pardo et al., 2015)
Bushland	+4-17	(Kutikoff et al., 2019)
Oasis–desert	+3-6	(Xu et al., 2017)

CHAPTER 2: MATERIALS AND METHODS

Abstract

A portable tripod EC tower system has an infrared gas analyzer (IRGA), net radiometer, infrared thermometers (IRs), thermocouples, and 2D- and 3D-sonic anemometers installed 6 m above the soil surface (approximately 2-m above the maize canopy). The setup consists of six thermocouples at heights of 1, 11, 111*, 170*, 210* and 303* cm from the soil surface toward the above canopy for temperature and water vapor measurement (* denote concurrent measurements of water vapor and carbon dioxide), and four IRs: two at the angle of 45° and the other two at 0° angle (Downward direction) at 6-m height above the soil. CO2 and water vapor sampling tubes are of the same length into a switching solenoid. Each height is sampled for 15 seconds; 8-second sampling time and 7-second equilibrium time. The CO2 concentration and water vapor are measured at a frequency of 1 minute, while above canopy wind speed, infrared temperature and thermocouples temperature are measured at the frequency of 5 Hz. Thermocouples provide a temperature profile by height while the IRs provide intra-canopy temperatures; soil heat flux is calculated at a soil depth of 6 cm, and soil T probes are located at 4.5 and 1.5 cm soil profiles.

Experimental Site Location

The current study was conducted in rural Philadelphia, Loudon County Tennessee, USA (longitude: 84.4651 and latitude: 35.6729) **Figure 2.** The Study area was Twenty-three hectares of agricultural land maintained as a maize cropping system. The site has a mean annual precipitation of 132-142 cm and a mean annual temperature of 12-15 °C. At this site, the sunrise varies from 0645 LT to 0740 LT, and sunset varies from 2024 LT to 1840 LT from May to

Figure 2. Map of the experimental site. The yellow pinpoint represents the location of the profile measurements system (source: Google Earth Pro)

October 2023.

The site has significant variation in slope and the current experimental location has a slope of 2-5% shown in **Figure 3**. Similarly, the elevation of the field varies between 280m to 250m, and the experimental site has elevation of 280m as shown in **Figure 4**. The soil belongs to the Alcoa Loam series and is classified as fine, thermic Rhodic Paleudult according to the USDA-NRCS (2018). The parent material of soil is residuum. (**Figure 5**)

Summary of Experimental Site Activities

The corn was planted on 25 April 2023. The tillage practice was vertical tillage on the site. The crop was planted with east-west row orientation with the inter row width of 30 inches. The plant population was counted biweekly, and at the end, the mean plant population was taken and found to be 74,000 plants/ha. During the summer, the prevailing wind comes from the southwest, while in winter, it comes from the northwest. The crop was harvested in the middle of October 2023.

Figure 6 represents the dynamics of sampling heights from which the CO_2 and H_2O measurements were made and used to calculate the storage terms. The h represents maize canopy height above the soil surface. The red line represents to height 1 which is at a height of 0.11m from the soil and constant throughout the growing season. The green line represents height 2 (h2) which is 0.5 (50%) m of plant height. The blue line represents height 3 (h3) 1m above the plant canopy and the purple line 4 (h4) is 2 m above the canopy height. Note that one height was permanently set at 0.11 m and the three other heights were adjusted as the crop grew. Sampling intake tubes were positioned on a 10-m steel mast at the respective positions. Air intake sampling tubes for CO_2 and H_2O, and thermocouples for temperature are mounted at the same height

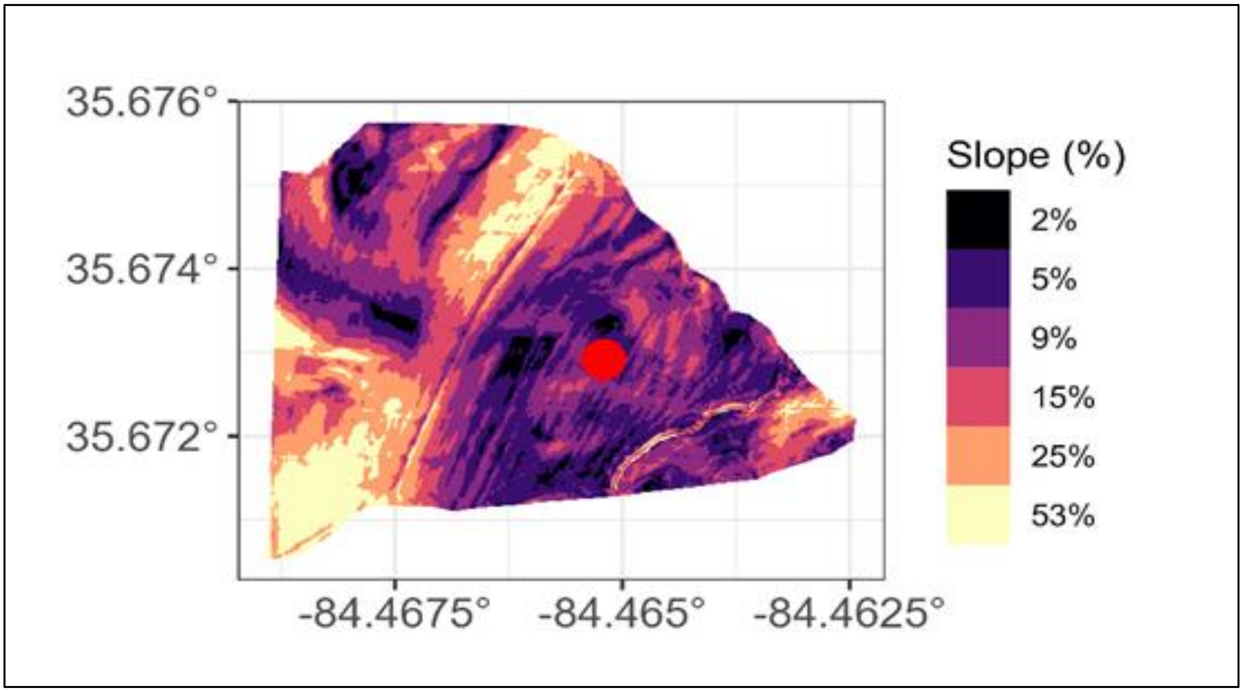

Figure 3. Slop of experimental site. The red point shows the location of instrumentation in the field.

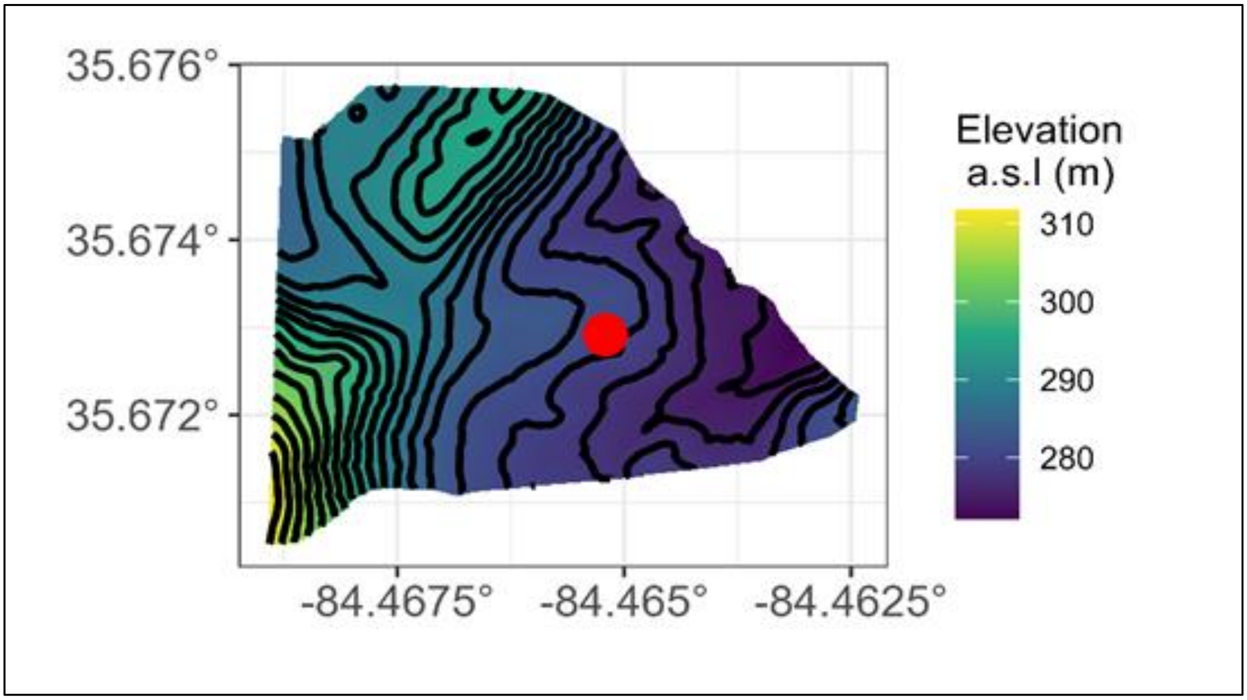

Figure 4. Elevation of experimental site. The red point shows the location of instrumentation in the field.

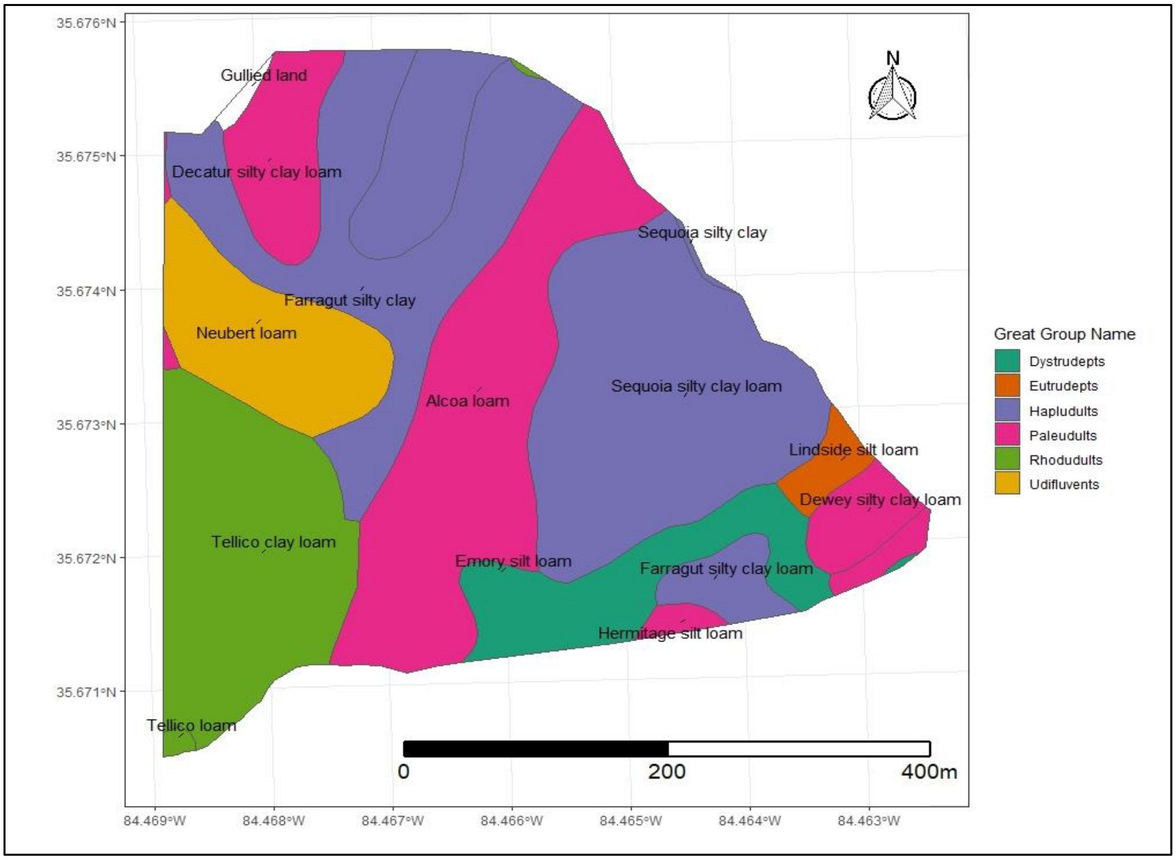

Figure 5. Soil series and surface texture overview of the experimental site.

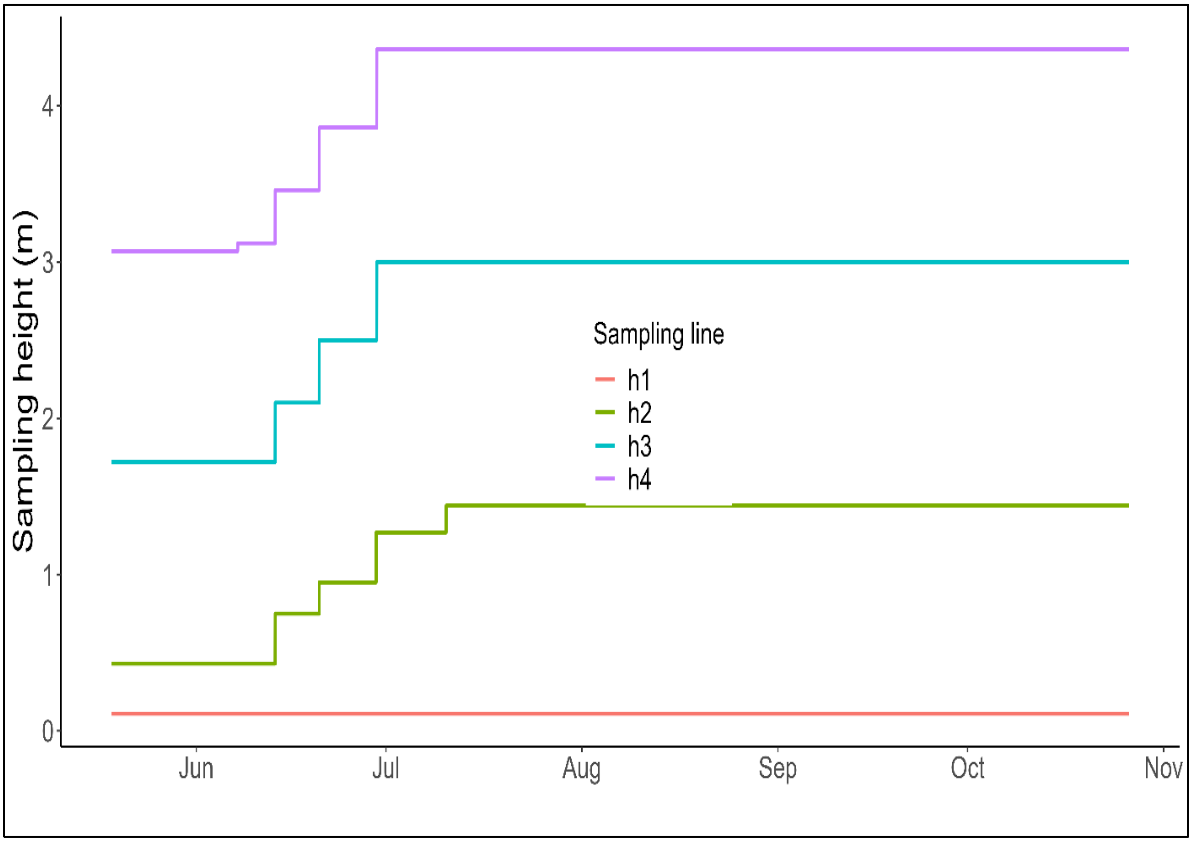

Figure 6. Dynamic of measurement heights throughout the study period.

within and above the canopy. Summary of the events accounted over the site during the complete growing season of maize are shown in **table 3 and table 4**.

Fluxes and Storage Terms Calculation

Carbon dioxide (CO_2) fluxes

Carbon dioxide is one of the most important variables because it is the main driver of NEE (photosynthesis and respiration). The flux can be calculated as:

$$F_{co2} = \rho_m \overline{w' c_{co2}'} \qquad (2)$$

Where ρ_m is the air molar density and $\overline{w'c'}$ is the covariance between the vertical wind speed (w) and the CO_2 concentration. The measurement unit is $\mu mol\ m^{-2}s^{-1}$.

Water Vapor (H_2O) Fluxes

The amount of water vapor exchanged. The flux can be calculated as

$$E_{h2o} = \rho_m \overline{w' c_{h2o}'} \qquad (3)$$

where ρ_m is the air molar density and the $\overline{w'c'}$ is covariance between the vertical wind speed (w) and the H_2O concentration. The measurement unit is $mmol\ m^{-2}s^{-1}$.

Latent Heat (LE) Fluxes

Latent heat flux is the amount of energy that is transferred due to the evaporation of water vapor. In fact, it is directly connected to the H_2O flux and can be calculated as:

$$LE = \lambda E \qquad (4)$$

where λ is the latent heat of vaporization of water and E is the H_2O flux (evaporation). The unit of measurement is W/m^2.

Sensible Heat (H) Fluxes

The sensible heat flux is the amount of energy exchanged as heat. The heat energy can

Table 3. Summary of the events accounted over the site during the complete growing season of maize.

TIMESTAMP	Events
04/20/2023	Plantation
05/11/2023	Measurement setup
05/18/2023	IRGASON installed at height of 163 cm
05/18/2023	Profile height adjusted (1st Bowen Ratio adjustment)
06/01/2023	Profile system raised
06/06/2023	IRGASON adjusted at height of 262 cm
06/06/2023	RMYOUNG-wind monitor adjusted at height of 533 cm
06/06/2023	RMYOUNG- wind monitor adjusted at height of 738 cm
06/07/2023	2nd time Bowen Ratio adjusted
06/07/2023	IRs height adjusted
06/07/2023	Thermocouples 2 & 4 replaced
06/13/2023	IRGASON adjusted at height of 295 cm
06/20/2023	IRGASON adjusted at height of 362 cm
06/29/ 2023	IRGASON adjusted at height of 413 cm
07/14/2023	LAI (5.667)
07/24/2023	LAI (5.431)
08/08/2023	LAI (5.151)
09/05/2023	LAI (3.638)
10/13/2023	Harvested

Table 4. Summary of events related to IRs throughout the study period.

TIMESTAMP	Angle to plant canopy	Direction	Distance from center (cm)	Distance from Each other (cm)	Distance from soil (cm)
05/18/2023	90	E	50	100	328
05/18/2023	90	W	50	100	328
05/18/2023	45	N	278	556	328
05/18/2023	45	S	278	556	328
06/07/2023	90	E	50	100	430
06/07/2023	90	W	50	100	430
06/07/2023	45	N	278	556	431
06/07/2023	45	S	278	556	428

be transferred through the movement of air masses. The sensible heat flux can be calculated as:

$$H = \rho_a c_p \overline{w'T'} \quad (5)$$

Where ρa is the air density, c_p is the air heat capacity and the $w'T'$ is covariance between the vertical wind speed (w) and air temperature (T). The measurement unit is W/m^2.

Storage terms (Jc)

Storage terms/fluxes of scalar quantities (CO_2, water vapor, etc.) were calculated using the ICOS methodology (Montagnani et al., 2018) using the Eq.5. For the case of CO_2,

$$J_c = \overline{\rho_d} \sum_{i=1}^{N} \left(\frac{\Delta c}{\Delta t} \right)_i \Delta z_i . \quad (6)$$

Here, J_c is the storage term of CO_2 within the i_{th} layer over which Δc is measured, Δc/Δt is the molar density at height i_{th} over time period Δt. Δz_i is the thickness of this layer and Δt is the measurement time step; $\bar{\rho}_d$ is dry air density, and N is the number of layers (number of measurements points).

Soil Heat Storage (ΔS)

The soil heat storage (SHS) is calculated on the base of soil temperature (T) and volumetric heat capacity (C) using this relationship.

$$\Delta S = C \ (\Delta T/\Delta t) \ z \times 1 \times 10^6 \quad (7)$$

Where ΔS is change in heat storage above the soil heat flux plate ($W \ m^{-2}$), z is the reference depth to where heat flux is measured (0.06 m), ΔT is the change in soil temperature above the heat flux plate take from the average of soil temperature measurement at 0.015 m and 0.045 m depths, Δt is the time step (s). C is calculated by using this equation:

$$C = C_m (1 - \phi_f) + C_w \times \theta \tag{8}$$

C_m is the volumetric heat capacity of soil (2.35 MJ m^{-3} K^{-1}) and C_w is volumetric heat capacity of water (4.14 MJ m^{-3} K^{-1}). θ soil volumetric water contents (m^3 m^{-3}) measured by the soil moisture senser. φ_f soil porosity which is calculated by the following equation:

$$\phi_f = 1 - (\rho_b / \rho_s) \tag{9}$$

P_b is soil bulk density (Mg m^{-3}), P_s particle density (Mg m^{-3}).

CHAPTER 3: DEVELOPMENT OF MULTIPORT SYSTEM TO MEASURE VERTICAL FLUXES

Abstract

Significant studies evaluated the temporal exchanges of CO_2, H_2O, and heat. However, few studies explored variation in the spatio-temporal scales to monitor these fluxes between vegetation and atmosphere. We develop a multiport instrument to measure air samples from four different heights using an Infrared Gas Analyzer (IRGA). After testing in the laboratory, the instrument was deployed to measure [H_20], [CO_2], and heat from air over the maize field in eastern Tennessee. The dataset collected from this system was further used to calculate different types of storage terms using ICOS and EC methodology.

Introduction

In the last few decades, significant work has attempted to enhance our knowledge to understand the gas exchange between soils, plants, and atmosphere. These improvements have been incorporated into land-surface models and numerically-based weather prediction as well as into assessment of atmospheric fluxes of carbon dioxide (Lamas Galdo et al., 2021), water vapor (Wang et al., 2023), and heat over vegetated landscapes (e.g., Hoeltgebaum and Nelson, 2023). Eddy covariance (EC) is a widely accepted method to measure the turbulent fluxes of CO_2, H_2O, and heat in the ecosystem (Nicolini et al., 2018). Routine EC measurements are now made at more than 1000 locations globally (Fluxnet; Pastorello et al., 2020).

At most forest experimental sites, the measured energy budget is not always close to the balance expressed by the familiar relationship:

$$R_n - G = H + LE \quad (11)$$

where R_n is net radiation, G is ground heat flux, H is sensible heat flux and LE is latent heat flux (q.v. Wilson et al., 2002).

An important factor that emerged from forest ecosystem studies is that the storage term contributes to the forest's energy closure and influences quantification of evapotranspiration (McCaughy and Saxton, 1988; Hoeltgebaum and Nelson, 2023). Storage measurement is challenging due to temporal changes in CO_2, H_2O, and heat (Varmaghani et al., 2016). Globally, less than 30 % of studies apply a profile measurement method to calculate the temporal variations in storage terms (Papale, 2006). Many studies reported that the energy balance closure is an unsolved problem for a variety of vegetation types: the sum of latent and sensible heat fluxes were found to be 10-30% lower than the available energy (Twine et al., 2000; Wilson et al., 2002; Leuning et al., 2012; Russell et al. 2015; Liu et al. 2017; Raza et al., 2023).

There are number of possible reasons for energy balance closure errors resulting from EC experimentation, such as neglecting the canopy and soil storage terms, loss of high- or low-frequency flux components, non-optimal coordinate rotation, and the use of inappropriate averaging times (Massman and Lee, 2002; Meyers and Hollinger, 2004; Oetting et al., 2024). A standardized method for measuring these variables is needed.

In the case of agricultural systems, storage terms are usually considered small and are often ignored (Nicolini et al., 2018; Raza et al., 2024). Assessments of storage terms within agricultural ecosystems are few and differ from those documented by researchers in the case of forest ecosystems studies (Wilson et al., 2002; Mayocchi and Bristow, 19950). Most results of heat storage in forest environments focus on the atmospheric component of the total heat storage term.

Quantifying storage terms is challenging because measurements are required both within and above the canopy and is costly to develop a system to measure them (Yang et al., 1999).

Finnigan (2006) reported that the atmospheric heat storage term is underestimated when the average sampling time is large. Neglecting canopy storage terms in studies of Net Ecosystem Exchange (NEE) can also cause substantial errors in NEE (Raza et al., 2023). To understand the role of the storage terms in energy balance closure and NEE, new measurement and analysis approaches are required (Irmak et al., 2014).

This chapter describes a measurement system specifically designed to provide observations for assessing the quantities contributing to the diurnal CO_2/heat and H_2O cycles. A complete maize growing season from planting to harvest was selected to coincide with measurement procedures following the recommendations of FLUXNET (Wilson et al., 2002) and ICOS (Montagnani et al., 2018). Therefore, it is very important to develop a predictive system to better understand the exchange of CO_2, heat and water flux in the ecosystem. The objective of this chapter is to produce evidence of the EC process by showing a lag between different heights and the level of CO_2 that changes with time following sunrise.

Material and Methods

Apparatus Design and Operation

Those variables which are difficult to measure impose unique technical requirements for field experiments. As measurement systems become more complex, continuous data recording is likely to be interrupted resulting in data gaps due to multiple common and unique problems. Based upon our experiments, these problems can include solar power or battery failure, snakes and mice in equipment boxes, chewed wires, rats digging up wires, lightning, etc. (e.g., O'Dell et al., 2014; Hicks et al., 2020). Our eight field experiment sites (in Lesotho, Zimbabwe, Tennessee, and Ohio) have demonstrated the need for a reliable yet technically simple system to measure gas exchange within and above a growing crop (O'Dell et al., 2014; Hicks et al., 2022). To satisfy the basic requirements for time continuity and reliability of the data record, we developed a multi-port sampling system. The intent is to facilitate the routine acquisition of temperature, humidity, and carbon dioxide data within and above a crop canopy.

The analysis of the recorded observations requires attention to gradients of the variables measured as well as to the variables themselves. To avoid consequences of individual sensor offsets when gradients are computed, the new system is designed to use a single detection system, in this case an infrared CO_2/H_2O gas analyzer (IRGA; LI-COR-850, Lincoln, NE). In the application considered here, the system was used to measure flux at four heights within and above a maize canopy.

The system is designed to maintain continuous airflow through all intake tubes, to cycle through all four measurements in one minute (7.5 seconds for each height; 4.4 seconds to achieve equilibrium by IRGA and 3.1 seconds for sample analysis by IRGA) and to minimize the switching time between samplings. The system consists of two small pumps [Model TD-3LSA, Brailsford & CO., Inc. Antrium. NH, USA], one pump (purge pump) draws in the sampling air to maintain constant flow through all intake tubes to minimize hygroscopic interactions along the tube walls while another pump pulls the air through the IRGA. The sampling pump is mounted close to the IRGA so that air smoothly enters the IRGA at ambient pressure. During sampling, the airflow through a specific tube was maintained at the rate of 1000 ml min^{-1}. The flow rates through the other three tubes are then maintained at 700 ml min^{-1} by flow meters [LZQ-7 flowmeter, 101.3 KPa, Hilitland, China]. The switching between sampling tubes is controlled by four three-way brass and stainless-steel solenoid valves [231Y-6, Ronkonkoma, NY, USA].

Each sampling tube is 10.5 m long to ensure that each sampling height has the same transit time. The purge pump manifold and all sampling tubes are of the same kind of urethane [BEV-A-LINE, Polyethylene material, Cole Parmer, City, State]. Before passing through the analyzer, the air is passed through a 1-µm pore filter [LI-6262, LI-COR, Lincoln NE, USA] to avoid the accumulation of debris, dirt, particles, etc., that can cause contamination in the analyzer optical cells. The air outlet of the purge pump and IRGA are open directly to the atmosphere. The 5Hz (5x/second) frequency raw data were averaged into 15-minute runs.

Sampling time

The performance of the system for measurement of CO_2 and H_2O profiles was examined before its field deployment. The apparatus was first flushed with nitrogen (N_2) gas to create a carbon dioxide free environment. Subsequently, a known concentration of CO_2 (430 ppm) at ambient pressure was fed through the intake tubes and system outputs were measured. This process allowed determination of the minimum amount of time to reach a stable measurement reading. The laboratory tests showed that after the IRGA received the known [CO_2], it took approximately 1.8 seconds to achieve a steady output. During the laboratory evaluation period, the recorded error was less than 0.5% in [CO_2] between sampling heights. An accuracy error of less than 1% is well within the acceptable range for the IRGA now used according to the specifications provided by the manufacturer and much less than higher errors common in these types of measurements (Montagnani et al. 2012). **Figure 7** presents a schematic description of the apparatus.

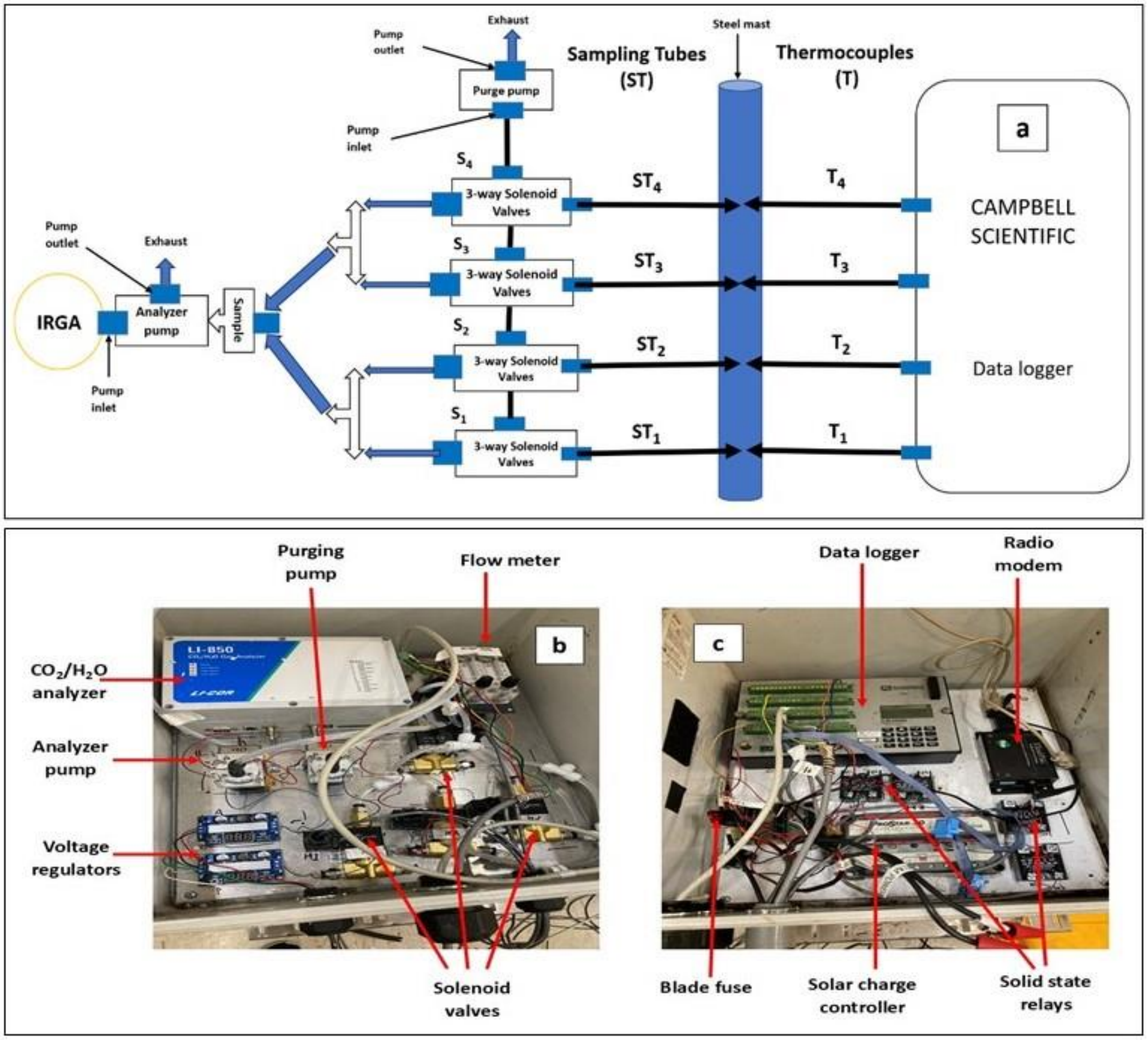

Figure 7. Details of the multi-port sampling system: (a) schematic diagram of the manifold for profile sampling of CO_2 and H_2O, (b) a photograph of the analyzer, pump, and manifold system, (c) the data logger for data collection.

Field Measurement Setup

The maize crop was planted on 25 April and the field instrumentation was installed one week later. Four intake sampling tubes were positioned at heights (m) of 0.11, 0.5h, 1+h, and 2+h, where h is the maize canopy height above the soil surface. Note that one height was permanently set at 0.11 m and the three other heights were adjusted as the maize grew. The sample intake tubes were positioned on a 15-foot-long steel mast. Thermocouples at the same height were mounted to measure temperature and were aspirated within a white PVC pipe shield of 1.9 cm diameter (**Figure 8a, b**) that also served as a radiation shield.

To provide the measurements necessary to interpret the gradient observations, a tripod tower was used to support the EC system and supporting micrometeorological measurements — an IRGASON [CO_2/H_2O] open path gas analyzer system, [Campbell Scientific, Logan, Utah], a net radiometer [Kipp & Zonen, OTT HydroMet B.V. Delft, Netherlands], infrared radiometers [IRs-S1-111-SS, Apogee Instruments Inc, City, State, USA], and type T thermocouples [Omega, City, State, USA]. The system was visually inspected every week for any leakage, condensation, and contamination. **Figure 9a, b** represents field setup to collected the data from vegetation stage to harvesting stage.

Results and Discussion

Vertical Profile of [CO_2]

Figure 10 presents average diurnal cycles of [CO_2] measured from May to October at four heights, two within the canopy and two above. Different colors correspond to different measurement heights. CO_2 variability was found to be higher at nighttime than in daytime. The greatest variability was recorded within the canopy at height 1 (0.11 m) and height 2 (0.4 – 1.4

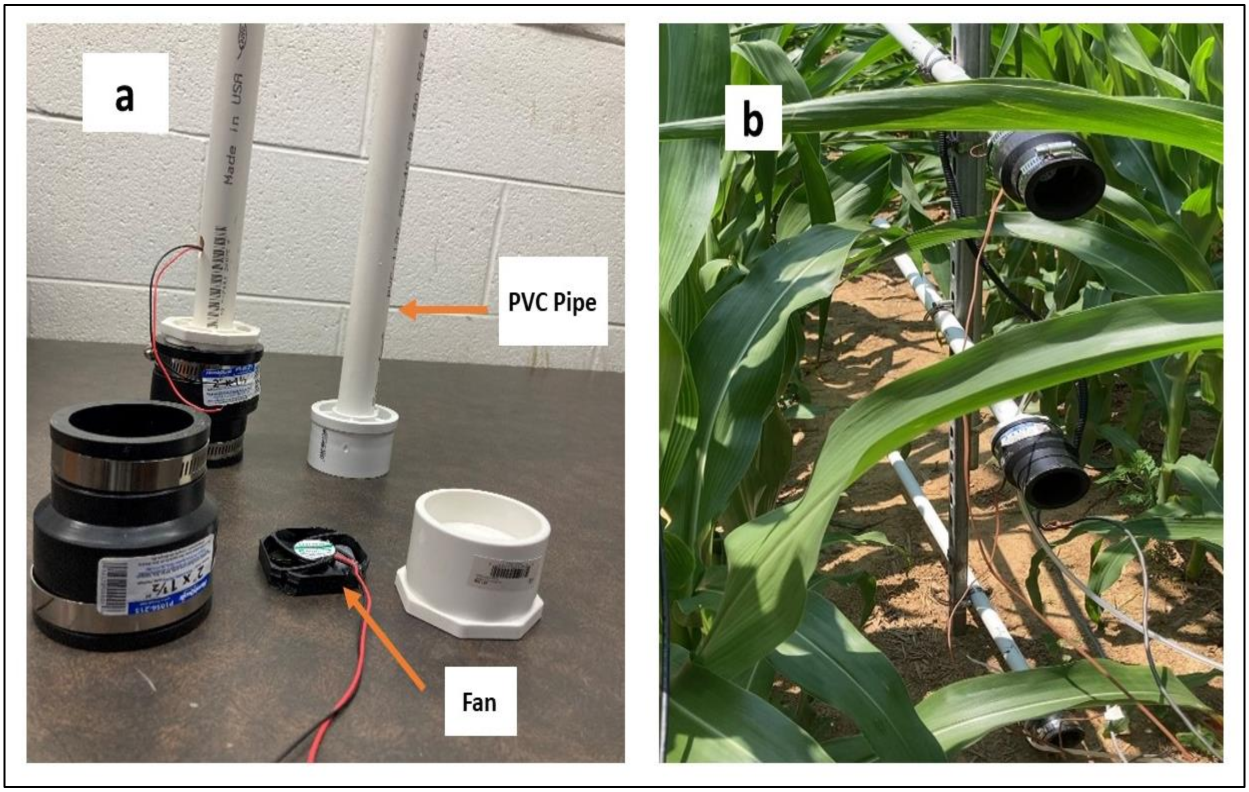

Figure 8. (a) Installation components at each height of the new profile system, showing the aspirated CO_2 intake tubes and thermocouples. (b) Deployment in a maize canopy; the two lowest heights are shown.

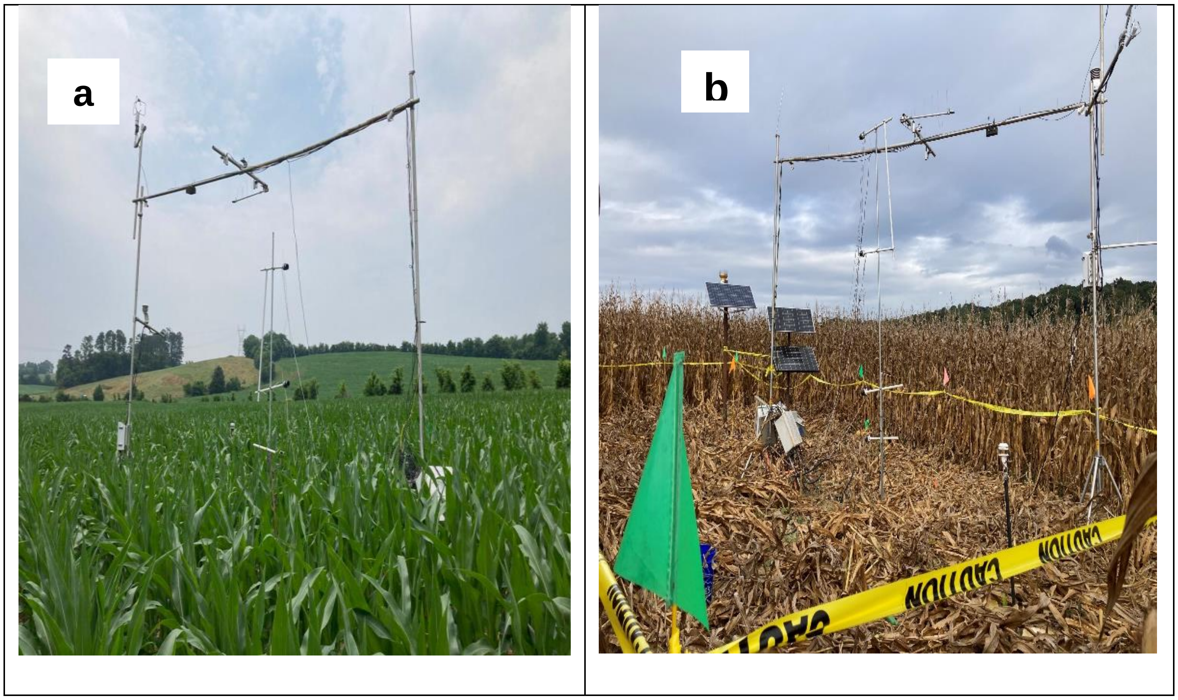

Figure 9. Field setup: Vegetation stage (a) to harvesting stage (b).

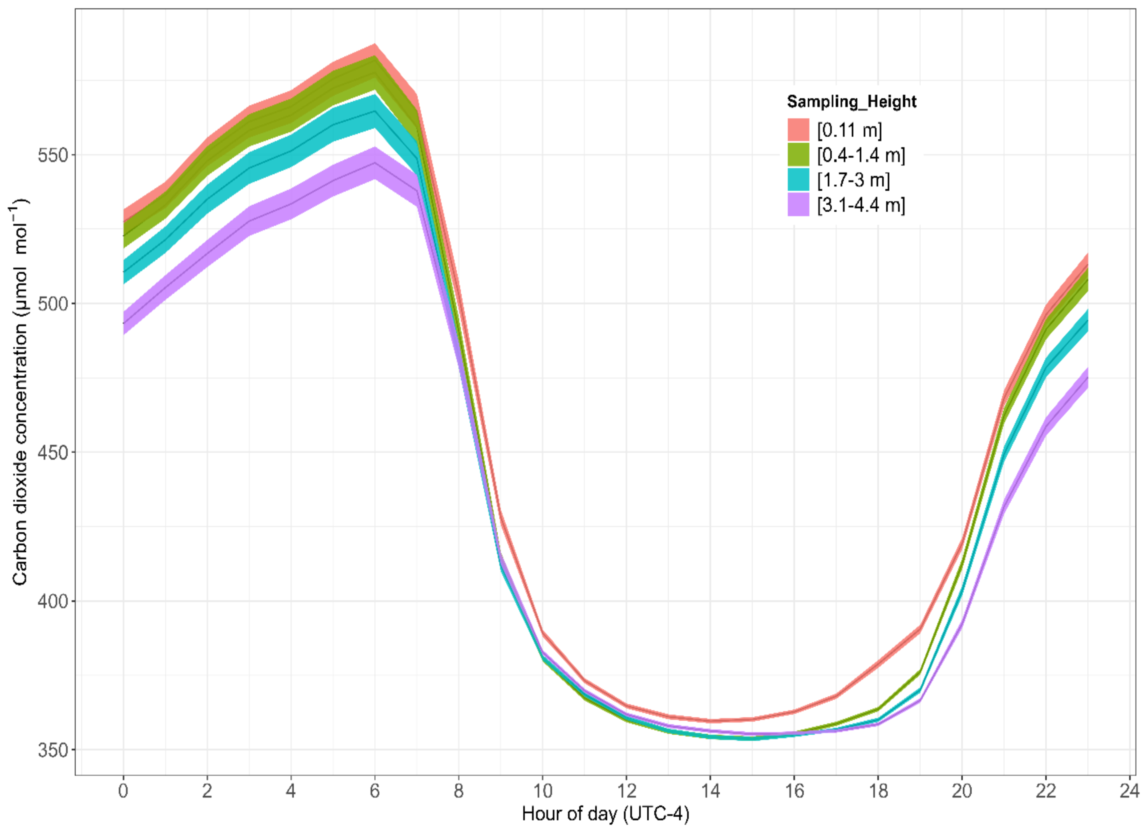

Figure 10. Average diurnal [CO_2] cycles over a complete maize growing season.

m).

During the night, the surface atmosphere often stabilized, and wind speeds decreased, allowing CO_2 emitted from the soil to accumulate. Hicks et al. (2021) also stated that during stable nighttime conditions, the [CO_2] increases at the surface. The concentrations of CO_2 observed below the canopy exceeded those elsewhere. Moreover, note that the increasing concentrations within the pool closely paralleled each other, providing support for the assumptions made elsewhere about CO_2 profile linearity.

About the average time of sunrise (0600 LT), the CO_2 average concentrations dropped rapidly as convection started to mix surface air with the overlying atmosphere and as photosynthesis commenced. At all heights, this initial decrease was followed by a more rapid loss rate until concentrations dropped to about 350 ppm in the afternoon (1200 to 1800 LT), much lower than ambient concentrations (~ 428 ppm), thereby reflecting the efficiency with which the maize crop extracted CO_2 from the air. Near sunset, [CO_2] started to increase and continued to build until reaching maximum values immediately before dawn. Concentrations within the canopy do not differ significantly, although the 0.11 m height values always exceed those higher above the soil surface. In general, [CO_2] decreased with increasing height.

The nocturnal accumulation of CO_2 observed here is not unusual. In many climatic regions, nighttime soil temperatures remain high enough to sustain microbial and soil respiration activities, resulting in CO_2 accumulation in the stratified air above the ground. After the sun rises, increased light intensity promotes higher photosynthesis rates.

Vertical Profile of [H_2O]

Figure 11 shows the average diurnal cycle constructed from 15-minute [H_2O] observations. At all heights, a sharp increase in [H_2O] was recorded in the morning at the same time as the sudden decrease for [CO_2] seen in **Figure 10**. Subsequently, [H_2O] peaked at about 0900 LT and, within the canopy maintained this concentration throughout the daylight hours. Above the canopy average concentration decreased and lower concentration constancy was attained. After the period around sunset had passed (about 2000 LT), [H_2O] started decreasing approximately linearly with time until sunrise approached. The [H_2O] generally decreased as the measurement height increased for both day and night because a constant source of water vapor was the soil surface, with crop evapotranspiration adding H_2O in the daytime and dewfall near sunset.

Figures 10 and **11** reveal considerably different cycles of CO_2 and H_2O. At night, **Figure 10** shows a more striking [CO_2] gradient than does **Figure 11** for [H_2O]. The reason is presumed to be that CO_2 continues to be emitted from the soil at night, whereas there is no parallel process influencing H_2O concentrations. This is a feature made apparent by the profile sampling system. In the daytime, there is little consistent [CO_2] gradient information derived from **Figure 10**, but for [H_2O] in **Figure 11** there is a clearly visible [H_2O] gradient structure. This suggests a slow-down of CO_2 exchange in the afternoons while evaporation continued.

Dew formation is another process that influences the [H_2O], especially during night and early morning hours due to the radiative cooling effect. During these times, due to radiation cooling, the surface temperature decreases, and vapor condenses as the temperature of the surface drops below the dew point. Sufficient water vapor in the air and radiation cooling are the

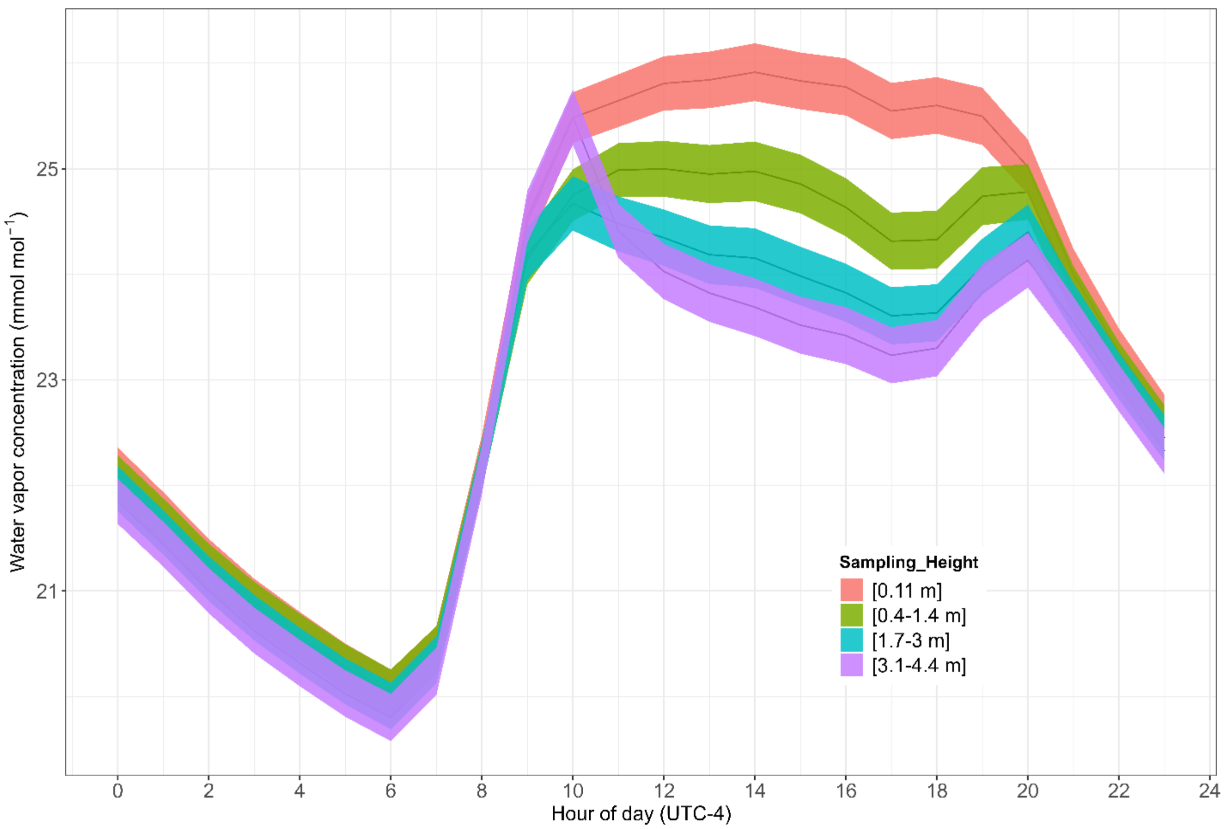

Figure 11. Average diurnal cycle of [H_2O] over a complete maize growing season.

two main requirements for dew formation. Wind speed, air humidity, and clearness of sky are also important factors that play a role in the dew formation. In short, dew formation reduces the [H_2O] in the air.

Vertical Profile of Temperature

Figure 12 represents the average temperature cycle over the complete maize growing season at a scale of 24 hours. It illustrates how temperature varies within the canopy of maize. Different colors indicate temperature variation at different sampling heights within the canopy. Generally, similar temperature trends were reported at all measurement heights. However, the maximum temperature was recorded during midday between 1400 LT and the minimum during the nighttime and in the morning. Interestingly, a higher temperature was recorded at a height of 0.4-1.4 m, which may be due to water vapor accumulation and/or absorption of heat in the water vapor. Minimal temperature difference at different heights suggests canopy ventilation and the effect of wind mixing. The diurnal cycle of temperature trend highlights the role of *Rn* in developing the microclimate within the canopy and temperature variations.

Conclusion

We developed a multiport system by following the ICOS method (Montagnani et al., (2018) to obtain reliable and accurate vertical profiles of [CO_2], temperature, and [H_2O] within and above of a maize canopy. The new multi-port profile system demonstrated its effectiveness in the measurement of CO_2 and H_2O concentrations at different heights. CO_2 concentrations were recorded greater during late night and early morning until 0600 LT. H_2O concentrations were significantly higher during the daytime compared to nighttime, peaking between 1200 LT and 1400 LT and then gradually decreasing. The multiple-height profile system aided substantially to

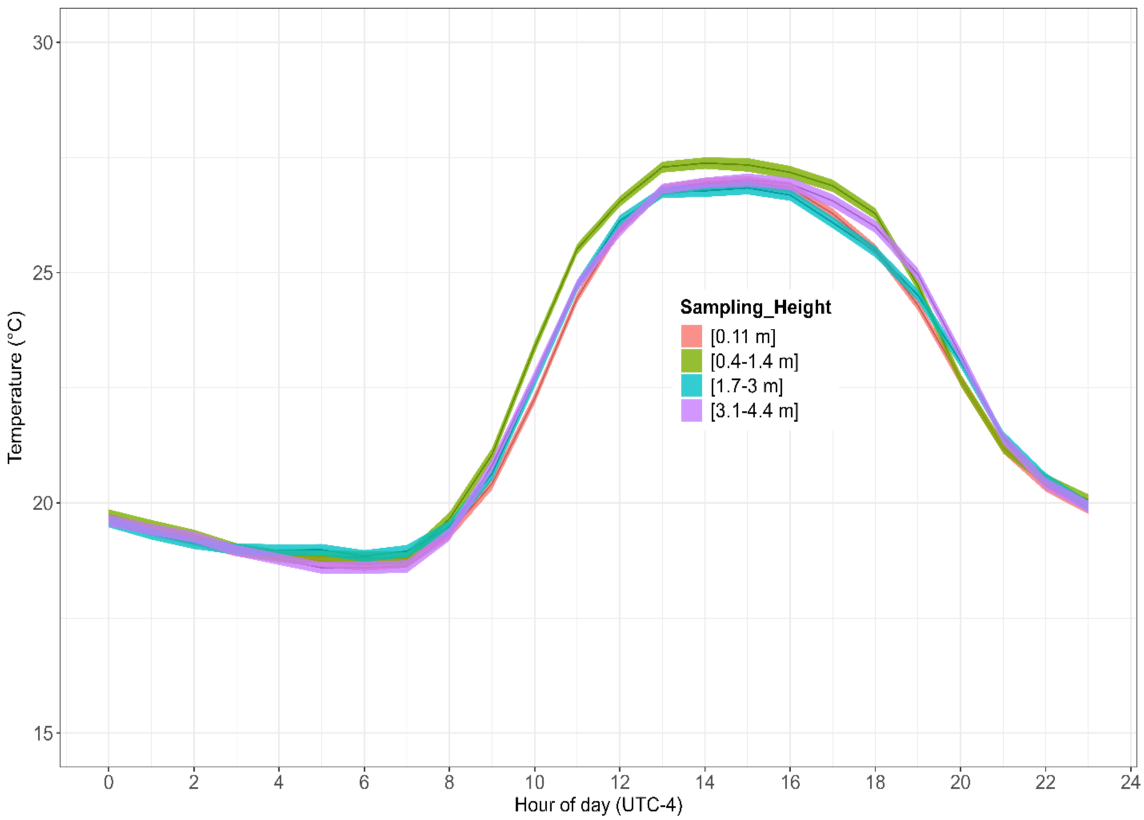

Figure 12. Average diurnal cycle of temperature over a complete maize growing season.

understanding CO_2 and H_2O concentration variations and their vertical profiles, thereby facilitating reliable assessments of their exchanges, storage, and overall balance within the growing maize ecosystem. This can be used to measure CO_2 and H_2O gradients over forest or bare soil by just modifying the height of the intake tubes.

CHAPTER 4: MEASUREMENT OF ENERGY BALANCE COMPONENTS OVER MAIZE

Abstract

For many types of land surfaces, imbalances in the surface energy balance (*Rn-G* ≠ *H*+*LE*) are a concerning issue. Usually for most agricultural crops surface energy balance studies, the role of canopy storage terms derived from canopy water contents, plant biomass, canopy heat storage (*LE* and *H* heat storage) and PE is neglected. Furthermore, the amount of heat stored above the ground heat flux plate is also not included in the surface energy balance closure equation. ICOS (Integrated Carbon Observation System) methodology was used to determine the energy storage terms and the Ochsner et al. (2027) correction was applied to correct the soil heat flux measurement. Our results showed that the maximum value found for canopy storage (20 W m^{-2}), and photosynthesis heat storage (18 W m^{-2}), latent energy storage (8 W m^{-}2), and sensible heat storage (2.5 W m^{-2}) during the daytime between 0900 LT and 1100 LT (local time). These values were significantly reduced during the nighttime.

Introduction

Both a rapid growing population and climate change are impacting agriculture globally resulting in changes in cropping patterns (O'Dell et al. 2020; Syed et al. 2022). Changing cropping patterns influence crop yield and water budgets due to shifting atmospheric [CO_2] levels and altering precipitation patterns (O'Dell et al. 2019; Brye et al. 2000). Globally, the temperature of the earth is projected to increase by ~4°C and CO_2 concentration will reach 540–970 ppm through the 21st century if greenhouse gas (GHGs) emission trends stay the same. Temperature and CO_2 are the two main factors which drive the global carbon cycle and agricultural yield (Prueger et al. 2004; Reiners 1968; Edwards 1975). However, naturally increasing [CO_2] has positive effects on crop yield because elevated levels of [CO_2] increases photosynthesis and decreases plant water requirement by limiting transpiration (Walker et al. 2021; Gray et al. 2016). Conversely, higher temperature increases the water requirement, causing drought and stress conditions that reduces growth and yield globally (Lobell et al., 2014; Rahimi-Moghaddam et al. 2018).

Micrometeorological methods are considered the most valid methods for measuring the direct response of plants to unmodified environmental conditions in the field. In micrometeorology, EC (direct method) and BREB (indirect method) are the most used methods to measure turbulent flux of CO_2, Heat and H_2O, and their exchanges (Brotzge and Crawford 2003; Alfieri et al. 2009; Sinclair et al. 1975; Chávez et al. 2009). However, most of the turbulent fluxes and gradients measured by these methods are not included in the surface energy budget when summing up available energy (Foken 2008; Moderow et al. 2009; Foken et al. 2010; Franssen et al. 2010; Mauder et al. 2010; Higgins 2012). For instance, heat storage terms (whether within canopy or in soil) receive less attention in such studies. According to Foken (2008), the extent of error associated with different vegetation surfaces can reach as high as 20-50% for storage terms. A 20-50% error can occur for ground heat flux (*G)* measurements without considering soil heat storage, 5-20% for *H*, 5-20% for *LE* and 5-20% for *Rn*. Studies reported that storage terms are consistently smaller in agricultural crops (often neglected) than forest ecosystems because agricultural ecosystems have less biomass, less complex canopy structure, and short vegetation exposed to sun and wind. Underestimating storage terms during energy balance closure studies can be a major reason for imbalances (Meyers, 2004; Varmaghani et al., 2016). Moreover, the advection and/or convection of heat and water is not often measured by traditional methods but are important when modeling *ET* over irrigated agricultural fields and especially in rainfed agriculture (Figuerola and Berliner 2005; Alfieri et al. 2012; Tanny et al. 2008). Therefore, it is important to find an alternative way to consider the advection and/or convection.

To better understand the process of water usage requires that we understand what influences evaporation and how it can be best measured (Bowen, 1926). Within the canopy airspace, convection heats the leaves, and when a spot on the leaf gets hot enough a buoyant cell is generated, and convective heat transfer starts (Defraeye et al., 2013; Bailey and Meneses, 1995). While details of this physical behavior remain obscure, this interaction changes continuously with height and time. When the sun rises, the air within a plant canopy will gradually warm and rising eddies will start to develop, all within the canopy airspace. This process would be evident by recording temperature within the canopy but probably only with high frequency measurements (Hicks, 1988). From an agricultural point of view, it is very important to understand the flux-gradient relationships because these relationships are needed to quantify the rate of water loss and to study the flux gradients between the crop and the air. This is important to the agricultural community because there is a growing need to conserve H_2O. Our aim is to explore these matters in a growing maize crop. The case of the maize canopy is of special interest because it is important to develop improved methods to manage grain production. There is an opportunity to explore matters that have otherwise been dominated by forest meteorologists at many different scales.

Micrometeorological approaches such as BREB and EC are the scientifically accepted techniques to calculate the flux gradient from a vegetated field and surrounding atmosphere (Oetting et al. 2019; Oetting et al. 2020; Irmak et al. 2014). For this study, a profile system was developed to investigate the exchanges of CO_2, heat, and H_2O from maize fields to the atmosphere by partitioning into below- and above-canopy profiles. Further, observations have been used to compute storage terms and overall energy balance closure of maize.

Results and Discussion

Plant Biomass, and Water Content

Figure 13 shows the trend of maize fresh and dry biomasses, and water content loss throughout the complete growing season. Color represents the variable, and the error bar represents +/- one standard error of the mean. Fresh biomass is an important parameter of the plant which indicates the potential growth of the plant and its interaction with plant water contents. Fresh biomass (blue line) corresponds to the total plant biomass including water. The plant fresh biomass was found lowest during the early season and rapidly increased by reaching the highest of 1200g per plant in August 2023 after that started decreasing slowly reaching 600g per plant in mid-September and then becoming constant. The period from June to August is the time when plants are in their rapid growth stages. The decreases in fresh biomass after August indicate that plants reached senescence and plant growth stopped. Additionally, at this stage, the water loss from the plant becomes highest which is the reason for lower fresh biomass.

The red line in the graph represents the maize dry biomass. It is the actual plant biomass. It can be seen in the graph that the dry biomass increased gradually and achieved maximum biomass of 450g per plant in September 2023. The dynamics of dry biomass are opposite to the fresh biomass and water contents because it represents the actual plant biomass and accumulation of resources. Reaching the highest in September indicates that plants reached

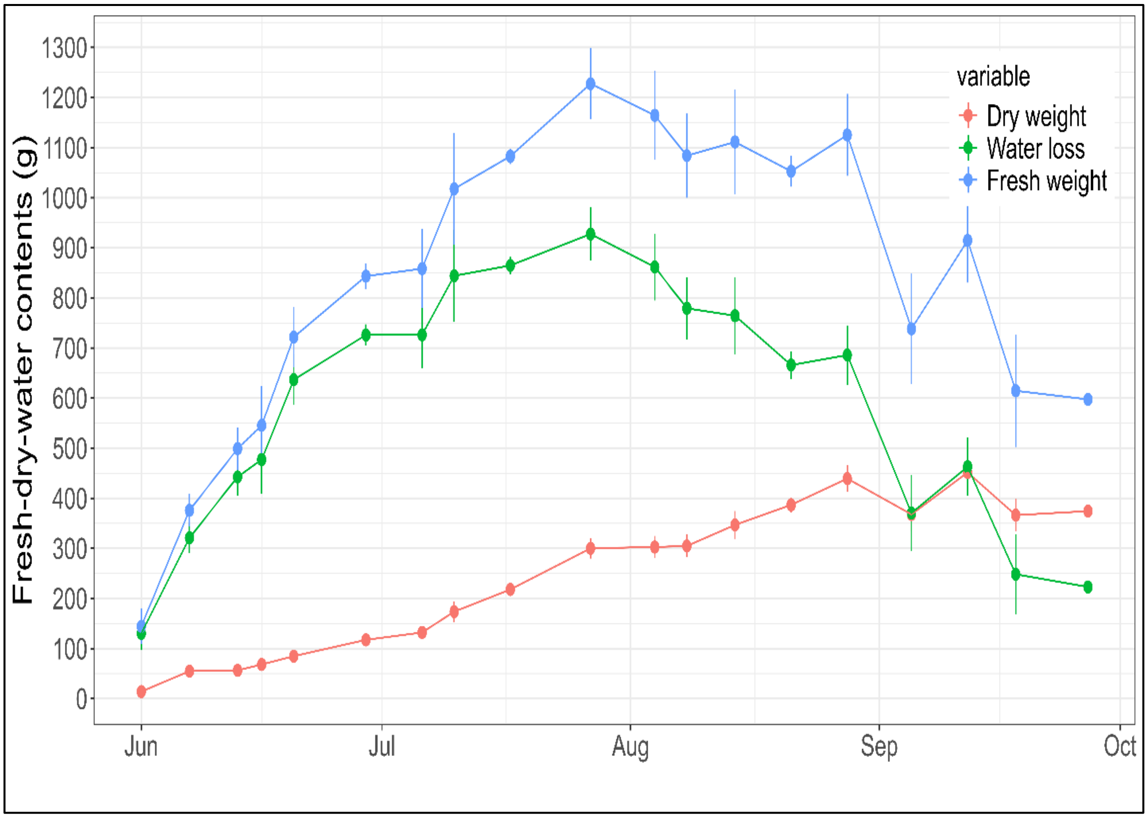

Figure 13. Average fresh, dry and water contents of maize.

maturity where the process of photosynthesis and uptakes of resources from soil and environment is reduced.

The green line in the graph represents water contents which indicates the difference between fresh- and dry-biomass. The plant water content follows the trend of plant fresh biomass. The plant water content gradually increases and starts to decrease from the same point when plant fresh biomass starts to decrease. This shows that plant fresh biomass and water contents are directly interconnected. In August, the plant water contents decreased sharply, indicating that the plant reached maturity and started drying. The water dynamic content throughout the growing season indicates that at the early growth stage, plants grow actively, and later when water content decreases plants approach maturity. A summary of maize different growth stages is given in **Table 5.**

It was noticed that during early November the plant water content and dry biomass become likely to be the same for a limited time. It explains the environmental as well as biological factors. The possible reasons include delay in harvesting after reaching maturity, kernel may continue respiration after maturity, loss of dry biomass due to CO_2 loss from plants, etc. At this stage, the maize cob has enough water content and is still active in evapotranspiration. Later, the cob biomass started to decline because of water loss and [CO_2] and overall biomass decreased.

Wind Speed (m s^{-1})

Figure 14 represents wind direction and speed over the maize field during the experimental period. The bar length indicates the percentage of wind for a specific time and specific direction, or in other words, how frequently wind is coming from a specific direction.

Table 5. Summary of maize growth stages

Month	**Day of the year**	**Growth Stage**
May-June	138-157	V5
June	158-163	V6
June	164-170	V7
June	171-180	V8
July	181-186	VT
July	187-190	R1-Silking
July	191-197	R2-Blister
July	198-207	R3-Milk
July	208-215	R4-Dough
August	216-232	R5-Dent
August-October	233-299	R6-Physiological Maturity

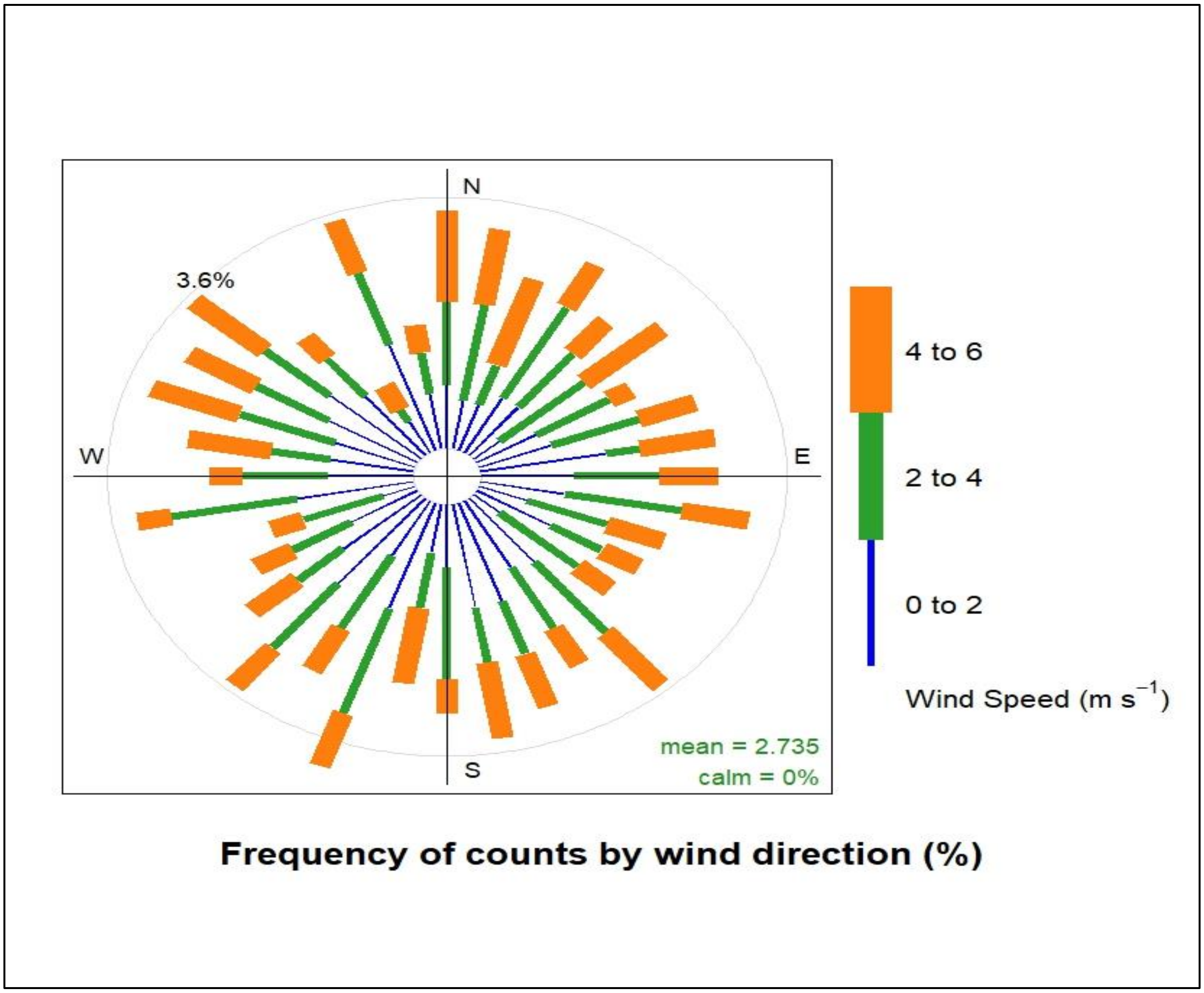

Figure 14. Wind direction and speed from EC system.

The wind speed varied between 0 and 6 m s^{-1} with an average speed of 2.735 m s^{-1}. The different color represents the range of wind speed. Similarly, there is no period (0%) when the calm wind conditions prevail. It means the wind never dropped below the measurable level and was always present. The graph indicates that only 3.6% of wind frequency comes from a single direction, which means the wind is coming from all directions, but most strongly north, northeast and south directions. Understanding wind direction and speed is important to study the flux exchanges between the surface and atmosphere. No calm conditions indicate that continuous mixing of turbulent fluxes occurs throughout the period, and maximum mixing occurs when the wind speeds it between 4-6 m s^{-1}. Wind direction also helps in flux footprint analysis to understand which direction is contributing most to measured fluxes. As most of the wind comes from the north, northeast and south directions, which can be a major source of fluxes, especially CO_2 and H_2O, etc. In short, the exchange of energy balance components and fluxes (CO_2, H_2O, heat, and storage terms) between soil, plant, and atmosphere are significantly influenced by the wind speed and direction.

Net Radiation (Rn)

Rn is the most important component of the energy balance equation. By definition, *Rn* is the balance between incoming and outgoing shortwave and longwave radiation and is dynamic throughout the growing season. **Figure 15** shows during the daytime, *Rn* was found positive and negative at nighttime. However, the diurnal behavior is interesting. *Rn* remains constantly lower than zero at nighttime but in the daytime, it was variable. During the daytime from 0800 LT the net radiation steadily increases and reaches a maximum of 1300 LT and then starts abruptly decreasing and reaches zero at 2000 LT. The vertical bar represents +/- one standard error of the

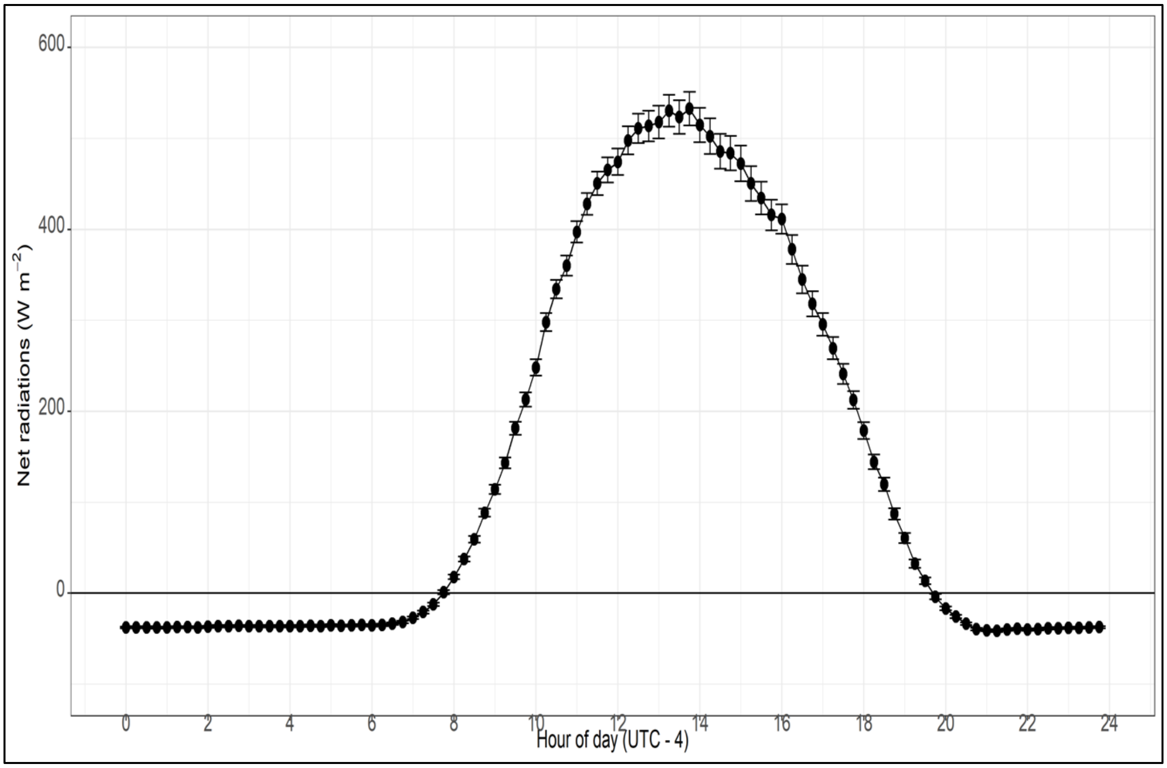

Figure 15. Average net radiation (*Rn*) for the entire growing period.

mean. Positive values during the daytime indicate the prevailing absorption of incoming solar radiation. During the nighttime and before 0600 LT there is no incoming solar radiation, while a negative value under zero is the indication of longwave radiation leaving the system and creating a situation of negative net radiation.

Between 1200 LT to 1400 LT, the highest net radiation is when the sun is high in the sky, and the system receives the highest radiation. It shows the variability in the net radiation during the daytime, especially 1200 LT to 1400 LT is highest because of variation in the environmental factors including clouds and haze. Other factors including wind speed, precipitation, etc., impact variability during the daytime.

Understanding net radiation patterns is important because it triggers important mechanisms like seed germination, growth and yield, photosynthesis, and evapotranspiration. During the daytime, the peak value of Rn shows the availability of energy to carry out these processes.

Latent Seat* (*LE*) *Fluxes

LE is the energy required to change the water into water vapor and its exchanges between the vegetation and overlying atmosphere. *LE* flux dynamic indicates how much *Rn* is partitioned into *LE* flux in other words for evapotranspiration. Ideally, *LE* flux is the main component of the energy balance. Correct estimation of *LE* flux can not only be important to resolve the problems of energy balance closure but also important to improve the irrigation scheduling and to reduce water loss. Agricultural ecosystems are strongly influenced by climate change and human activity. Scientifically, it is important to understand the exchange of energy and water between agricultural ecosystems and prevailing atmosphere to manage agricultural ecosystems. Therefore, understanding *LE* flux is important to manage the maize ecosystem.

LE flux during the nighttime from 2100 LT to 0600 LT was near zero in **Figure 16**. This is because at night there is no solar energy (*Rn*) available and no evapotranspiration (ET) from soil or plant surface. From 0700 LT the *LE* steadily increased and at 1500 LT reaches a maximum of almost 250 W m^{-2}. Variation of *LE* flux during the daytime between 1200 LT and 1600 LT is higher due to temperature variations (net radiation). Interestingly, the higher *LE* flux than zero was recorded at nighttime (after 2100 LT) because the site has an atmosphere that can remain hot at nighttime. This temperature is not enough for continuing evapotranspiration at low levels.

LE is accompanied by the loss or gain of energy. The negative LE at nighttime and early morning also negates the dew because during this process, vapor condenses, and energy is released. Thus, negative LE is an indication of dew formation.

Higher *LE* flux during the daytime means crops use more water to continue their physiological processes like photosynthesis and resulting evapotranspiration. At this time higher soil water content is important for better maize growth and yield.

Sensible Heat (H) Fluxes

H flux is the amount of energy involved in the exchange of heat between the plant surface and atmosphere. Like *LE*, *H* fluxes are also a key atmospheric component of the energy balance and are primarily influenced by several environmental factors, e.g., temperature, humidity, wind and solar radiation. Furthermore, *H* is also an important component to study the agricultural ecosystem efficiency. **Figure 17** shows the diurnal distribution of *H* flux over the complete

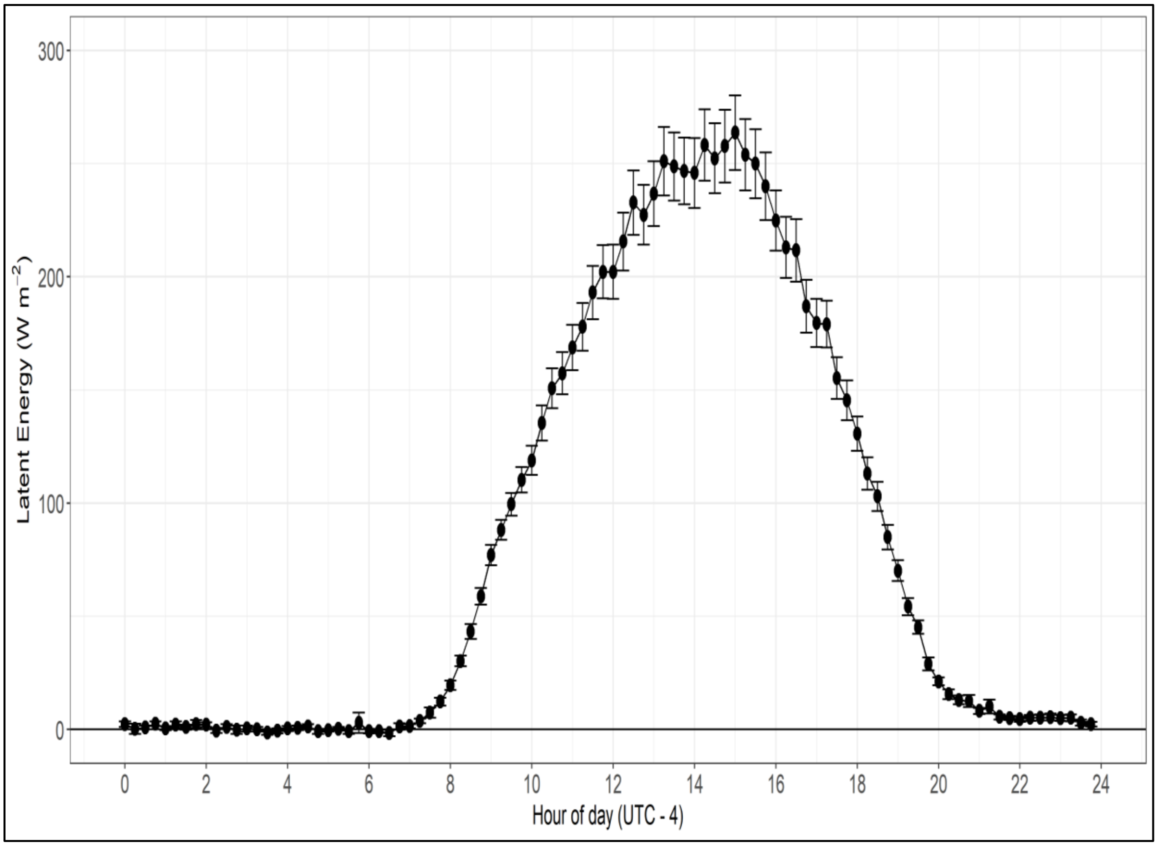

Figure 16. Average *LE* fluxes for the entire maize growing period.

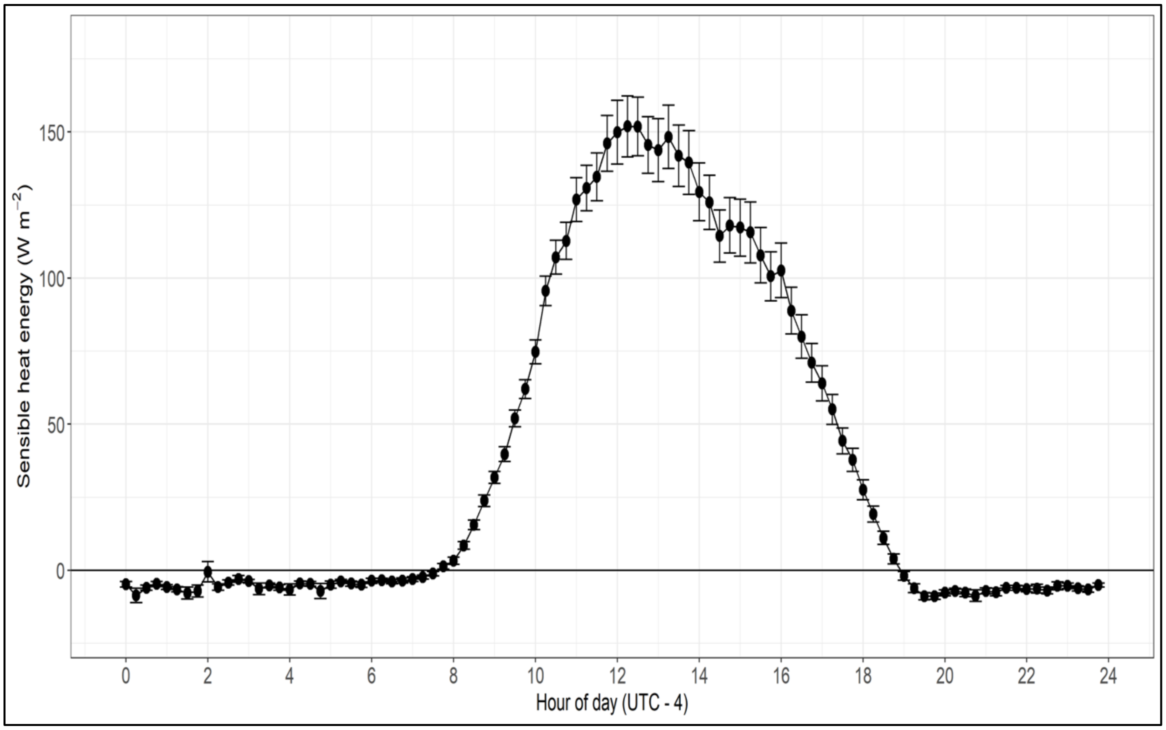

Figure 17. Average sensible heat flux for the entire maize growing period.

maize growing season. The *H* flux during the nighttime from 1900 LT to early morning before 0800 LT, found negative or below zero which is due to no sunlight. After 0800 LT as the sun appeared, sensible heat flux steadily increased and reached a maximum of 150 W m^{-2} (1200 LT and 1300 LT). After that it rapidly started decreasing and reached zero at 1900 LT near sunset. It attained a constant negative value till the sun rose the next day. During nighttime, due to the cooling effect, the loss of heat as latent and/or sensible from soil and from plant surface to air becomes lower.

Throughout the season, *H* flux was found lower than *LE* flux which was due to plant growth, dense canopy structure, and higher LAI. Denser canopies are responsible for higher partitioning of *Rn* into *LE* and ET as compared to *H* flux. *H* flux is lower because the system is dominated by transpiration. At the start of the growing season, the crop LAI is lower which leads to lower transpiration. It indicates that more *Rn* is partitioned to *H* as compared to *LE* because *H* is the heat exchanged by the process of convection. This indicates that higher β because at early growth stage of maize, more energy go to the atmoshpare to heat up the air.

Ground Heat (G0) Fluxes

Ground heat flux (*G0*) represents the amount of heat/energy that enters and/or is lost from soil over a specific time. Soil absorbs energy in the form of shortwave and longwave radiation. Soil absorbs sunlight as shortwave radiation to retain heat and release it into the environment as latent and sensible heat or longwave radiation. *G0* is the most variable and important component of the surface energy balance of any system.

Figure 18 represents the average dynamics of *G0* flux over a complete growing season of maize. During the nighttime from 2100 LT to 1000 LT, the *G0* is negative. This is because the

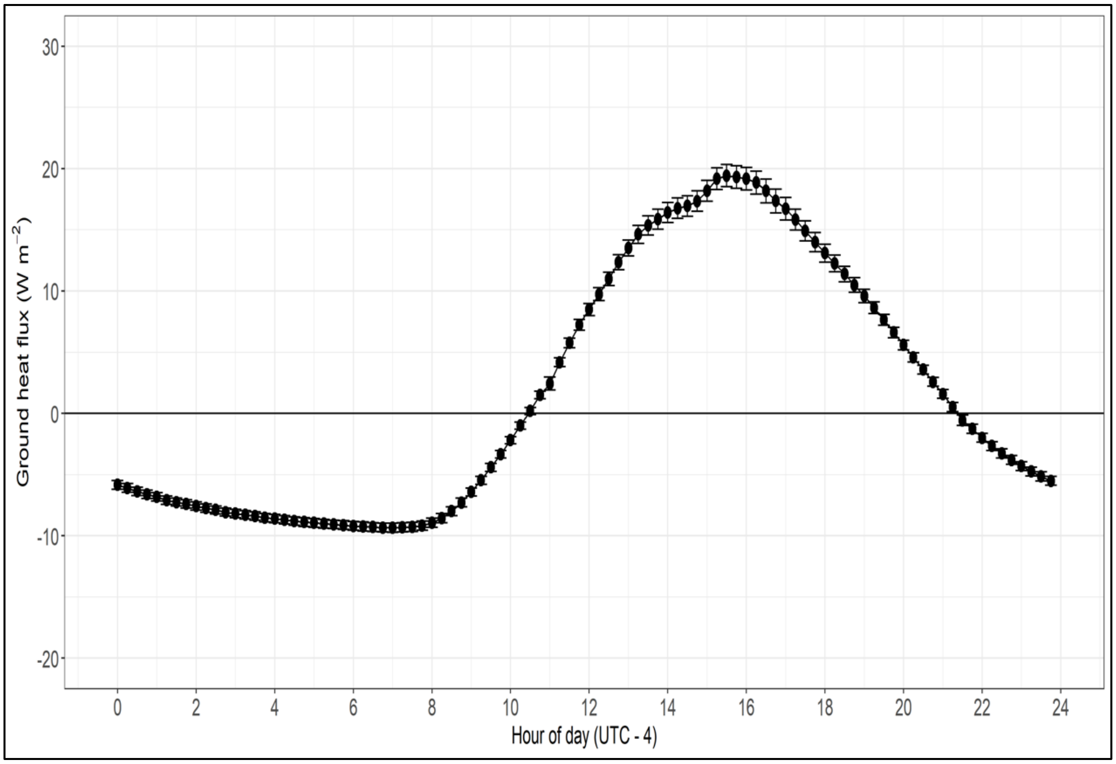

Figure 18. Average ground heat flux (G0) for the entire growing period.

absorbed heat is released in the form of longwave radiation into the atmosphere resulting in a cooling effect. At sunrise, the *G0* steadily starts to increase and attains a maximum 20 W m^{-2} value at 1500 LT and then slowly decreased and reached zero at 2100 LT and attained zero until 1000 LT the next day.

The negative *G0* means that the energy soil absorbed in daytime is released back to the atmosphere because of the surface cooling effect in the absence of solar radiation. The ground heat flux is negative because of the lower night temperature. After sunrise, solar radiation heats the soil surface, and the soil starts absorbing heat as energy. The maximum *G0* is between 1500 LT to 1600 LT, at that time the sun is near 90-degree angle to the soil surface and directly overhead resulting in higher *Rn* penetration into the plant canopy and the soil. It can be seen in the graph from the departure of the curve that ground heat flux is changing as the sun angle changes. *G0* provides insight into how net radiation is partitioned as heat into the ground.
All the common approaches or models used for *H, LE,* and *H/LE* require *G0* as an input to estimate the amount of available energy. Accurate estimation of *G0* will directly reduce the estimation error in *LE*- and *H*-fluxes measured by any approach and improve energy balance closure. *G0* is significantly influenced by soil moisture contents. Soil with higher moisture contents have higher thermal conductivity which transfers heat more easily but has higher thermal inertia taking more energy to change the soil temperature. Further, the *G0* is substantially influenced by the canopy closure (e.g. shading, LAI, etc.). Higher LAI provides shading effects on soil reducing the loss of water from soil and provides a cooling effect. Stomatal closure is also influenced by ground heat fluctuations. Understanding *G0* dynamics over agriculture ecosystems helps to develop soil and irrigation smart practices to achieve agricultural sustainability.

Storage Terms (Latent, sensible, canopy, photosynthesis and total)

Figure 19 represents the diurnal cycle of the overall energy storage terms and its components [canopy heat storage, photosynthesis heat storage (PE_storage), latent heat storage (LE_storage), sensible heat storage (H_storage), and total heat storage (total_storage)] over maize crops. The line width represents the standard error of the mean. **Figure 19** shows that the storage term was significantly higher during the daytime and lower at nighttime. These diurnal patterns of canopy, *H* and *LE* heat storage show similar behavior at night, until 0600 LT. During the night, these fluxes and differences between measurements above the surface and at the surface itself were small. As the air cooled during the night, sensible heat storage in the air mass remained negative. After sunrise, the air mass warmed and all the components of heat storage rose to a maximum value between 1200 LT and 1230 LT. Afterwards, the sensible heat storage rate declined, reaching negative values a few hours before sunset and attaining a minimum value a few hours before midnight. The sensible heat storage subsequently trended to a near-zero constancy until being disrupted by sunrise at about 0700 LT. However, canopy heat and photosynthesis storage were found to be highest at this time and stayed positive for longer times compared to others. Similarly, canopy storage is negative for a long time compared to others. Photosynthesis storage (PE_storage) stayed positive during the day because plants did actively photosynthesize in the presence of sunlight while it became zero as sunset occurred and stayed zero till the next day sunrise. The diurnal variations PE_storage are influenced by light intensity, [CO_2], canopy architecture, LAI, temperature, and water availability. The variation in these parameters influences the daily flux of PE_storage. Higher [CO_2] during the daytime is responsible for higher photosynthesis and resultantly higher energy use. Photosynthesis is also

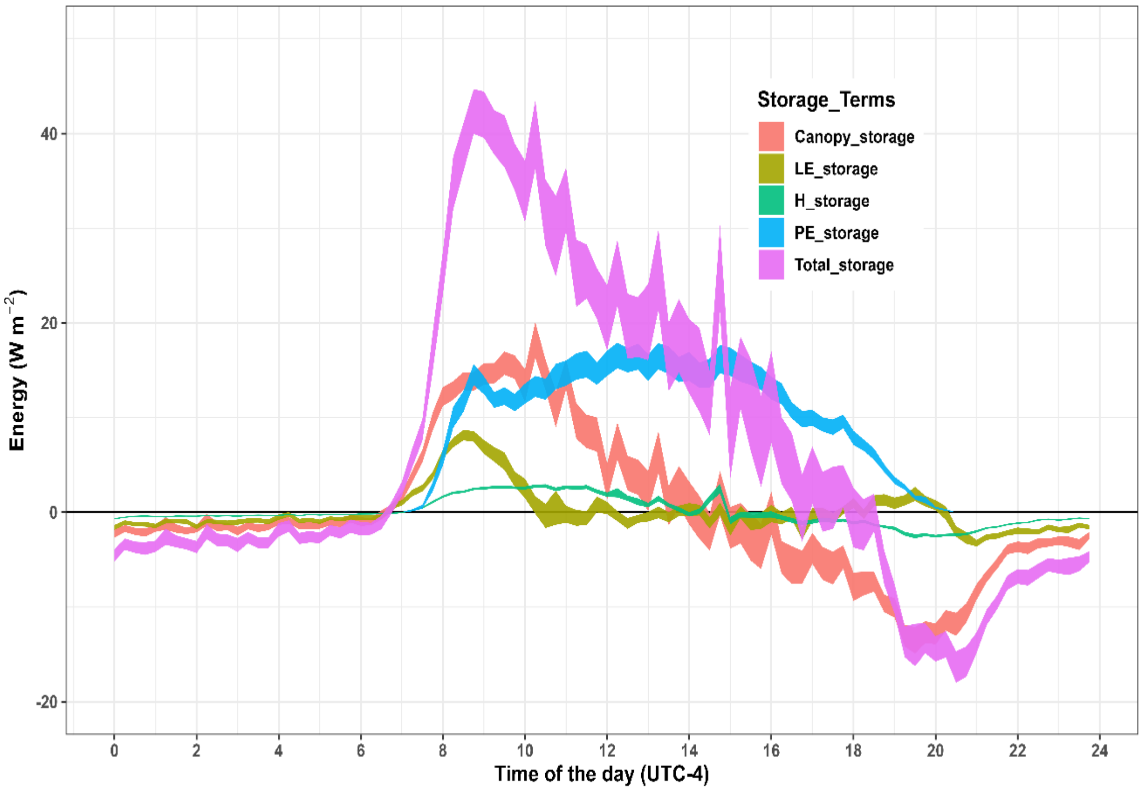

Figure 19. Average diurnal cycle of storage terms for the entire growing period.

directly influenced by light intensity because light is required to excite the photons to commence photosystem I and II for ATP formation. Furthermore, optimal temperature is also required to drive both photosystems I and II. So, plants met this temperature, light, and [CO_2] requirement only during the daytime. Therefore, higher photosynthesis rate and higher utilization of energy during the daytime as compared to nighttime.

The total heat storage (total_storage) is the sum of all the storage terms that reflect how radiation energy is distributed among different energy components to drive the function of the ecosystem.

The diurnal variations in heat storage are influenced by, for example, solar radiation, boundary layer stability, ground heat flux, precipitation and plant physiology. The variation in canopy structure, biology and microclimate changed the canopy storage and influenced the daily integrated fluxes. Forest studies report that the exchanges of CO_2 and H_2O between vegetation and atmosphere are regulated by canopy characteristics (biological as well as physical) e.g., leaf morphology, leaf roughness, and LAI. In this context, the present results provide valuable insights into the energy dynamics within the maize canopy and contribute to a deeper understanding of its environmental response to plant biophysical processes during different periods of the day.

Effect of Storage Terms on Energy Balance

Figures 20 and **21** represent the effect of storage terms with and without including in the turbulent fluxes (*H*, *LE*) on available energy (*Rn-G0*). The *Rn* during daytime is the major factor responsible for driving energy fluctuations. The blue line indicates the relationship of turbulent flux with available energy while the blue dotted line is the reference line (1:1) indicating ideal

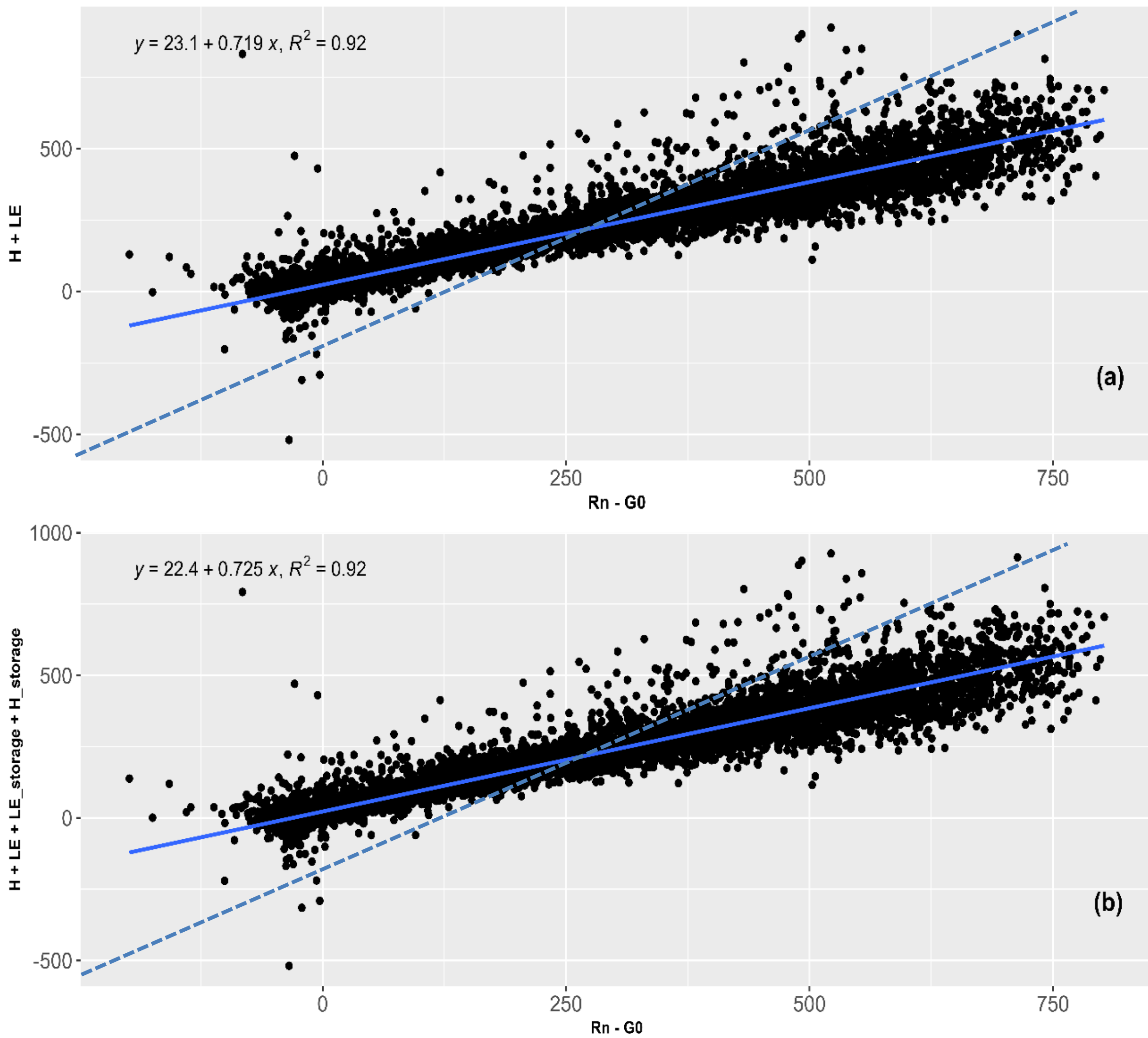

Figure. 20. Scatter plot of energy balance over maize: (a) available energy (*Rn - G0*) vs turbulent flux (*LE + H*), (b) available energy (*Rn - G0*) vs storage flux (*LE + H + LE_storage + H_storage*).

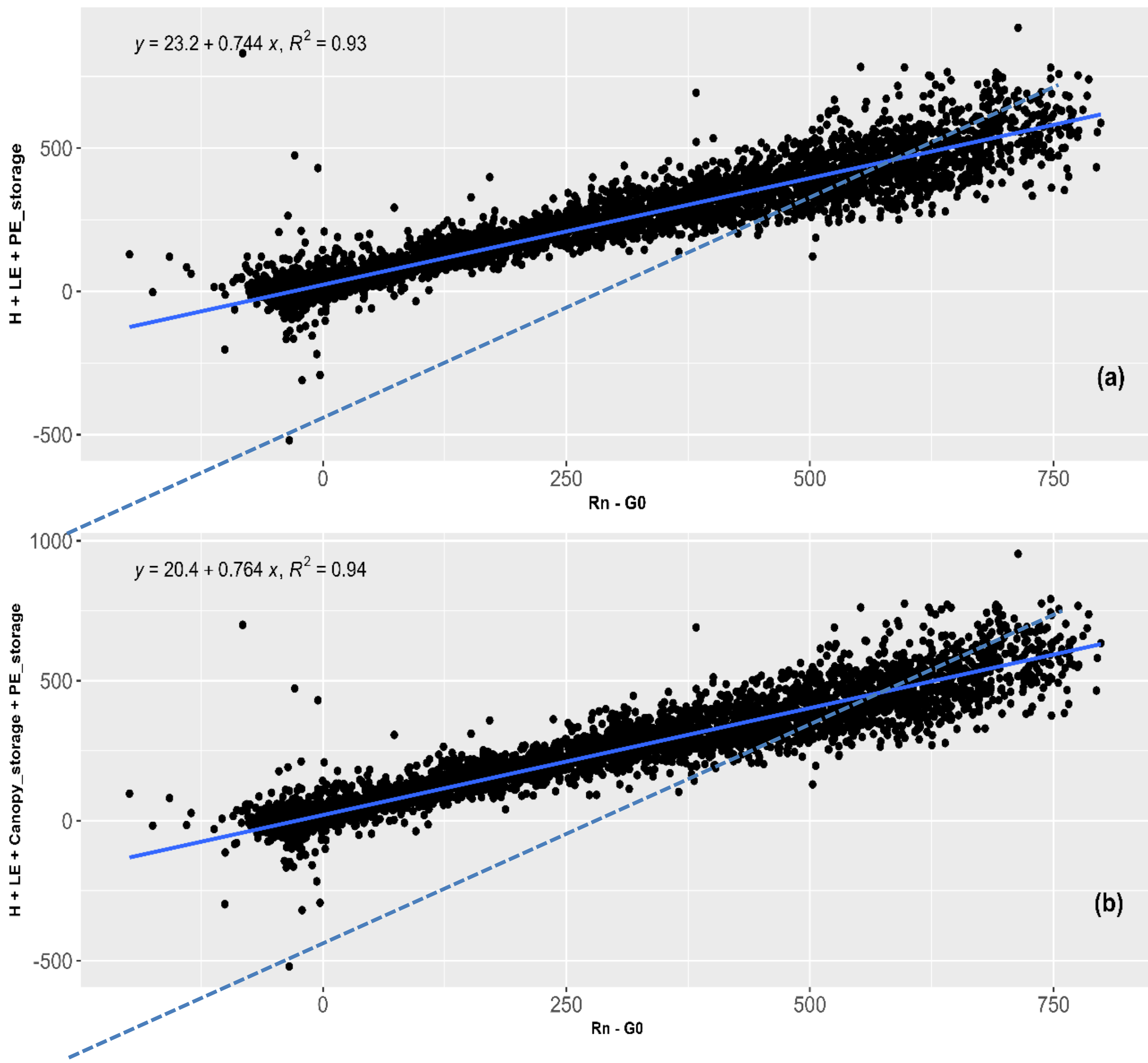

Figure. 21. Scatter plot of energy balance over maize: (a) available energy (*Rn - G0*) vs PE_storage (photosynthesis storage) flux, (b) available energy (*Rn - G0*) vs storage flux (canopy+ photosynthesis).

closure. The r square value of 0.92 indicates that the surface energy balance is closed. The closer the r square value is to 1, the more the energy balance is closed. However, there is no effect of latent, and/or sensible heat storage (**Figure 20 a, b**) was found on energy balance closure. However, when canopy and photosynthesis storage terms (**Figure 21 a, b**) were accounted for the overall energy balance closure improved (r^2 value increased from 0.92 to 0.94). Canopy storage is the amount of energy (*Rn*) in the form of heat absorbed in the biomass of maize. Photosynthesis storage (PE) equals the energy plant uses during photosynthesis. The higher r-square value indicates a strong correlation between available energy and turbulent flux. The lower r^2 value indicates the extent of discrepancies in energy balance. Simply, some energy dissipates in other processes which are not accounted (e.g. photosynthesis), called residual energy. This indicates residual energy is important to count to achieve energy balance closure. During this study, considering canopy and photosynthesis storage terms recovered almost 25% of energy which was not accounted.

Conclusion

Exploring the relationship between soil, plant, and atmosphere increases our ability to understand critical processes occurring in the environment like evapotranspiration and NEE, etc. The partitioning of energy balance fluxes indicates how the solar radiation available energy (*Rn-G0*) is subdivided into turbulent fluxes (*H*, *LE*) and storage terms and highlights those fluxes can contribute to the surface balance issue. Measuring residual energy sources and accounting for turbulent fluxes improves energy balance closure. In field studies, storage terms (canopy, ground, photosynthesis, latent, and sensible storage terms) are occasionally measured and we measured them in the current study. In this study, we measured latent, sensible, canopy and photosynthesis heat storage and accounted for these factors in the overall energy balance closure. There was no effect of latent and sensible heat storage on energy balance closure, but photosynthesis and canopy heat storage have improved the overall energy balance. On considering canopy storage terms, the r^2 value increased from 0.92 to 0.94, showing that energy balance closure improved by considering this factor. The study concluded that on this site the energy balance is already significantly closed (r^2 value of 0.92) even though storage terms are considered or not. Therefore, turbulent fluxes are the major component of energy balance over this site.

CHAPTER 5: MEASURING H_20 AND CO_2 VERTICAL FLUX AND THEIR STORAGE WITHIN THE MAIZE CANOPY

Abstract

Precise measurements of H_20 and CO_2 fluxes can help estimate accurate evapotranspiration (ET) and net ecosystem exchange (NEE), the negative effect of climate change on crop production, and irrigation scheduling. This study evaluates the vertical fluxes of H_20 and CO_2 over maize to estimate CO_2 flux, ET, and storage of CO_2 and H_2O within the canopy. Study results indicate that [CO_2] were higher during late night and early morning until 0600 LT. [H_2O] were significantly higher during the daytime compared to nighttime, peaking between 1200 LT and 1400 LT and then gradually decreasing. Due to photosynthesis, CO_2 storage becomes negative (depletion) during the daytime while storage increases (accumulation) at night. The current study shows that significant turbulent fluxes of H_2O and CO_2 were found between the tasseling stage (VT) and early reproductive stage of maize while the lowest were found at early vegetative and maturity stages. However, during the study, diurnal H_2O storage fluxes were significant, but CO_2 storage flux was not large but significant variation was found at different growth stages of maize.

Introduction

The concentration of CO_2 has been increasing, and agricultural activities can play a main role mitigating global climate. The agroecosystem is not only a source of CO_2 in the atmosphere but has a natural potential to reduce the [CO_2] through C-sequestration (Griscom et al., 2017; Fargione et al., 2018). It is reported that atmospheric [CO_2] is influenced by the NEE (how much CO_2 is fixed by photosynthesis and how much is released by respiration) and some other factors including environmental, management, micrometeorology, and biological drivers (Humphrey et al. 2021). The flux of CO_2 in the agricultural ecosystem varies seasonally and is directly linked to plant growth (Li et al. 2016; Schmidt et al. 2012). Crops are a C-sink during the crop growing period (from emergence to harvest) and act like a carbon-sink. C4 crops, especially Maize, are considered a major sink of CO_2 due to its potential to sequester atmospheric CO_2 (Maier et al. 2022).

Water vapor in the agroecosystem is comprised of soil-plant evaporation (E) and plant transpiration (T). Both E and T are affected by different plant processes (e.g., LAI) and environmental factors e.g., temperature, soil moisture, and humidity (Skaggs et al., 2018; Sulman et al., 2016; Wagle et al., 2021). Exchanges of CO_2 and H_2O near the soil surface and in the lower boundary layer are fundamentally important to regulate the natural continuum of the plant-soil-atmosphere (Silva et al., 2017).

In exchange mechanisms, plant canopies receive less attention. Plant canopies accumulate various quantities e.g., CO_2, and water vapor. This accumulation is temporal and sometimes changes with the environment quickly especially when wind speed is high. This accumulation is known as CO_2 storage and H_2O storage. Additionally, the plant canopy also regulates the microclimate and partitions the available energy into heat fluxes (LE, H, and ET). A theoretical estimation is that approximately 6% of photosynthesis energy is utilized for the process of photosynthesis through the process of C-assimilation by C4 and 4.6% for C3 plant (Zhu et al., 2008). The C4 plants have more potential for C-sequestration than C3 because C4 plants have higher efficiency for photosynthesis, can do photosynthesis at lower [CO2], and higher performance under stress conditions (can partially close the stomata, and reduce water loss to maintain photosynthesis).

At the leaf level, stomata control the exchange of CO_2 (fixed for photosynthesis) and H_2O (transpiration) with the overlying atmosphere (Lawson & Blatt, 2014). A strong relationship exists between the CO_2 uptake and H_2O flux; when CO_2 uptake is higher, higher H_2O flux contributes to ET. Canopy architecture, surface roughness, wind speed, atmospheric stability, soil respiration, etc., are important factors that control CO_2 and H_2O fluxes and their storage in the canopy and the broader ecosystem (Zhu et al., 2008).

From the last few decades, studies have mainly focused on the [CO_2] investigation over cropping systems to study the net exchanges of [CO_2] with the environment, but less attention has been given to the process of how the [CO_2] behaves vertically and how much is stored in the canopy. CO_2 storing within the canopy is ignored when partitioning the NEE into its components, which may cause inaccuracies in modelling. The measurement of CO_2 flux and its storage work as an additional empirical base to parameterize GPP, Re, and NEE to model the carbon cycle. Storage term calculation could be useful to evaluate whether a dense cropping system is beneficial or not.

More importantly, at nighttime a stable boundary layer (SBL) forms under calm wind conditions that traps CO_2. Due to the temperature rise after sunrise, the SBL begins to weaken. The trapped CO_2 mixes with air, disperses, and decreases CO_2 storage at sunrise (Stull, 2012). This is not reported much in the literature; therefore, it is important to measure how [CO_2] and [H_2O] temporarily fluctuate vertically, and the amount stored within the canopy.

The objective is to measure the [CO_2], [H_2O], and their storage flux from a maize canopy to elucidate how the canopy airspace communicates with the outside airspace.

Objective

- Determine how [CO_2] and [H_2O] change vertically within the maize canopy
- Evaluate the nocturnal and diurnal behavior of CO_2 and H_2O flux
- Calculate the CO_2 and H_2O storage flux in the early morning and late night

Materials and Methods

Storage terms (CO_2 and H_2O) refer to depletion or accumulation of scalar quantities (CO_2, H_2O, etc.,) in a hypothetical control volume. Fluxes (CO_2 and H_2O) refer to how CO_2 or H_2O exchange between a surface and the overlying atmosphere. Both of these terms are different concepts and how both are different is shown in **Figure 22**.

Firstly, four intake tubes were installed at heights of 0.11m, 0.5h, 1+h, and 2+h (h is maize canopy height in meters) to measure how [CO_2] and [H_2O] varied vertically. An infrared CO_2/H_2O gas analyzer was used to quantify [H_2O] and [CO_2] at the different heights. Height 1 is fixed, and the other 3 heights changed as the canopy grew to capture spatio-temporal variation in [H_2O] and [CO_2]. After that, fluxes of [H_2O] and [CO_2] were computed using equation numbers 12 and 13 respectively using the EC method.

$$F_{co2} = \rho_m \overline{w' c_{co2}'} \qquad (12)$$

Where ρ_m is air molar density and $\overline{w'c'}$ is covariance between [CO_2] and vertical wind speed (w), and unit is $\mu mol\ m^{-2}s^{-1}$.

$$E_{h2o} = \rho_m \overline{w' c_{h2o}'} \qquad (13)$$

where $\overline{w'c'}$ is covariance between [H_2O] and vertical wind speed (w), and unit is $\mu mol\ m^{-2}s^{-1}$.Finally, the CO_2 storage term was calculated by ICOS methodology (Montagnani et al., 2018) using equation 14

$$J_c = \overline{\rho_d} \sum_{i=1}^{N} \left(\frac{\Delta c}{\Delta t} \right)_i \Delta z_i.$$

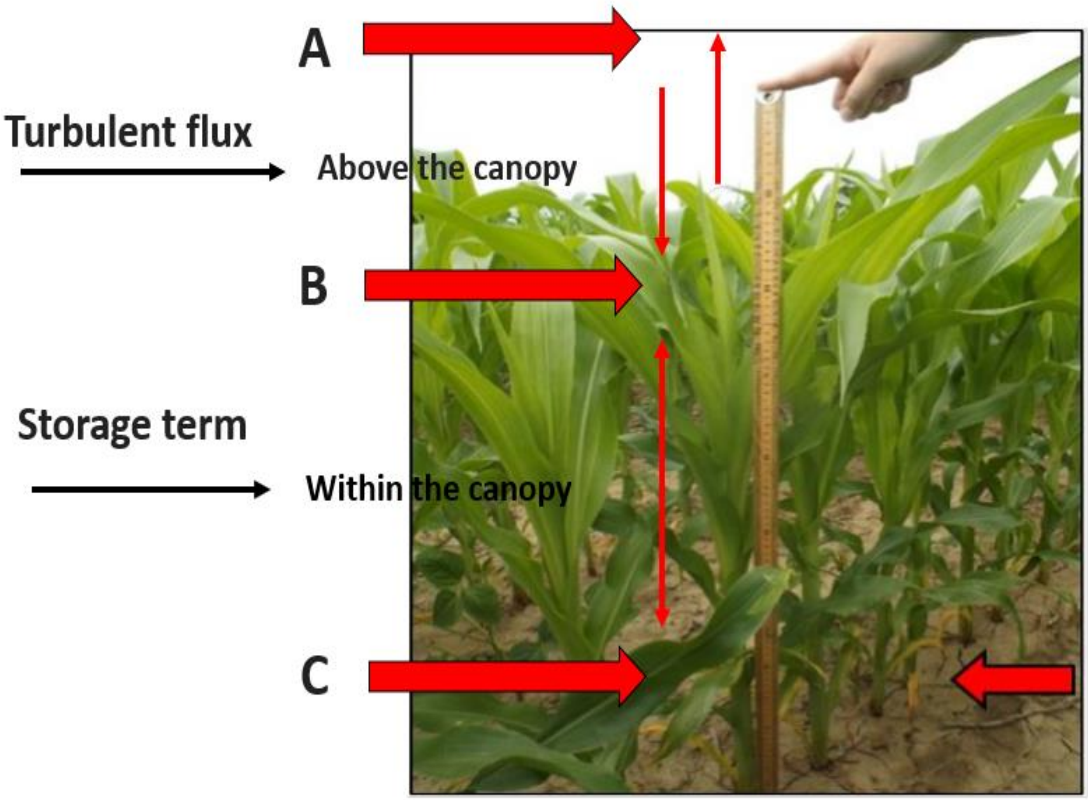

Figure. 22. Overall canopy view to difference between flux and storage terms (source: Taqi Raza).

(14)

Where J_c is the storage term of CO_2 within the i_{th} layer over which Δc is measured, Δz_i is the thickness of this layer and Δt is the measurement time step; $\bar{\rho}_d$ is dry air density, and N is number of layers (number of measurements points). Fifteen-minute average data was used to study the seasonal trend of [CO_2] and [H_2O] on a daily scale. The monthly trend of CO_2 storage was calculated on a daily basis. Finally, evapotranspiration (ET) was calculated using this formula:

$$ET = LE/\lambda \quad (15)$$

Where LE is latent energy and λ is latent heat of vaporization (2.45×106 J/kg)

Results and Discussion

CO_2 Storage Fluxes Over Different Growth Stages

Studying CO_2 storage at different growth stages is important because it shows how the growing stage influences CO_2 stored in the canopy and vice versa. Different stages are associated with different phenomena of plant growth and development like photosynthesis, C-assimilation, C-uptake, etc. Evaluating the CO_2 storage by growth stage would help determine at what stage the plant more efficiently captures CO_2. Growth stage monitoring also suggests at which grow stage wind speed has a more apparent influence on the microclimate of the canopy. Fifteen-minute average data was used to compute the maize storage terms at different growth stages shown in **Figure 23**. CO_2 storage changes with crop growth stage because the plant structure, rate of respiration and photosynthesis also change. At V5-V7 (called vegetative stage), CO_2 storage was stable and lower. This is because plants are in their early stage of growth and have a less dense canopy, and environmental factors, especially wind speed have more influence on the

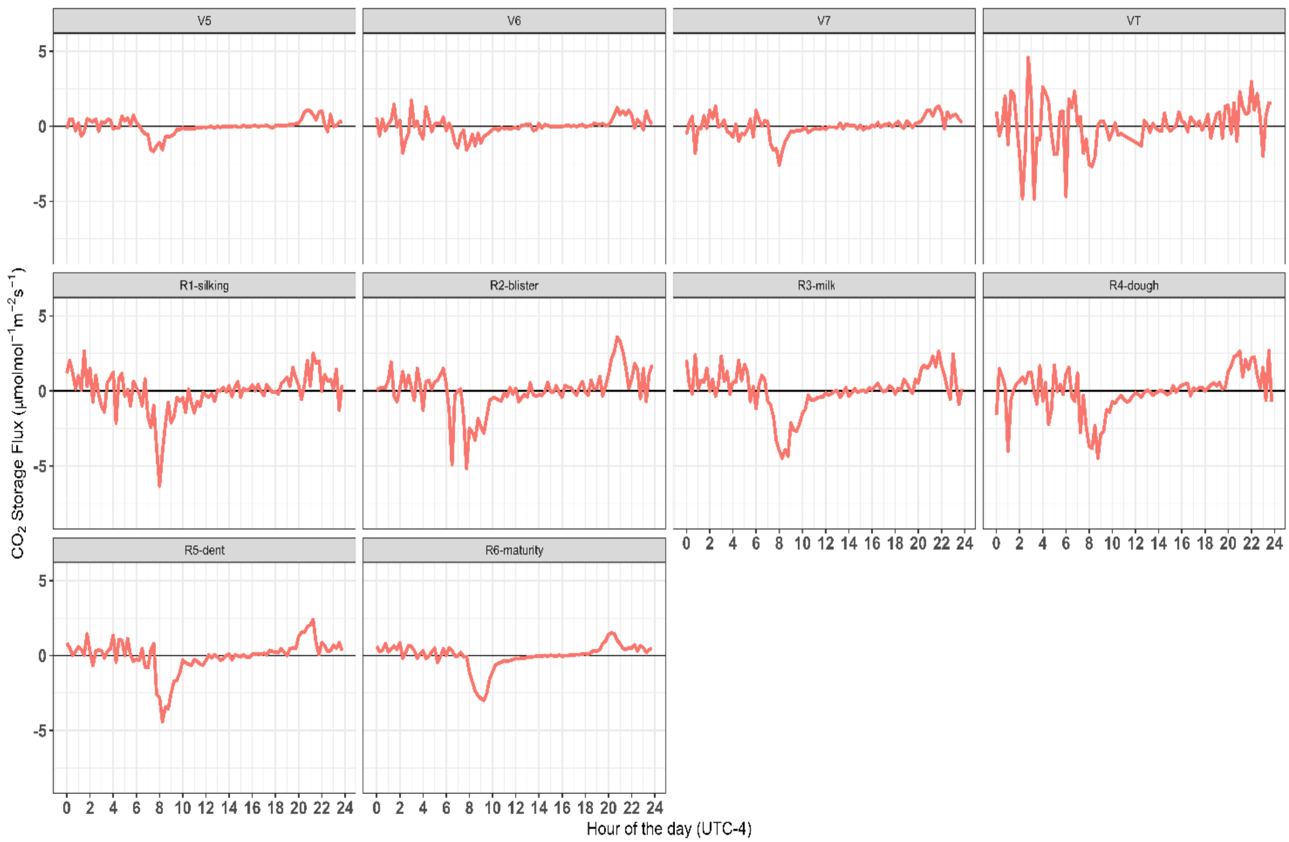

Figure. 23. Diurnal patterns of CO_2 storage flux fluctuations over different growth stages of maize.

storage of CO_2 in the canopy. However, significant storage flux variation was found when the plant shifted toward the tasseling stage (VT) and reproductive stages (R1-R4) because the plant is green and has a dense canopy. At these stages, a dense canopy serves as a place to store CO_2, and the wind has less effect on the stored CO_2 with the canopy. At reproductive stages (R5-R6), the plant reaches maturity, and CO_2 storage flux is reduced significantly as compared to VT and R1-R4 stages because the plant canopy is reduced, and the plant senesces. The trend of CO_2 storage over the different growth stages reflects how CO_2 changes within the canopy as plants grow. The highest CO_2 storage (2.5 uml m^{-2} s^{-1}) was found when the plant was at tasseling and from R1-R4. The lowest CO_2 storage was found at the early growth stage and when plants shift toward senescence. At R6 (dent stage), CO_2 storage reduction is not only due to the wind effect but also due to grain filling, uptake and utilization of CO_2. **Figure 23** also clearly indicates the pooling effect of CO_2. The nighttime CO_2 storage flux is higher because the process of photosynthesis stops, and the wind has a low effect as compared to daytime. During the daytime, CO_2 storage was found near zero, even negative because plants utilized all the CO_2 for photosynthesis. The transitional behavior of CO_2 storage flux during different growth stages indicates its importance for modelers and farmers.

H_2O Storage Flux Over Different Growth Stages

Like CO_2 storage flux, diurnal H_2O storage fluxes were also calculated over different growth stages of maize. H_2O storage flux is the amount of water vapor that is stored within the control volume of the maize canopy over a specific period. **Figure 24** represents the variation in the H_2O storage flux over different growth stages. At the early growth stages (V5-V7), the H_2O storage did not fluctuate much and was found stable with values near to zero except for a few

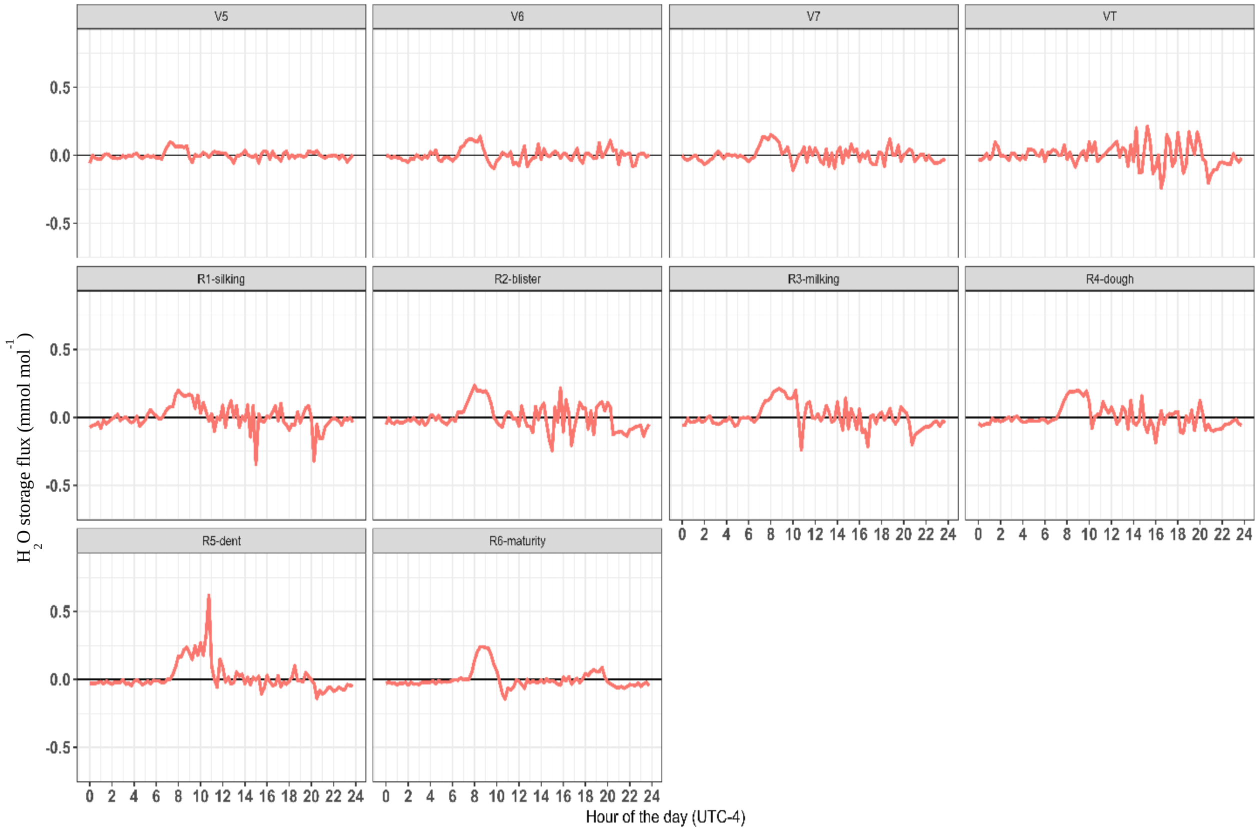

Figure. 24. Diurnal patterns of H_2O storage flux fluctuations over different growth stages of maize.

hours (0700-1000 LT). This is because plants are in their early stage of growth and leaf architecture is scattered. At this stage, the plant canopy is not fully closed because the leaves are small, and the transpiration rate is low. Open plant canopies have more prominent wind effects, and water vapor is easily transferred resulting in minimal storage. When plants entered stage VT-R4, the H_2O storage flux was found significantly higher with more variability. This is because plant activities become prominent, LAI increases, stomatal conductance increases, and ET increases. Plant demand for water increases, and water vapor because of transpiration accumulates temporarily within the canopy temporally before exchanging with the overlying atmosphere. At this stage, the plant developed a closed canopy, and the effect of wind became less.

During the R5-R6 stages, the H_2O storage flux becomes minimal with only a few peaks during specific periods. This is because plants enter grain filling and senescence stages and at this stage, the stomatal activities and respiration are again reduced. **Figure 24** summarizes that the H_2O storage flux was minimal during early- and late- growth stage while relatively higher during VT to R3 because of higher canopy and more evapotranspiration. These trends at different growth stages can be useful in irrigation scheduling and water management.

CO_2 fluxes Over Different Growth Stages

CO_2 flux is the process of CO_2 exchange between the vegetation and surrounding atmosphere. In the case of a maize field, it is between the maize canopies and the overlying atmosphere. It is the most important parameter that mimics the process of net ecosystem exchange (NEE). CO_2 flux is directly affected by environmental factors, soil activities, and plant physiology. Soil respiration, photosynthesis, and environmental conditions (e.g. temperature) are the major controlling factors of CO_2 flux over the agricultural system.

Figure 25 represents the diurnal flux of CO_2 over the different growth stages of maize. Positive CO_2 flux indicates the CO_2 released into the atmosphere and negative CO_2 flux shows the uptake of CO_2 by the plant from the surrounding atmosphere. **Figure 25** represents that during the daytime CO_2 flux was negative which indicates photosynthesis. At nighttime, the positive CO_2 flux indicates photosynthesis and CO_2 uptake are stopped (due to no solar energy) and all the CO_2 released from respiration goes directly to the atmosphere. Generally, the CO_2 flux was lower at stage V5 compared to other stages. At stage V5, it is lower because plants are in the initial growth stage when the LAI is small, and uptake is lower. While at the R6 stage, the plant is at maturity stage, senescence starts (yellow leaves) and CO_2 uptake is again reduced. At stages (V5-R2), the extent of CO_2 flux (both positive and negative) was more significant because at this stage plants are growing rapidly, have developed significant LAI, and have a dense canopy. During the daytime plants uptake more CO_2 to maintain the process of photosynthesis and drive reproductive stages. At this stage, plant development and grain filling started and the need for CO_2 increased. The variability of CO_2 flux at this stage indicates higher environmental stability. However, at later reproductive stages (R3-R5), the CO_2 flux has stronger variability that may be due to higher metabolic processes as the plant enters silk and milk stages. Furthermore, variability indicates that environmental conditions are unstable. At stage R6, the plant reached senescence, developed yellow leaves and photosynthesis declined. At the maturity stage, the plant is dried and yellow but has still fair CO_2 flux because of respiration from the grain (plant

Figure. 25. Diurnal patterns of CO_2 flux fluctuations over different growth stages of maize.

respiration). Understanding CO_2 flux at different growth stages helps to achieve higher maize production by developing management strategies at various growth stages.

Evapotranspiration Fluxes Over Different Growth Stages

Evapotranspiration (*ET*) is a major mechanism of H_2O loss from agricultural fields and significantly influences crop production. Different factors influence evapotranspiration including temperature, wind speed, leaf area index, water vapor deficit, atmospheric stability, and soil moisture content. During the process of photosynthesis, plants uptake CO_2 and release water into the atmosphere through the process of respiration. At the leaf level, canopy architecture and LAI are the most important controlling factors of evapotranspiration in maize. **Figure 26** represents the diurnal pattern of ET over different growth stages of maize. **Figure 26** indicates that ET pattern is influenced by daily solar radiation. Generally, ET was found lowest during the early hours of the day and highest midday and then again started decreasing as the day moved toward the night. At the vegetation stage from V5-V7, the magnitude of the ET was found to be almost 0.4 mm hour $^{-1}$ during 1200-1400 LT. As the plant reaches the VT stage, the ET rate increases significantly and is persistent till reproductive stage R4. During the reproductive stage, the ET increased due to plant metabolic activities and grain formation. At this stage, the plant has the highest LAI and increases CO_2 uptake to maintain photosynthesis and release the highest water. When plants enter stages R5-R6, the plant reaches maturity, and the ET decreases. At this stage, senescence starts and CO_2 uptake and photosynthesis decline. At this stage, the uptake of water from soil also declines due to lower metabolic activities, and water loss becomes minimal. The pattern of water loss at different growth stages mimics that plant demand for water increased as

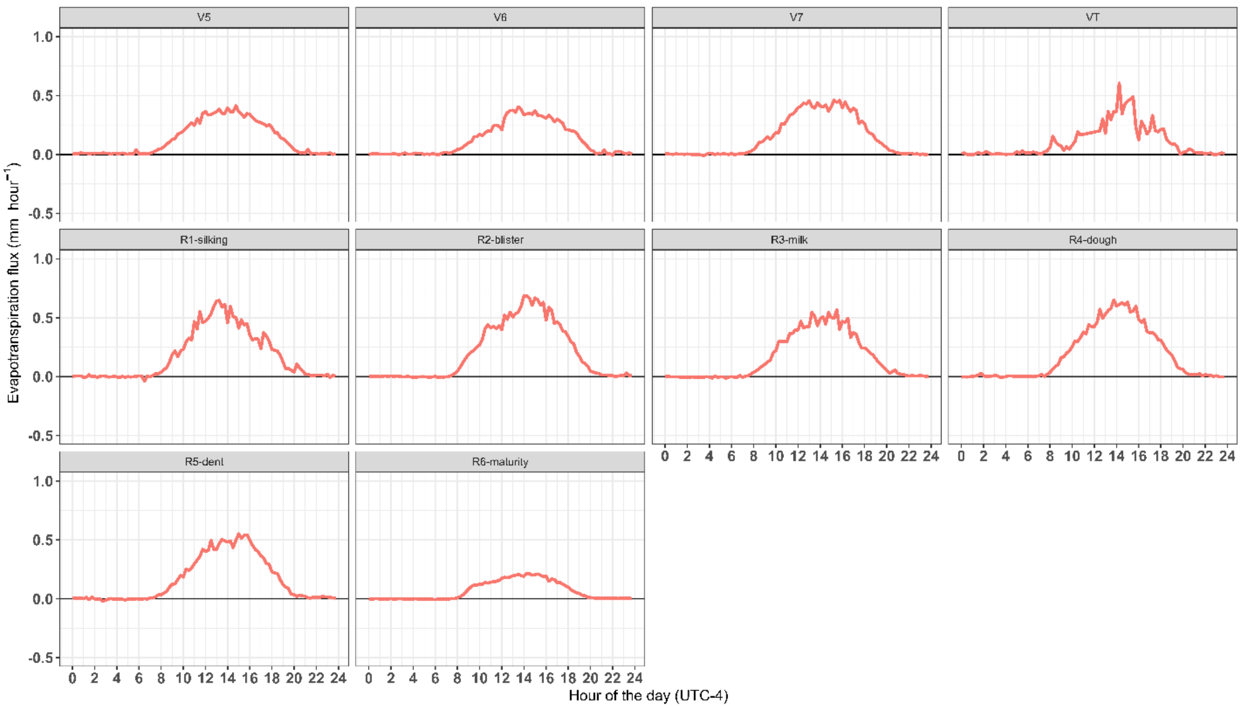

Figure. 26. Diurnal patterns of evapotranspiration fluctuations over different growth stages of maize.

plants enter tasseling till reproductive stage R4. At these stages, irrigation is more important to maximize maize production.

Conclusion

Understanding the variation in [CO_2], and [H_2O] in the vertical profile of maize canopy enhances knowledge of canopy structure and its role in fluxes exchanged between soil, plant, and the atmosphere. This profile-based study within the maize canopy has an advantage in understanding how inside canopy atmosphere communicates with the overlying atmosphere under different environmental conditions like varying boundary layers (both PBL and SBL), wind speed, etc. It also improves the knowledge of microclimate and storage of gases within the canopy and their role in NEE. Furthermore, within canopy studies provide an idea of how eddies develop and mix within the canopy due to the wind. Narrow or wide strip cultivation shows how tillage practices can influence the eddies development and turbulent fluxes. Our current study results indicate that [CO_2] was higher during late night and early morning until 0600 LT. [H_2O] were statistically higher during the daytime compared to nighttime, peaking between 1200 LT and 1400 LT and then gradually decreasing. CO_2 storage becomes negative (depletion) during the daytime while storage increases (accumulation) at night. The current study also indicates that significant turbulent fluxes of H_2O (*ET*) and CO_2 were found between tasseling and early maize reproductive stage while the lowest were found at early vegetative and maturity stages. These results indicate that soil moisture, wind speed, surface resistance, and temperature are the most controlling factors within the profile in developing vertical profiles of [CO_2], [H_2O], and their storage.

CHAPTER 6: EVALUATION OF CO_2 AND ENERGY BALANCE FLUXES FROM A MAIZE CANOPY IN EAST TENNESSEE USING THE SURFATM MODEL

Abstract

Field crops can emit or store carbon depending on the season and cropping practices. A process-based modeling approach allowed us to predict the transfer pattern of the CO_2 fluxes and energy between vegetation, soil, and the atmosphere. A SURFATM-CO_2 model was developed to simulate the CO_2 exchanges between vegetation, soil, and the atmosphere. The model couples soil respiration, considering its temperature sensitivity, with photosynthesis and plant respiration by taking into account the plant CO_2 compensation point. The SURFATM-CO_2 process model was evaluated using field measurements obtained from a multiport profile system consisting of 4 vertical measurement heights to monitor the spatio-temporal variation of temperature, CO_2, and H_2O, within and above maize canopy in east Tennessee. The 5Hz frequency raw data were averaged into 15-minute runs and used as input for the SURFATM model to simulate CO_2 and energy balance fluxes. The main objective of the study was to comprehend the exchanges of CO_2 between vegetation, soil and atmosphere compartments. The findings of the SURFATM-CO_2 model highlight the ability of the SURFATM-model to capture canopy-atmosphere interaction as well as provide a base for model application in the studies of carbon dynamics, and cropland ecosystem management.

Introduction

In the current study, a two-layer resistance and bi-directional model for CO_2 and heat is parameterized for a maize canopy. In maize, photosynthesis is the main process of CO_2 exchange and is influenced by different factors like temperature, light intensity, air quality, soil moisture, water availability, growth stage, and canopy conductance (Wang et al., 2021). Modeling CO_2 exchange and energy balance are of special interest in maize canopies because their understanding is important to develop improved methods to manage maize production and water loss under changing climate scenarios. The concept of resistance is used to combine energy balance and CO_2 exchange in the SURFATM-CO_2 model. In the model, the CO_2 stomatal (photosynthesis) compensation point, soil CO_2 (respiration) compensation point, and leaf cuticular layer were incorporated. After that, CO_2, water, and energy fluxes were derived from the East Tennessee, USA measurement campaign (using a multiport profile system consisting of 4 vertical measurement heights) was used as input to evaluate the SURFATM-CO_2 model. In both United States and France, maize is a major cereal crop by quantity production and harvested area (USDA, 2022; FranceAgriMer, 2021). Maize is a C4 plant and very efficient in converting CO_2 into biomass accumulation, but uncertainties remain regarding the magnitudes and controlling factors of CO_2 exchanges, and surface energy balance over maize cropping systems (Sage & Zhu, 2011; Bernacchi et al., 2006). The study aims to simulate energy balance and CO_2 fluxes by the SURFATM model. Furthermore, measured and simulated surface energy balance components, and CO_2 flux (net ecosystem exchange (NEE), gross primary production (GPP) and ecosystem respiration (Reco)) were compared.

Model Description

SURFATM-CO_2 is a one-dimensional model with bi-directional soil-plant-atmosphere-transfer properties to simulate CO_2, *LE* and *H* fluxes between the biological surfaces and the overlying atmosphere. This model is based on the idea of resistance and comprises of three coupled models: (i) a pollutant exchange model (Nemitz et al., 2000), (ii) an energy budget model (Choudhury and Monteith, 1988) and (iii) a soil-water balance model, that recognizes the vegetation and soil exchange processes. Previously, the model has accomplished satisfactory results for NH_3 exchanges over various canopy types, such as grassland, wheat, and Maize (Personne et al., 2009, Ferrara et al., 2014; Lichiheb et al., 2019) and could be adapted to several pollutants, as it has been adapted for ozone and pesticides (Stella et al., 2011; Lichiheb et al., 2014). In the current study, a resistive scheme was used for water vapor, heat and CO_2. It includes the same aerodynamic resistance both within and above of canopy, and so far, the same transfer resistance for boundary-layer and stomatal.

Methodology

Crop CO_2 Flux Modeling Using SURFATM-CO_2

SURFATM-CO_2 is a model that stimulates/run at daily time step. The model adopted the SAYFE-CO_2 model to compute CO_2 fluxes, carbon budget and SURFATM model for surface energy balance. Full details of SAYFE-CO_2 model and SURFATM model are provided by Pique et al. (2020a,b) and Lichiheb et al. (2014). In SURFATM-CO_2, initially gross primary production (GPP) is estimated to use APAR as function of GPP. The major components of the model are described below in the form of equations and parameters are given in the table below. Each table describes the methods to estimate parameters, range and the notation.

Gross Primary Production (GPP) Computation

In the first step, the model is trained to compute photosynthesis (GPP) using the equation number 16

$$GPP = R_g * \mathcal{E}_c * f_T(T_a) * f ELUE * f APAR * SR10 \qquad (16)$$

Where, R_g is incoming global radiation, and $\mathcal{E}_c$ is climate efficiency.

$f_T(T_a)$ is a temperature stress function that depends on the mean air temperature at 2m.

For stress function following different scenarios were used to calculate $f_T(T_a)$

for $T_{min} < T_a < T_{opt}$

$f_T(T_a) = 1 - (T_{opt} – T_a/T_{opt} - T_{min})^{\beta}$ (17)

for $T_{opy} < T_a < T_{max}$

$f_T(T_a) = 1 - (T_{opt} – T_a/T_{opt} - T_{max})^{\beta}$ (18)

for $T_a < T_{min}$ or $T_{max} < T_a$ (19)

$f_T(T_a) = 0$

where, $^{\beta}$ is polynomial degree, T_{opt} is optimal temperature, T_{min} is minimum temperature, and T_{max} is maximum temperature.

In equation 2, fELUE is effective light use efficiency which is calculated by equation 20

$f\mathrm{ELUE} = \mathrm{LUE}_a * \exp(R_{diff}/R_g) * \mathrm{LUE}_b$ (21)

where LUE_a is the light use efficiency (for direct radiation) and LUE_b is a correction coefficient. This coefficient is used due to effect of diffuse radiation (R_{diff}) radiation on ELUE.

fAPAR is fraction of absorbed photosynthetically active radiation which is calculated by the

$f\mathrm{APAR} = 1 - \exp^{(-K_{ext} * \mathrm{GLAI})}$ (22)

where K_{ext} is a coefficient of light interception and GLAI is green leaf area index.

SR10 explains how photosynthetic efficiency during senescence. The value of SR10 is used 1 from the period of sowing to senescence and from the senescence to crop harvest is calculated by the equation

$\mathrm{SR10} = \mathrm{GLAI}/\mathrm{GLAI}_{max} * \mathrm{Cs}$ (23)

Where is corrective factor for GPP during senescence.

Ecosystem Respiration (Re) Computation

In the second step, net ecosystem exchange (NEE) was computed from GPP and ecosystem respiration (Re) using the equation

$$NEE = GPP - Re \quad (24)$$

The Re consists of autotrophic respiration (R_a) and heterotrophic respiration (R_h).

$$Re = R_a + R_h \quad (25)$$

In equation 10, R_a is calculated from the equation

$$R_a = R_m + R_{gr} \quad (26)$$

R_a is divided into R_m (maintenance respiration; Amthor, 2000), and R_{gr} (growth respiration; Choudhury, 2000). R_m is influenced by factors; R10 (basal respiration at 10 C), + Q10 (temperature sensitivity for respiration), temperature (T) and SR10. and R_{gr}

$$R_m = R10.\ Q10^{-0.1.\ (T-10)}.\ SR10 \quad (27)$$

While R_{gr} is calculated by the equation

$$R_{gr} = (1-Yg).\ (GPP-R_m) \quad (28)$$

Where Y_g is growth conversation efficiency.

In equation 10, R_h is calculated by equation 29

$$Rh = a * \exp^{(b* Tsoil)} \quad (29)$$

Where,

$$a = R_{href} \quad (30)$$

R_{href} is the reference respiration rate at 0°C, and b expresses RH sensitivity to temperature.

$$Q10 = \exp^{(b* 10)} \quad (31)$$

Q10 and R_{href} both are heterotopic respiration parameters.

Results and Discussion

Comparison of Measured and Simulated LE, H and G0 Fluxes

The measured fluxes (*LE_m*, *H_m*, and *G_m*) were compared with the simulated fluxes (*LE_s*, *H_s*, and *G_s*) shown in **Figure 27. 28** and **29** respectively. The yellow line represents the measured flux while the blue line represents the simulated flux by the SURFATM model. The figures clearly indicate that the measured fluxes have close agreement with the simulated energy balance components. The flux amplitude was found almost the same in both measured and simulated flux. The other reason may be the model is unable to capture the rapid changes in the LE flux, net radiation, soil moisture, etc. Furthermore, the study results also suggest that although the model captures the overall flux trends very well, there is still a need for parameter adjustment to achieve better accuracy and agreement between measured and simulated fluxes.

However, in the case of ground heat flux, there is a slight forward shift in the measured flux, which may be due to several reasons. For example, the model was already trained to consider a fixed value of heat stored in soil in the simulation while our measured value directly measures continuous variation of soil heat storage in addition to ground heat flux.

Comparison of Measured and Simulated GPP, Re and NEE Fluxes

Like energy balance components, measured GPP, Re, and NEE were compared with the simulated NEE, GPP, and Reco shown in **Figures 30, 31**, and **32** respectively. The yellow line represents the measured flux while the blue line represents the simulated flux by the SURFATM model. However, in the case of Reco, the yellow line represents simulated by the SURFATM model, and blue represents measured Reco. The overall diurnal trend and pattern of measured and simulated NEE, GPP, and Reco were found to be consistent.

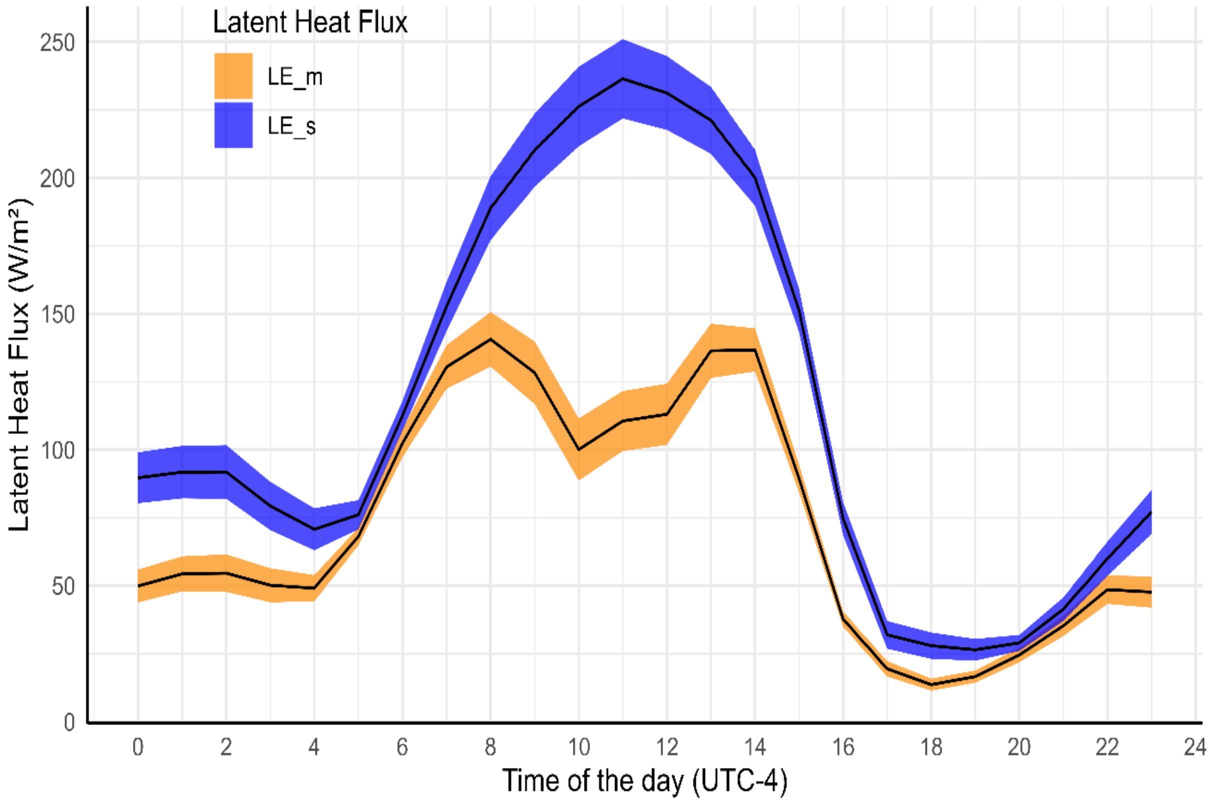

Figure. 27. Comparison of measured (yellow-line), simulated (blue-line) *LE* flux.

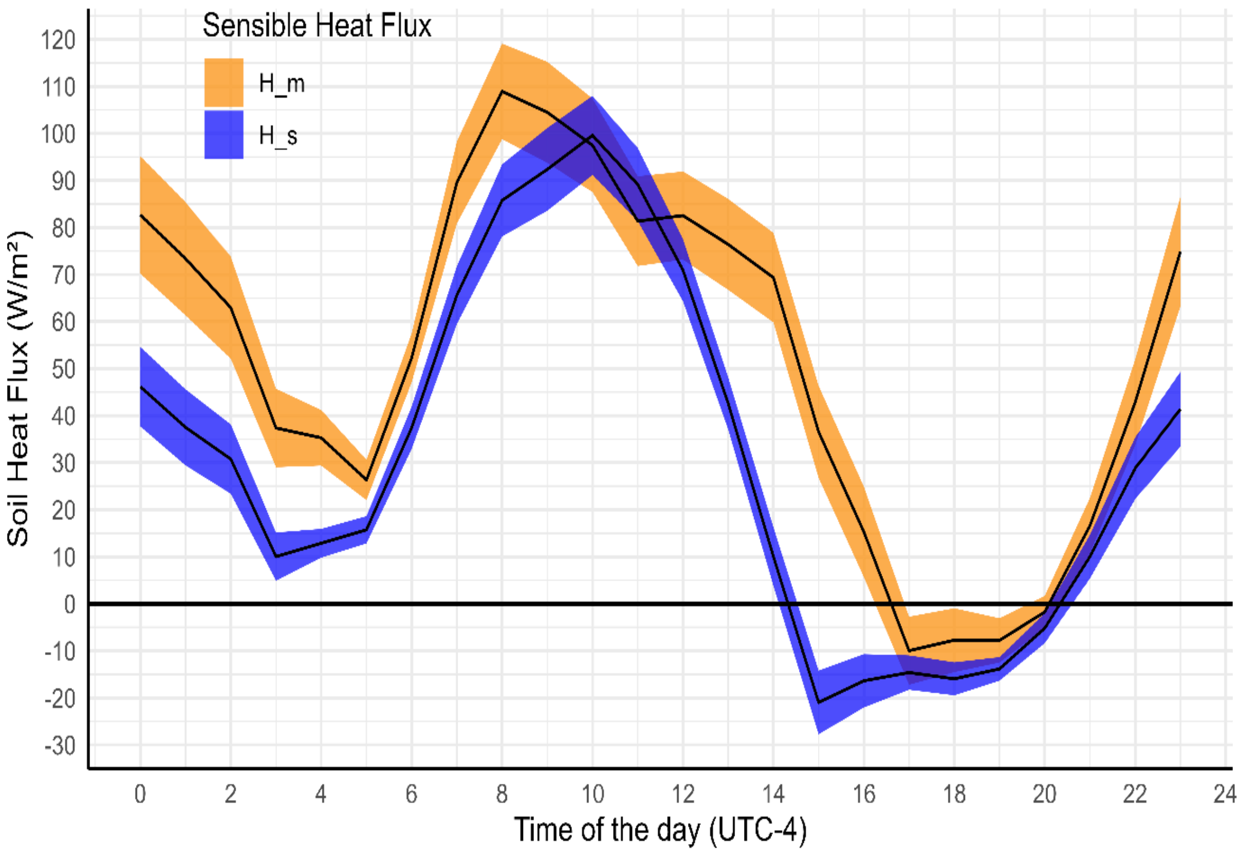

Figure. 28. Comparison of measured (yellow-line), simulated (blue-line) *H* flux.

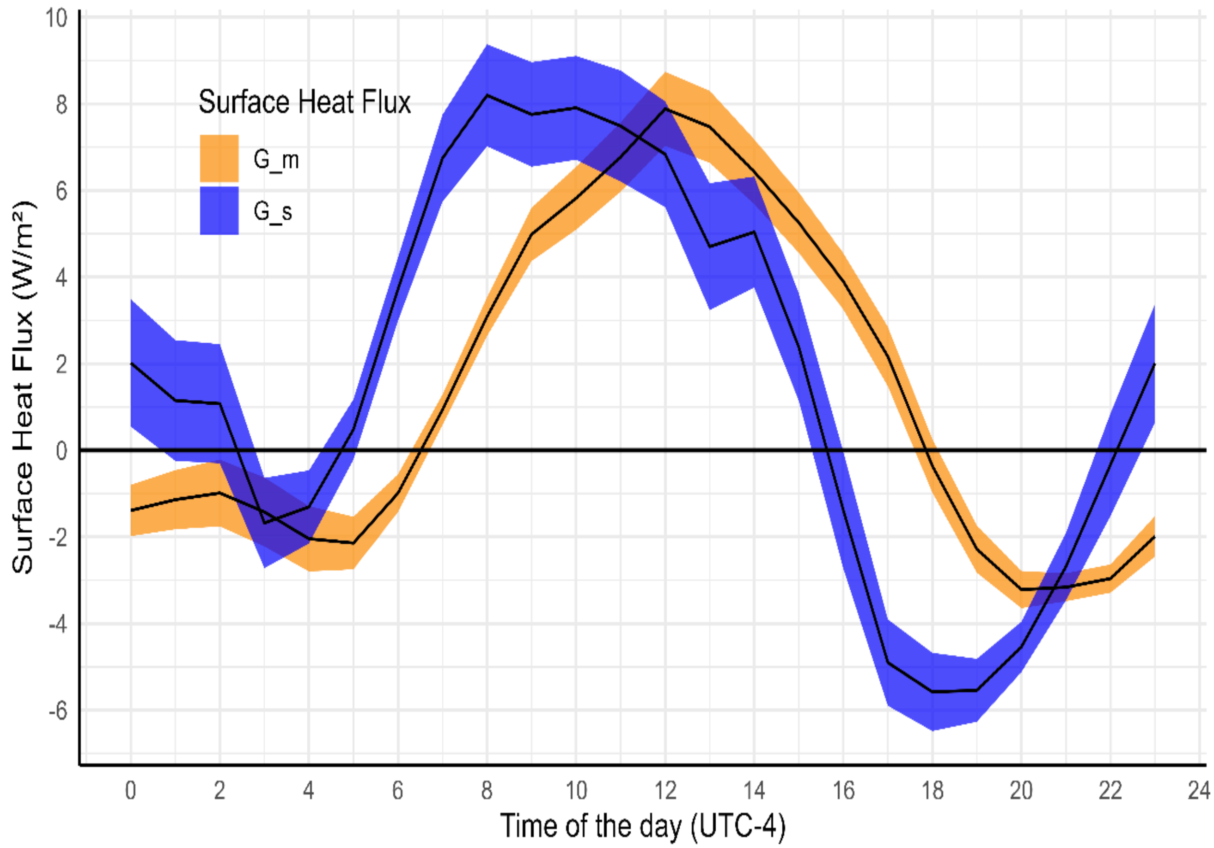

Figure. 29. Comparison of measured (yellow-line), simulated (blue-line) *G* flux.

The diurnal pattern of GPP in **Figure 30** represents that overall GPP was found higher during the daytime as compared to night because of plant photosynthesis activities. Plants are active in photosynthesis during the daytime while negative during the nighttime, which means the plant has minimized the process of photosynthesis resultantly GPP is minimal. The measured GPP_m indicates a higher negative value during the daytime and is more scattered as compared to the simulated GPP_s. This reflects the variation in environmental factors such as net radiation as well as the influence of plant canopy etc. Overall, simulated GPP_s were found 27% higher than measured GPP_m. Simulated GPP_s found less scatter which may be due to model parameterization and assumptions.

In the case of Re, the measured Re_m was found consistently higher (12.94%) as compared to the simulated Re_s by the SURFATM model shown in **Figure 30**. The disagreement between simulated and measured Reco could be due to field observation as well as model assumption. For example, models simulate autotrophic and heterotrophic respiration separately. Different adjustable parameters are used to derive the respiration which may influence the accuracy of the model. Similarly, the local environmental conditions and the heterogeneity of the maize canopy captured by the field measurements are not captured by the model. Although the model efficiently reflects a similar GPP trend, it is unable to represent the same magnitude, which suggests that adjustable parameters are required to better the model accuracy.

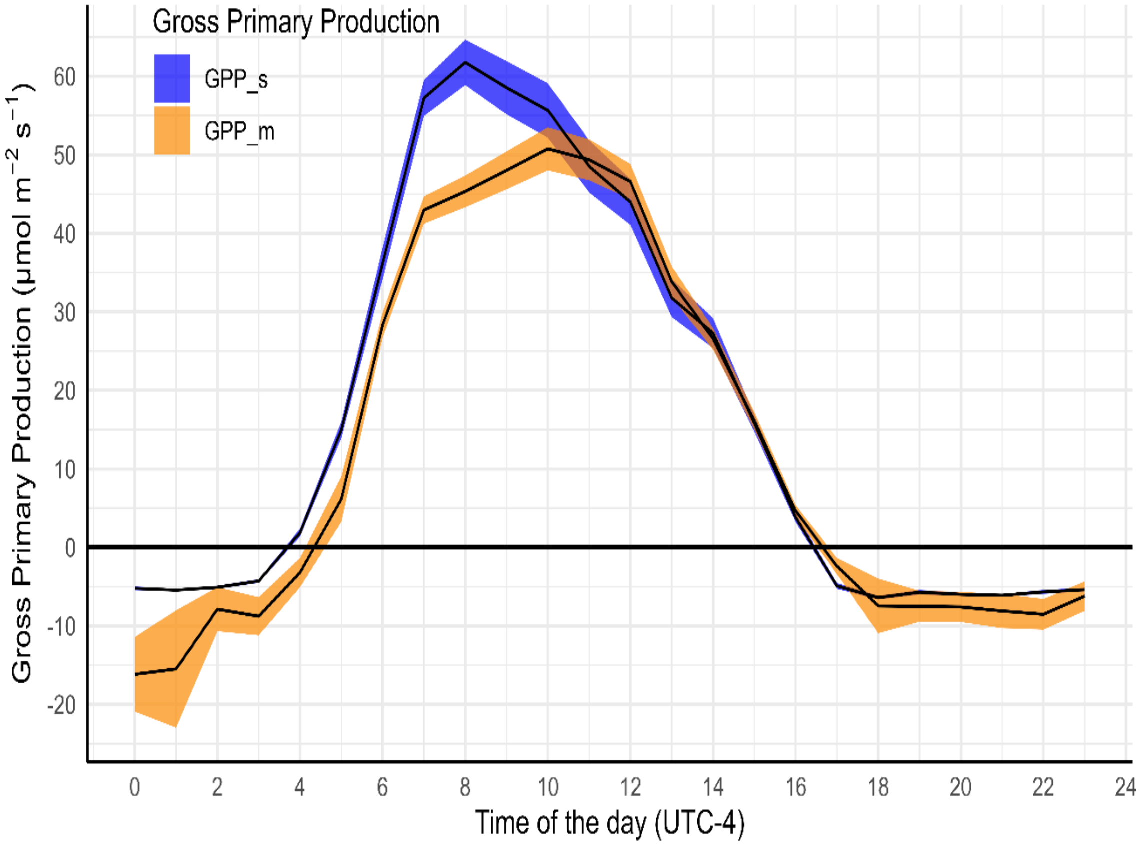

Figure. 30. Comparison of measured (yellow-line), simulated (blue-line) GPP flux.

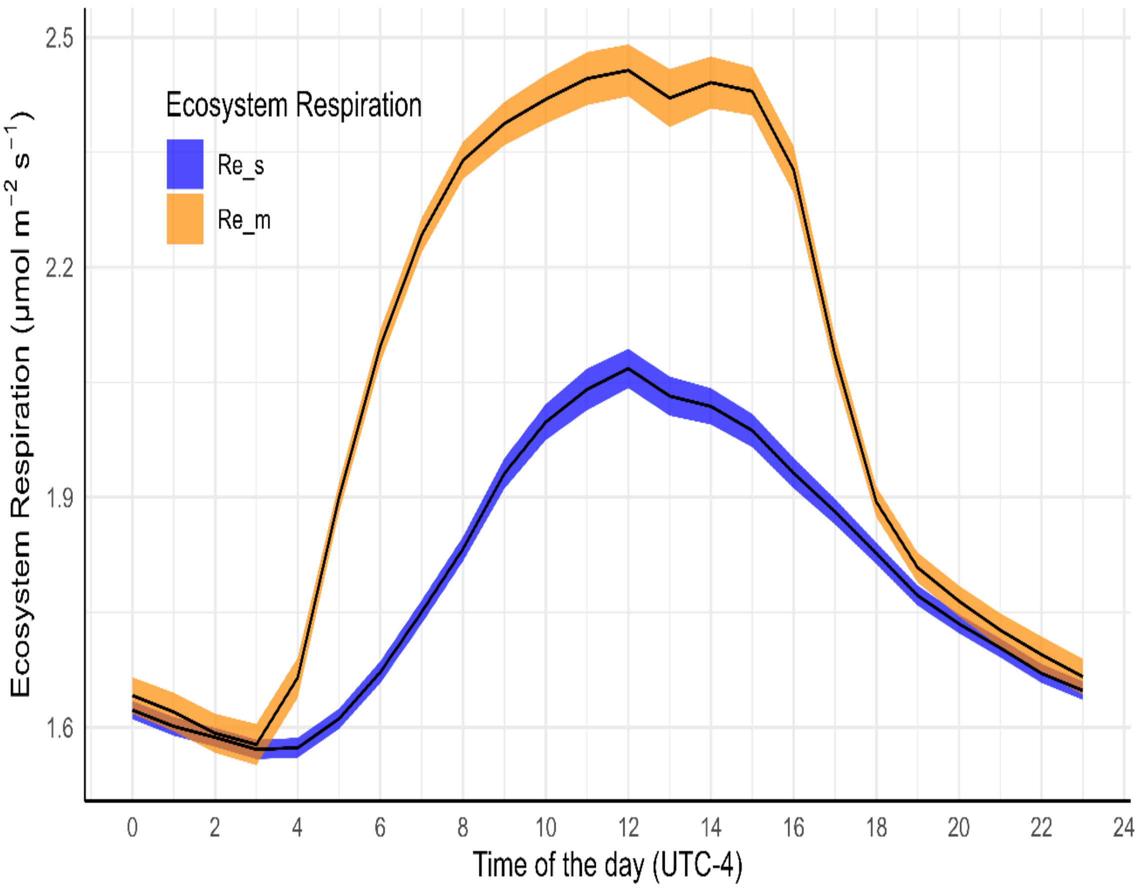

Figure. 31 Continued. Comparison of measured (blue-line) and simulated (yellow-line) Re flux.

As previously explained, the general trend of measured GPP_m and Re_m was higher as well as more scattered than the simulated. Similarly, measured NEE_m was also found more scattered and higher during the daytime as compared to the simulated NEE_s shown in **Figure 31**. During the daytime, the GPP is dominant due to photosynthesis and responsible for negative NEE (uptake of the CO_2). As the measured GPP increases, it is likely to indicate the higher negative NEE value. Compared to daytime, nighttime Re becomes a dominant process and the release of CO_2 and NEE becomes positive. It was calculated that during the daytime from 0600 LT to 1800 LT, the simulated NEE was 7% higher than measured NEE_m. in other words, during the daytime simulated NEE absorbed more carbon as compared to nighttime. The measured NEE_m indicates the higher variation reflecting that variation in the CO_2 ecosystem exchanges.

Conclusion

This comparison study between field measured and simulated fluxes by the SURFTAM model suggests that there is a good agreement between energy components (LE, H, and G0) and CO_2 flux (GPP, Re, and NEE). However, measured fluxes were more scattered and trended higher when compared to simulated fluxes by the SURFATM model. These comparisons suggest that reevaluation of the input dataset is needed as well as to refine adjustable parameters required to achieve a good correlation between measured and simulated fluxes. Furthermore, instrumentation errors, weather conditions, data gaps, etc. may also be responsible for input data discrepancies during the calculation of measured and simulated fluxes. In summary, while the SURFATM model captured a good correlation between energy balance components and GPP

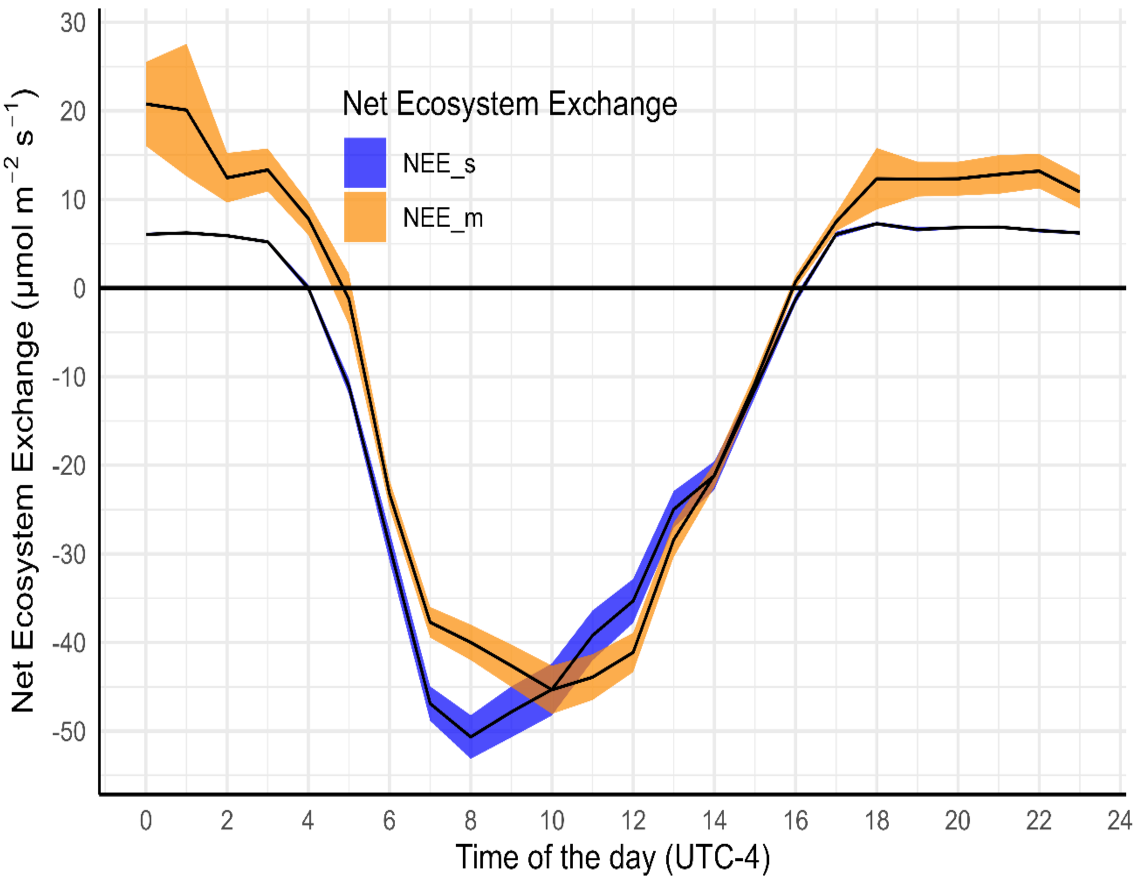

Figure. 32. Comparison of measured (yellow-line), simulated (blue-line) NEE flux.

flux, refining the input data and adjusting the parameters may help to achieve better accuracy between measured and simulated flux.

REFERENCES

Anderson, R.G., Wang, D., 2014. Energy budget closure observed in paired Eddy Covariance towers with increased and continuous daily turbulence. Agricultural and forest meteorology, 184, 204-209. https://doi.org/10.1016/j.agrformet.2013.09.012

Bailey, B.J., Meneses, J.F., 1994. Modelling leaf convective heat transfer. Greenhouse Environment Control and Automation 399, 191-198.

Baldocchi, D., 2014. Measuring fluxes of trace gases and energy between ecosystems and the atmosphere–the state and future of the eddy covariance method. Global change biology, 20(12), 3600-3609. https://doi.org/10.17660/ActaHortic.1995.399.22

Barr, A.G., Van der Kamp, G., Black, T.A., McCaughey, J.H., Nesic, Z., 2012. Energy balance closure at the BERMS flux towers in relation to the water balance of the White Gull Creek watershed 1999–2009. Agricultural and Forest Meteorology, 153, 3-13. https://doi.org/10.1016/j.agrformet.2011.05.017

Blake, G.R. and Hartge, K.H., 1986. Bulk density. Methods of soil analysis: Part 1 Physical and mineralogical methods, 5, 363-375.

Bowen, I.S., 1926. The ratio of heat losses by conduction and by evaporation from any water surface. Physical Review, 27(6), 779. http://dx.doi.org/10.1103/PhysRev.27.779

Burba, G., 2013. Eddy covariance method for scientific, industrial, agricultural and regulatory applications: A field book on measuring ecosystem gas exchange and areal emission rates. LI-Cor Biosciences.

Canadell, J.G., Monteiro, P.M., Costa, M.H., Da Cunha, L.C., Cox, P.M., Eliseev, A.V., Henson, S., Ishii, M., Jaccard, S., Koven, C. and Lohila, A., 2021. Global carbon and other biogeochemical cycles and feedbacks. IPCC AR6 WGI, final government distribution, pp.chapter-5.

Cava, D., Contini, D., Donateo, A., Martano, P., 2008. Analysis of short-term closure of the surface energy balance above short vegetation. Agricultural and forest meteorology, 148(1), 82-93. https://doi.org/10.1016/j.agrformet.2007.09.003

Chen, N., Wang, A., An, J., Zhang, Y., Ji, R., Jia, Q., Zhao, Z, Guan, D., 2020. Modeling canopy carbon and water fluxes using a multilayered model over a temperate meadow in Inner Mongolia. International Journal of Plant Production, 14, 141-154. https://doi.org/10.1007/s42106-019-00074-4.

Choudhury, B.J. and Monteith, J.L., 1988. A four-layer model for the heat budget of homogeneous land surfaces. Quarterly Journal of the Royal Meteorological Society, 114(480), 373-398. https://doi.org/10.1002/qj.49711448006

da Silva, P.F., de Sousa Lima, J.R., Antonino, A.C.D., Souza, R., de Souza, E.S., Silva, J.R.I., Alves, E.M., 2017. Seasonal patterns of carbon dioxide, water and energy fluxes over the Caatinga and grassland in the semi-arid region of Brazil. Journal of Arid Environments, 147, 71-82. https://doi.org/10.1016/j.jaridenv.2017.09.003

Defraeye, T., Verboven, P., Ho, Q.T., Nicolai, B., 2013. Convective heat and mass exchange predictions at leaf surfaces: Applications, methods and perspectives. Computers and Electronics in Agriculture, 96, 180-201. https://doi.org/10.1016/j.compag.2013.05.008

Duell, E.B., Zaiger, K., Bever, J.D., Wilson, G.W., 2019. Climate affects plant-soil feedback of native and invasive grasses: negative feedbacks in stable but not in variable environments. Frontiers in Ecology and Evolution, 7, 419.

https://doi.org/10.3389/fevo.2019.00419Eder, F., Schmidt, M., Damian, T., Träumner, K., Mauder, M., 2015. Mesoscale eddies affect near-surface turbulent exchange: Evidence from lidar and tower measurements. Journal of Applied Meteorology and Climatology, 54(1), 189-206. https://doi.org/10.1175/JAMC-D-14-0140.1

Fargione, J. E., Bassett, S., Boucher, T., Bridgham, S. D., Conant, R. T., Cook-Patton, S. C., Ellis, P. W., Falcucci, A., Fourqurean, J. W., Gopalakrishna, T., Gu, H., Henderson, B., Hurteau, M. D., Kroeger, K. D., Kroeger, T., Lark, T. J., Leavitt, S. M., Lomax, G., McDonald, R. I., Megonigal, J. P., Miteva, D. A., Richardson, C. J., Sanderman, J., Shoch, D., Spawn, S. A., Veldman, J. W., Williams, C. A., Woodbury, P. B., Zganjar, C., Baranski, M., Elias, P., Houghton, R. A., Landis, E., McGlynn, E., Schlesinger, W. H., Siikamaki, J. V., Sutton-Grier, A. E., Griscom, B. W.: Natural climate solutions for the United States, *Science advances*, 4. https://doi.org/10.1126/sciadv.aat1869, 2018

Ferrara, R.M., Loubet, B., Decuq, C., Palumbo, A.D., Di Tommasi, P., Magliulo, V., Masson, S., Personne, E., Cellier, P., Rana, G., 2014. Ammonia volatilisation following urea fertilisation in an irrigated sorghum crop in Italy. Agricultural and Forest Meteorology, 195, 179-191. https://doi.org/10.1016/j.agrformet.2014.05.010

Finnigan, J., 2006. The storage term in eddy flux calculations. Agricultural and Forest Meteorology, 136(3-4), 108-113. https://doi.org/10.1016/j.agrformet.2004.12.010.

Foken, T., 1998. Die scheinbar ungeschlossene Energiebilanz am Erdboden-eine Herausforderung an die Experimentelle Meteorologie. Sitzungsberichte der Leibniz-Sozietät, 24(5), 131-150.

Foken, T., 2008. The energy balance closure problem: An overview. Ecological Applications, 18(6), 1351-1367. https://doi.org/10.1890/06-0922.1

Foken, T., Aubinet, M., Finnigan, J.J., Leclerc, M.Y., Mauder, M., Paw U, K.T., 2011. Results of a panel discussion about the energy balance closure correction for trace gases. Bulletin of the American Meteorological Society, 92(4), ES13-ES18.Frank, J.M., Massman, W.J., Ewers, B.E., 2013. Underestimates of sensible heat flux due to vertical velocity measurement errors in non-orthogonal sonic anemometers. Agricultural and Forest Meteorology, 171, 72-81. https://doi.org/10.1016/j.agrformet.2012.11.005

Franssen, H.H., Stöckli, R., Lehner, I., Rotenberg, E., Seneviratne, S.I., 2010. Energy balance closure of eddy-covariance data: A multisite analysis for European FLUXNET stations. Agricultural and Forest Meteorology, 150(12), 1553-1567. https://doi.org/10.1016/j.agrformet.2010.08.005

Galmiche, M., Hunt, J.C.R., 2002. The formation of shear and density layers in stably stratified turbulent flows: linear processes. Journal of Fluid Mechanics, 455, 243-262.https://doi.org/10.1017/S002211200100739X.

Gao, Z., Russell, E.S., Missik, J.E., Huang, M., Chen, X., Strickland, C.E., Clayton, R., Arntzen, E., Ma, Y., Liu, H., 2017. A novel approach to evaluate soil heat flux calculation: An analytical review of nine methods. Journal of Geophysical Research: Atmospheres, 122(13), 6934-6949. https://doi.org/10.1002/2017JD027160

Goulden, M.L., Munger, J.W., Fan, S.M., Daube, B.C., Wofsy, S.C., 1996. Measurements of carbon sequestration by long-term eddy covariance: Methods and a critical evaluation of accuracy. Global change biology, 2(3), 169-182. https://doi.org/10.1111/j.1365-2486.1996.tb00070.x,

Grace, J.B., 2006. Structural equation modeling and natural systems. Cambridge University Press.

Griscom, B. W., Adams, J., Ellis, P. W., Houghton, R. A., Lomax, G., Miteva, D. A., Schlesinger, W. H., Shoch, D., Siikamaki, J. V., Smith, P., Woodbury, P., Zganjar, C., Blackman, A., Campari, J., Conant, R. T., Delgado, C., Elias, P., Gopalakrishna, T., Hamsik, M. R., Herrero, M., Kiesecker, J., Landis, E., Laestadius, L., Leavitt, S. M., Minnemeyer, S., Polasky, S., Potapov, P., Putz, F. E., Sanderman, J., Silvius, M., Wollenberg, E., and Fargione, J.: Natural climate solutions, Griscom, B.W., Adams, J., Ellis, P.W., Houghton, R.A., Lomax, G., Miteva, D.A., Schlesinger, W.H., Shoch, D., Siikamäki, J.V., Smith, P., Woodbury, P., 2017. Natural climate solutions. Proceedings of the National Academy of Sciences. 114, 11645–11650. https://doi.org/10.1073/pnas.1710465114, 2017.

Held, I.M. and Soden, B.J., 2000. Water vapor feedback and global warming. Annual review of energy and the environment, *25*(1), 441-475.

Hicks, B.B., Eash, N.S., O'Dell, D.L., Oetting, J.N., 2020. Augmented Bowen ratio analysis–I: site adequacy, fetch and heat storage (ABRA). Agricultural and Forest Meteorology, 290, 108035. https://doi.org/10.1016/j.agrformet.2020.108035,

Hicks, B.B., Lichiheb, N., O'Dell, D.L., Oetting, J.N., Eash, N.S., Heuer, M., Myles, L., 2021. A statistical approach to surface renewal: The virtual chamber concept. Agrosystems, Geosciences & Environment, 4(1), e20141. https://doi.org/10.1002/agg2.20141.

Hicks, B.B., O'Dell, D.L., Eash, N.S., Sauer, T.J., 2015. Nocturnal intermittency in surface CO2 concentrations in sub-Saharan Africa. Agricultural and Forest Meteorology, 200, 129-134. https://doi.org/10.1016/j.agrformet.2014.09.007.

Hicks, B.B., Oetting, J.N., Eash, N.S., O'Dell, D.L., 2022. Augmented Bowen ratio analysis, II: Ohio comparisons. Agricultural and Forest Meteorology, 313,108760. https://doi.org/10.1016/j.agrformet.2021.108760.

Hoeltgebaum, L.E., Dias, N.L., 2023. Evaluation of the storage and evapotranspiration terms of the water budget for an agricultural watershed using local and remote-sensing measurements. Agricultural and Forest Meteorology, 341, 109615. https://doi.org/10.1016/j.agrformet.2023.109615.

Horst, T.W., Semmer, S.R., Maclean, G., 2015. Correction of a non-orthogonal, three-component sonic anemometer for flow distortion by transducer shadowing. Boundary-Layer Meteorology, 155, 371-395. https://doi.org/10.1007/s10546-015-0010-3

Humphrey, V., Berg, A., Ciais, P., Gentine, P., Jung, M., Reichstein, M., Seneviratne, S.I., Frankenberg, C., 2021. Soil moisture–atmosphere feedback dominates land carbon uptake variability. Nature, 592(7852), 65-69. https://doi.org/10.1038/s41586-021-03325-5

Irmak, S., Payero, J.O., Kilic, A., Odhiambo, L.O., Rudnick, D., Sharma, V., Billesbach, D., 2014. On the magnitude and dynamics of eddy covariance system residual energy (energy balance closure error) in subsurface drip-irrigated maize field during growing and non-growing (dormant) seasons. Irrigation science, 32, 471-483. https://doi.org/10.1007/s00271-014-0443-3

Irmak, S., Skaggs, K.E., Chatterjee, S., 2014. A review of the Bowen ratio surface energy balance method for quantifying evapotranspiration and other energy fluxes. Transactions of the ASABE, 57(6), .657-1674. https://doi.org/10.13031/trans.57.10686.

Jarvis, P.G., Massheder, J.M., Hale, S.E., Moncrieff, J.B., Rayment, M., Scott, S.L., 1997. Seasonal variation of carbon dioxide, water vapor, and energy exchanges of a boreal black spruce forest. Journal of Geophysical Research: Atmospheres, 102(D24), 28953-28966. https://doi.org/10.1029/97JD01176

Kochendorfer, J., Meyers, T.P., Frank, J., Massman, W.J., Heuer, M.W., 2012. How well can we measure the vertical wind speed? Implications for fluxes of energy and mass. Boundary-layer meteorology, 145, 383-398. https://doi.org/10.1007/s10546-012-9738-1

Kutikoff, S., Lin, X., Evett, S., Gowda, P., Moorhead, J., Marek, G., Colaizzi, P., Aiken, R., Brauer, D., 2019. Heat storage and its effect on the surface energy balance closure under advective conditions. Agricultural and Forest Meteorology, 265, .6-69. https://doi.org/10.1016/j.agrformet.2018.10.018

Lal, R., 2007. Soil science and the carbon civilization. Soil Science Society of America Journal, 71(5), pp.1425-1437. https://doi.org/10.2136/sssaj2007.0001

Lamas Galdo, M.I., Rodriguez García, J.D., Rebollido Lorenzo, J.M., 2021. Numerical model to analyze the physicochemical mechanisms involved in CO2 absorption by an aqueous ammonia droplet. International Journal of Environmental Research and Public Health, 18(8), 4119. https://doi.org/10.3390/ijerph18084119. 2021.

Law, B.E., Falge, E., Gu, L., Baldocchi, D.D., Bakwin, P., Berbigier, P., Davis, K., Dolman, A.J., Falk, M., Fuentes, J.D. and Goldstein, A., 2002. Environmental controls over carbon dioxide and water vapor exchange of terrestrial vegetation. Agricultural and Forest Meteorology, *113*(1-4), 97-120.

Leuning, R., 2000. Estimation of scalar source/sink distributions in plant canopies using Lagrangian dispersion analysis: Corrections for atmospheric stability and comparison with a multilayer canopy model. Boundary-Layer Meteorology, 96(1), 293-314. https://doi.org/10.1023/A:1002449700617.

Leuning, R., van Gorsel, E., Massman, W.J., Isaac, P.R., 2012. Reflections on the surface energy imbalance problem. Agricultural and Forest Meteorology, 156, 65-74. https://doi.org/10.1016/j.agrformet.2011.12.002

Li HongQin, L.H., Zhang FaWei, Z.F., Li YingNian, L.Y., Wang JunBang, W.J., Zhang LeiMing, Z.L., Zhao Liang, Z.L., Cao GuangMin, C.G., Zhao XinQuan, Z.X. and Du MingYuan, D.M., 2016. Seasonal and inter-annual variations in CO2 fluxes over 10 years in an alpine shrubland on the Qinghai-Tibetan Plateau, China. Agricultural and Forest Meteorology, 228-229, 95-103. https://doi.org/10.1016/j.agrformet.2016.06.020

Lichiheb, N., Myles, L., Personne, E., Heuer, M., Buban, M., Nelson, A. J., Bernacchi, C., 2019. Implementation of the effect of urease inhibitor on ammonia emissions following urea-based fertilizer application at a Zea mays field in central Illinois: a study with SURFATM-NH3 model. Agricultural and Forest Meteorology, 269, 78-87. https://doi.org/10.1016/j.agrformet.2019.02.005

Lichiheb, N., Personne, E., Bedos, C. and Barriuso, E., 2014. Adaptation of a resistive model to pesticide volatilization from plants at the field scale: Comparison with a dataset. Atmospheric Environment, 83, 260-268. https://doi.org/10.1016/j.atmosenv.2013.11.004

Luo, Y., 2007. Terrestrial carbon–cycle feedback to climate warming. Annual Review of Ecology, Evolution, and Systematics. *38*(1), 683-712.

Maier, R., Hörtnagl, L., Buchmann, N., 2022. Greenhouse gas fluxes (CO2, N2O and CH4) of pea and maize during two cropping seasons: Drivers, budgets, and emission factors for nitrous oxide. Science of the Total Environment, *849*, 157541. https://doi.org/10.1016/j.scitotenv.2022.157541

Masseroni, D., Corbari, C., Mancini, M., 2014. Limitations and improvements of the energy balance closure with reference to experimental data measured over a maize field. Atmósfera 27, 335–352. https://doi.org/10.1016/S0187-6236(14)70033-5

Massman, W.J., Lee, X., 2002. Eddy covariance flux corrections and uncertainties in long-term studies of carbon and energy exchanges. Agricultural and Forest Meteorology, 113(1-4), 121-144. https://doi.org/10.1016/S0168-1923(02)00105-3.

Mauder, M., Desjardins, R.L., Pattey, E. and Worth, D., 2010. An attempt to close the daytime surface energy balance using spatially-averaged flux measurements. Boundary Layer Meteorology, 136, 175-191. https://doi.org/10.1007/s10546-010-9497-9

Mauder, M., Jung, M., Stoy, P., Nelson, J., Wanner, L., 2024. Energy balance closure at FLUXNET sites revisited. Agricultural and Forest Meteorology, 358, p.110235. https://doi.org/10.1016/j.agrformet.2024.110235

Mayocchi, C.L., Bristow, K.L., 1995. Soil surface heat flux: some general questions and comments on measurements. Agricultural and forest meteorology, 75(1-3), 43-50. https://doi.org/10.1016/0168-1923(94)02198-S.

McCaughey, J.H., Saxton, W.L., 1988. Energy balance storage terms in a mixed forest. Agricultural and Forest Meteorology, 44(1), 1-18. https://doi.org/10.1016/0168-1923(88)90029-9.

Meyers, T.P., Hollinger, S.E., 2004. An assessment of storage terms in the surface energy balance of maize and soybean. Agricultural and Forest Meteorology, 125(1-2), 105-115. https://doi.org/10.1016/j.agrformet.2004.03.001.

Montagnani, L., Grünwald, T., Kowalski, A., Mammarella, I., Merbold, L., Metzger, S., Sedlák, P., Siebicke, L., 2018. Estimating the storage term in eddy covariance measurements: the ICOS methodology. International Agrophysics, 32(4), 551- http://dx.doi.org/567. 10.1515/intag-2017-0037

Nemitz, E., Sutton, M.A., Schjoerring, J.K., Husted, S., Wyers, G.P., 2000. Resistance modelling of ammonia exchange over oilseed rape. Agricultural and Forest Meteorology, 105(4), 405-425. https://doi.org/10.1016/S0168-1923(00)00206-9

Nicolini, G., Aubinet, M., Feigenwinter, C., Heinesch, B., Lindroth, A., Mamadou, O., Moderow, U., Mölder, M., Montagnani, L., Rebmann, C., Papale, D., 2018. Impact of CO2 storage flux sampling uncertainty on net ecosystem exchange measured by eddy covariance. Agricultural and Forest Meteorology, 248, 228-239. http://dx.doi.org/10.1016/j.agrformet.2017.09.025.

Ochsner, T.E., Sauer, T.J., Horton, R., 2007. Soil heat storage measurements in energy balance studies. Agronomy Journal, 99(1), 311-319.

O'Dell, D., Sauer, T.J., Hicks, B.B., Lambert, D.M., Smith, D.R., Bruns, W.A., Basson, A., Marake, M.V., Walker, F., Wilcox, M.D., Eash, N.S., 2014. Bowen ratio energy balance measurement of carbon dioxide (CO2) fluxes of no-till and conventional tillage agriculture in Lesotho. Open Journal of Soil Science 4(3): 87-97. http://hdl.handle.net/10919/70228.

O'Dell, D., Sauer, T.J., Hicks, B.B., Thierfelder, C., Lambert, D.M., Logan, J., Eash, N.S., 2015. A short-term assessment of carbon dioxide fluxes under contrasting agricultural and soil management practices in Zimbabwe. Journal of Agricultural Science., 7 (2), http://dx.doi.org/10.5539/jas.v7n3p32. 2015.

Oetting, J., Hicks, B., Eash, N., 2024. On recursive partitioning to refine coordinate rotation in Eddy covariance applications. Agricultural and Forest Meteorology, 346, 109873. https://doi.org/10.1016/j.agrformet.2023.109873.

Papale, D., Reichstein, M., Aubinet, M., Canfora, E., Bernhofer, C., Kutsch, W., Longdoz, B., Rambal, S., Valentini, R., Vesala, T.,Yakir, D., 2006. Towards a standardized processing of Net Ecosystem Exchange measured with eddy covariance technique: algorithms and uncertainty estimation. Biogeosciences, 3(4), 571-583. https://doi.org/10.5194/bg-3-571-2006.

Pardo, N., Sánchez, M.L., Pérez, I.A., García, M.A., 2015. Energy balance and partitioning over a rotating rapeseed crop. Agricultural Water Management, 161, 31-40. https://doi.org/10.1016/j.agwat.2015.07.015

Pastorello, G., Trotta, C., Canfora, E., Chu, H., Christianson, D., Cheah, Y.W., Poindexter, C., Chen, J., Elbashandy, A., Humphrey, M., Isaac, P., 2020. The FLUXNET2015 dataset and the ONEFlux processing pipeline for eddy covariance data. Scientific data, 7(1), p.225. https://doi.org/10.6084/m9.figshare.12295910.

Personne, E., Loubet, B., Herrmann, B., Mattsson, M., Schjoerring, J. K., Nemitz, E., Cellier, P., 2009. SURFATM-NH3: a model combining the surface energy balance and bi-directional exchanges of ammonia applied at the field scale. Biogeosciences, 6(8), 1371-1388. https://doi.org/10.5194/bg-6-1371-2009

Pique, G., Fieuzal, R., Al Bitar, A., Veloso, A., Tallec, T., Brut, A., Ferlicoq, M., Zawilski, B., Dejoux, J.F., Gibrin, H., Ceschia, E., 2020a. Estimation of daily CO2 fluxes and of the components of the carbon budget for winter wheat by the assimilation of Sentinel 2-like remote sensing data into a crop model. *Geoderma*, *376*, 114428. https://doi.org/10.1016/j.geoderma.2020.114428

Pique, G., Fieuzal, R., Debaeke, P., Al Bitar, A., Tallec, T., Ceschia, E., 2020. Combining high-resolution remote sensing products with a crop model to estimate carbon and water budget components: application to sunflower. Remote Sensing, 12(18), 2967. https://doi.org/10.3390/rs12182967

Raza, T., Hicks, B., Oetting, J., Eash, N., 2023, January. On the agricultural eddy covariance storage term: measuring carbon dioxide concentrations and energy exchange inside a maize canopy. In 103rd AMS Annual Meeting. AMS.

Raza, T., Oetting, J., Eash, N., Hicks, B.B., Lichiheb, N., 2024, January. Assessing energy balance closure over maize canopy using multiport system and canopy net storage. In 104th AMS Annual Meeting. AMS.

Russell, E.S., Liu, H., Gao, Z., Finn, D., Lamb, B., 2015. Impacts of soil heat flux calculation methods on the surface energy balance closure. Agricultural and Forest Meteorology, 214, 189-200. https://doi.org/10.1016/j.agrformet.2015.08.255

Schmidt, M., Reichenau, T.G., Fiener, P., Schneider, K., 2012. The carbon budget of a winter wheat field: An eddy covariance analysis of seasonal and inter-annual variability. Agricultural and Forest Meteorology, 165,114-126. https://doi.org/10.1016/j.agrformet.2012.05.012

Stella, P., Personne, E., Loubet, B., Lamaud, E., Ceschia, E., Béziat, P., Bonnefond, J.M., Irvine, M., Keravec, P., Mascher, N., Cellier, P., 2011. Predicting and partitioning ozone fluxes to maize crops from sowing to harvest: the Surfatm-O 3 model. Biogeosciences, 8(10), 2869-2886. https://doi.org/10.5194/bg-8-2869-201

Stoy, P.C., Mauder, M., Foken, T., Marcolla, B., Boegh, E., Ibrom, A., Arain, M.A., Arneth, A., Aurela, M., Bernhofer, C., Cescatti, A., 2013. A data-driven analysis of energy balance closure across FLUXNET research sites: The role of landscape scale heterogeneity. Agricultural and forest meteorology, 171, 137-152. https://doi.org/10.1016/j.agrformet.2012.11.004

Twine, T.E., Kustas, W.P., Norman, J.M., Cook, D.R., Houser, P., Meyers, T.P., Prueger, J.H., Starks, P.J., Wesely, M.L., 2000. Correcting eddy-covariance flux underestimates over a grassland. Agricultural and forest meteorology, 103(3), 279-300. https://doi.org/10.1016/S0168-1923(00)00123-4

Twine, T.E., Kustas, W.P., Norman, J.M., Cook, D.R., Houser, P., Meyers, T.P., Prueger, J.H., Starks, P.J., Wesely, M.L., 2000. Correcting eddy-covariance flux underestimates over a grassland. Agricultural and forest meteorology, 103(3), 279-300. https://doi.org/10.1016/S0168-1923(00)00123-4.

USDA-NRCS (2018). Soil Survey Staff, Natural Resources Conservation Service, United States Department of Agriculture. Web Soil Survey. Available online at the following link: https://websoilsurvey.sc.egov.usda.gov/App/WebSoilSurvey.aspx Accessed [10/12/2018}

Varmaghani, A., Eichinger, W.E., Prueger, J.H., 2016. A diagnostic approach towards the causes of energy balance closure problem. Open Journal of Modern Hydrology, 6(02), 101. https://doi.org/10.4236/ojmh.2016.62009.

Verma, S.B., Rosenberg, N.J., 1976. Vertical profiles of carbon dioxide concentration in stable stratification. Agricultural Meteorology, 16(3), .359-369. https://doi.org/10.1016/0002-1571(76)90005-4.

Wang, X., Zhong, L., Ma, Y., Fu, Y., Han, C., Li, P., Wang, Z., Qi, Y., 2023. Estimation of hourly actual evapotranspiration over the Tibetan Plateau from multi-source data. Atmospheric Research, 281, 106475. https://doi.org/10.1016/j.atmosres.2022.106475.

Wilson, K., Goldstein, A., Falge, E., Aubinet, M., Baldocchi, D., Berbigier, P., Bernhofer, C., Ceulemans, R., Dolman, H., Field, C., Grelle, A., 2002. Energy balance closure at FLUXNET sites. Agricultural and forest meteorology, 113(1-4), 223-243. https://doi.org/10.1016/S0168-1923(02)00109-0.

Xu, Z., Ma, Y., Liu, S., Shi, W., Wang, J., 2017. Assessment of the energy balance closure under advective conditions and its impact using remote sensing data. Journal of Applied Meteorology and Climatology, 56(1), .127-140. https://doi.org/10.1175/JAMC-D-16-0096.1

Yang, P.C., Black, T.A., Neumann, H.H., Novak, M.D., Blanken, P.D., 1999. Spatial and temporal variability of CO2 concentration and flux in a boreal aspen forest. Journal of Geophysical Research: Atmospheres, 104(D22), 27653-27661. https://doi.org/10.1029/1999JD900295.

Yue, P., Li, Y., Zhang, Q., Zhang, L., 2012. Surface energy-balance closure in a gully region of the Loess Plateau at SACOL on eastern edge of Tibetan Plateau. Journal of Meteorology Society of Japan, 90(2), 173-184. https://doi.org/10.2151/jmsj.2012-C12

Zalewski, M., Kiedrzyńska, E., Wagner, I., Izydorczyk, K., Boczek, J.M., Jurczak, T., Krauze, K., Frankiewicz, P., Godlewska, M., Wojtal-Frankiewicz, A., Łapińska, M., 2021. Ecohydrology and adaptation to global change. Ecohydrology & Hydrobiology, 21(3), 393-410. https://doi.org/10.1016/j.ecohyd.2021.08.001

Zhu, X.G., Long, S.P., Ort, D.R., 2008. What is the maximum efficiency with which photosynthesis can convert solar energy into biomass?. Current opinion in biotechnology, 19(2), 153-159. https://doi.org/10.1016/j.copbio.2008.02.004

Zuo, J., Wang, J., Huang, J., Li, W., Wang, G., Ren, H., 2011. Estimation of ground heat flux and its impact on the surface energy budget for a semi-arid grassland. Sciences in Cold and Arid Regions, 3(1), 41-50. https://doi.org/10.3724/SP.J.1226.2011.00041

VITA

Taqi Raza was born in Punjab, Pakistan. He attended the University of Agriculture Faisalabad, Pakistan and graduated with a bachelor’s and master’s degrees in agriculture with majoring Soil Science.